

PERKIN-ELMER
OPTICAL TECHNOLOGY DIVISION

(NASA-CR-143682) INTERNAL ULTRAVIOLET
EXPLORER (IUE) STUDY PROGRAM. VOLUME 1:
TECHNOLOGY DISCUSSION Final Report, Feb. -
Aug. 1974 (Perkin-Elmer Corp., Danbury,
Conn.)

N75-16598

Unclas
10905

CSCL 22B G3/15

International Ultraviolet Explorer (IUE) Study Program

FINAL REPORT

PRICES SUBJECT TO CHANGE

Volume 1 - Technical Discussion

NAS5-23327
SPO 21015

Period of Performance

FEBRUARY 1974 - AUGUST 1974

Reproduced by
**NATIONAL TECHNICAL
INFORMATION SERVICE**
U.S. Department of Commerce
Springfield, VA. 22151

Prepared for:

GODDARD SPACE FLIGHT CENTER
Theoretical Astrophysics Branch

N O T I C E

THIS DOCUMENT HAS BEEN REPRODUCED FROM THE BEST COPY FURNISHED US BY THE SPONSORING AGENCY. ALTHOUGH IT IS RECOGNIZED THAT CERTAIN PORTIONS ARE ILLEGIBLE, IT IS BEING RELEASED IN THE INTEREST OF MAKING AVAILABLE AS MUCH INFORMATION AS POSSIBLE.

Engineering Report: ER-267

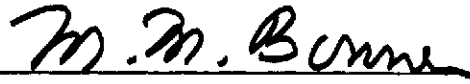
Date: November 1974

Prepared By: T. S. Turner, Jr.

Subject: International Ultraviolet Explorer (IUE)
Study Program - Final Report (Preliminary)

Publication Review:

This document has been reviewed and is approved.



Dr. M.M. Bonner, Director, Advanced Systems

Abstract:

The results of a simulation study to predict the IUE imaging chain performance are presented, including simulation photographs and transparencies of ultraviolet echelle spectra. Errors in wavelength determination and radiometric measurements due to system degradation are indicated to be minor. Some order overlap is predicted at the bottom of the echelle format.

PRECEDING PAGE BLANK NOT FILMED

TABLE OF CONTENTS

<u>Section</u>	<u>Title</u>	<u>Page</u>
1	INTRODUCTION	1-1
2	SYSTEM MATHEMATICAL MODEL	2-1
2.1	Model Summary and Block Diagram	2-1
2.2	Destructive Readout of SEC Vidicon	2-1
2.2.1	One-Dimensional Readout Model	2-3
2.2.2	Space-Invariant Approximation - Effective PSF	2-5
2.2.3	Extension to Two Dimensions	2-6
2.2.4	Computer Algorithm for Destructive Readout ..	2-9
2.2.5	Effective PSF Features	2-10
2.3	UV Converter	2-20
2.3.1	Introduction	2-20
2.3.2	MTF Derivation from Square Wave Response Date	2-22
2.3.3	Best Fit to Johnson Formula	2-22
2.3.4	Re-Inversion to SQR - Comparison with Original Data	2-25
2.4	Guidance PSF	2-25
2.4.1	NASA-Furnished Specification of Truncated Gaussian Servo Jitter PSF	2-25
2.4.2	MTF Derivation	2-25
2.5	UV Spectrograph	2-28
2.6	System MTF and PSF	2-28
2.7	Computer Implementation	2-29
3	PREPARATION OF INPUT ECHELLOGRAM	3-1
4	SIMULATIONS	4-1
5	DISCUSSION OF RESULTS	5-1
5.1	Effects of Destructive Readout	5-1
5.2	Effects of Guidance and UV Converter Smear	5-3
6	SUMMARY AND CONCLUSIONS	6-1
	REFERENCES	
Appendix A	COMPUTER PRINTOUTS OF SIMULATIONS 1-7	
Appendix B	EXPANSION FORMULAE FOR HANKEL TRANSFORM OF TRUNCATED GAUSSIAN POINT SPREAD FUNCTION	

LIST OF ILLUSTRATIONS

<u>Figure</u>	<u>Title</u>	<u>Page</u>
1	International Ultraviolet Explorer (IUE) Scientific Instrument Functional Block Diagram ...	2-2
2	Destructive Readout of Uniformly Charged Target	2-4
3	Readout Raster and Pixel Labeling	2-8
4	Computer Subroutine for Destructive R/O of SEC Vidicon	2-11
5	Gaussian Beam Current Distribution (PSF for Non-Destructive R/O)	2-12
6	Effective PSF for SEC Vidicon Destructive R/O (100 Percent Discharge)	2-13
7	Effective PSF for SEC Vidicon Destructive R/O (100 Percent Discharge)	2-14
8	Processing Spot for 100 Percent Discharge $\Delta X = \Delta Y = 1.551\sigma$	2-15
9	Processing Spot for 100 Percent Discharge $\Delta X = \Delta Y = 2.35\sigma$	2-16
10	X - and Y - Profiles of Effective PSF	2-17
11	X - and Y - Profiles of Effective PSF	2-19
12	X - and Y - Profiles of Effective PSF	2-21
13	Square Wave Response of Proximity Focused Converters Average of Bendix Tubes Number 401, 402, 403-25 and 407X	2-23
14	Sine Wave Response of Proximity Focused UV Converter (Calculated from Square Wave Response Data and Fitted to Johnson Formula)	2-24
15	Point Source Guidance MTF	2-27
16	Cascaded Point Source Guidance and UV Converter MTF's	2-30
17	Instrument PSF's (Not including destructive R/O)	2-31
18	NASA Echellogram "REDPSF" (750 x 750) Reproduced on LSIG Showing Subsection Used for Simulations	3-2

LIST OF ILLUSTRATIONS (Continued)

<u>Figure</u>	<u>Title</u>	<u>Page</u>
19	Simulated Slit Scan of Echelle Order Along Order Direction	5-2
20	Simulation Profiles in Cross-Order Direction at Bottom Center of Echelle Format	5-4

SECTION 1

INTRODUCTION

The Perkin-Elmer Corporation Optical Technology Division in Danbury, Connecticut has performed a six month scientific study contract for the NASA/Goddard Space Flight Center, Theoretical Astrophysics Branch, Greenbelt, Maryland. (Contract No. NAS 5-23327). The study program consisted of the development of a computerized mathematical model and the production of simulated ultraviolet (UV) spectrograms on film with the aid of the Perkin-Elmer Line Scan Image Generator (LSIG). This model was used as a basis to predict the optical performance of the International Ultraviolet Explorer (IUE) Scientific Instrument which is scheduled for launch in December 1976.

The two questions of major concern in the study program were, first, the effect of the destructive readout process in the SEC vidicon camera on the accuracy of spectroradiometric data in the UV spectrogram (or "echellogram", since it is produced by crossed echelle and concave spherical gratings), and second, the question of the extent of overlap between adjacent echelle orders.

The results of the study indicate that the answer to the first question is that, to the extent that linear modeling accurately represents the imaging system, the errors in wavelength determination and radiometry introduced by destructive readout are not serious, possibly even negligible. The second question has not been completely answered. Order overlap is significant at the bottom of the echelle format where the orders are most closely spaced. Further work in the area of image enhancement, particularly desmearing in the cross-order direction, is suggested.

Section 2 discusses the development of the math model. Section 3 describes the preparation of the input echellogram computer tapes which were linearly interpolated from the NASA-furnished data. Section 4 gives the details of the simulation procedures, Section 5 discusses the results, and gives

recommendations for further work. Section 6 contains a brief summary and lists the major conclusions. Selected computer printouts of the simulation tapes are included in Appendix A, and a derivation of a series expansion formula for evaluating a Hankel integral transform is presented in Appendix B.

Positive film transparencies and photographic prints of the simulated echellograms are furnished in Volume II of this report.

SECTION 2

SYSTEM MATHEMATICAL MODEL

2.1 MODEL SUMMARY AND BLOCK DIAGRAM

A simplified functional block diagram of the International Ultraviolet Explorer (IUE) Scientific Instrument is shown in Figure 1. (A complete description of the Scientific Instrument is given in Reference 1.)

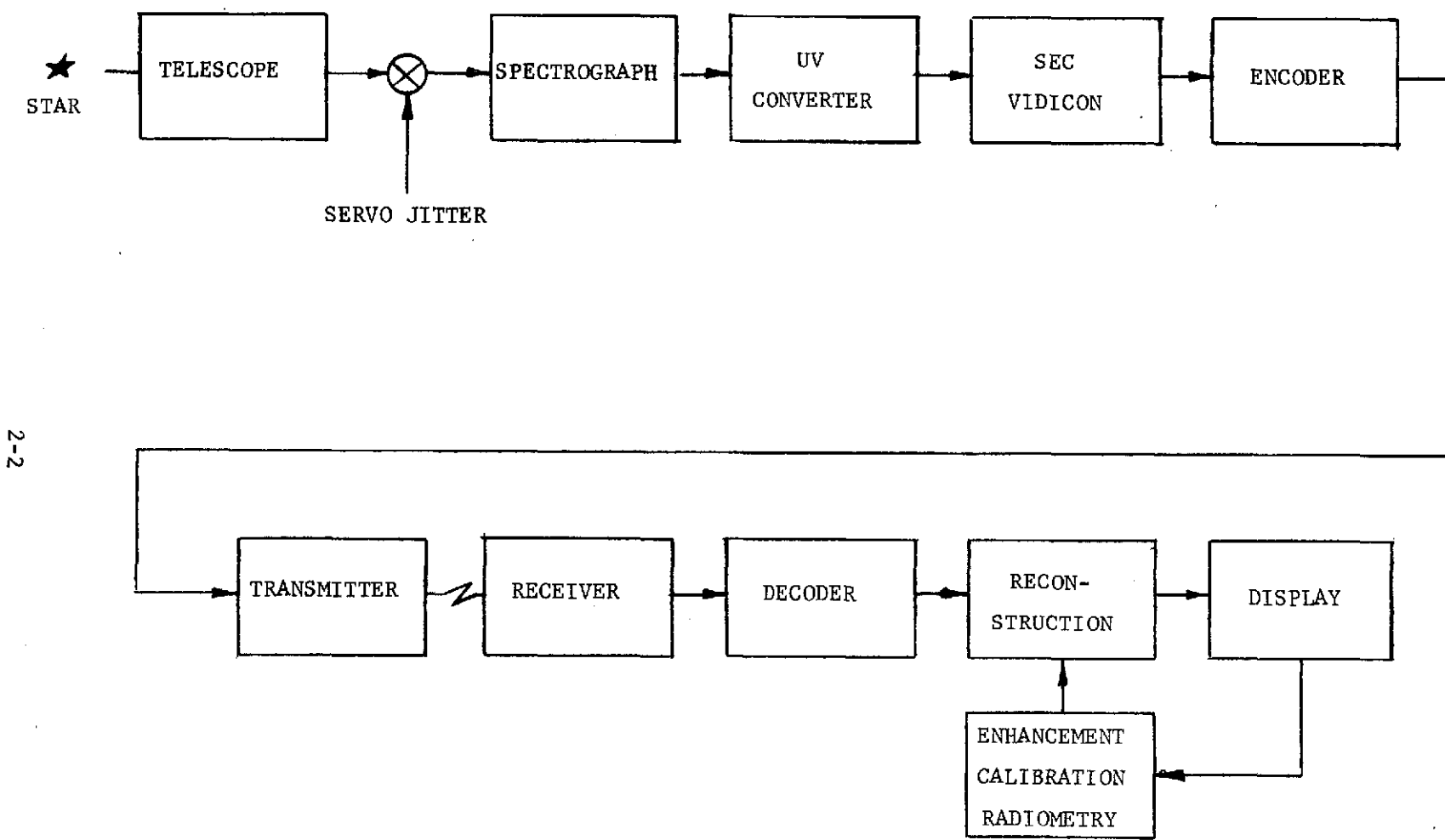
In this study program we have concerned ourselves with analysis of performance degradations of only the imaging portion of the system chain extending from the telescope through the SEC vidicon camera, since effects of noise in the transmission link and reconstruction artifacts are deemed to be minor considerations relative to the questions pertaining to the discharge overlap in the SEC readout process and loss of resolution in the UV converter.

In the following paragraphs a linear analytical model suitable for computer simulation of the imaging chain effects on UV echelle spectra is developed. The destructive readout process is first discussed, and a computer algorithm for generating an "effective" point spread function (PSF) for destructive readout is presented in Paragraph 2.2. This is followed by a discussion of the derivations of the UV converter and guidance (servo jitter) transfer functions in Paragraphs 2.3 and 2.4. The echelle spectrograph is assumed to make a negligible contribution to performance degradations, as discussed in Paragraph 2.5. Cascaded transfer functions and PSF's are presented in Paragraph 2.6, and finally, a discussion of the implementation of the model on the computer is given in Paragraph 2.7. The Perkin-Elmer IBM 370/158 system was used for all the modeling computations.

2.2 DESTRUCTIVE READOUT OF SEC VIDICON

We start with the following basic assumptions concerning the destructive readout process:

- a. The digitally addressed read beam current profile is circular Gaussian (although other profiles may be substituted in the model).



2-2

Figure 1. International Ultraviolet Explorer (IUE) Scientific Instrument Functional Block Diagram

b. The charge removed from a uniformly charged region of the SEC target during a single capacitive discharge read operation is proportional to the integral of the product of the charge density Q times the beam current profile over the spatial extent of the beam. In other words, a single read operation makes a Gaussian-shaped "hole" in the original uniform charge density (see Figure 2-b).

c. Target lag effects are negligible.

The linearity of the analytical model rests on the latter two assumptions.

In the following development, we first expand and generalize the one-dimensional approach outlined in some preliminary calculations done at NASA. Next, we make the important simplifying approximation which neglects the previous read operations more than a few pixels (3-4) removed from the current beam address. This approximation has the very useful result of rendering the readout integral space-invariant, which allows us to use the powerful convolution theorem for Fourier transforms. The next step is a straightforward extension to two dimensions. Finally, the discrete sum approximation to the readout integral is made, which is necessary for computer calculations.

2.2.1 One-Dimensional Readout Model

The following is depicted graphically in Figure 2 for a digitally addressed Gaussian beam profile spaced by its full-width-half-maximum (FWHM) width. The charge readout at the first beam address x_1 is given by

$$M_1 = \int_{-\infty}^{\infty} QG(x-x_1)dx, \quad (2.1)$$

where Q is the (uniform) charge density on the target, and $G(x-x_1)$ is the beam current profile, appropriately normalized, centered at x_1 (Figure 2-a). The charge density remaining at this point is clearly $Q[1-G(x-x_1)]$ (see Figure 2-b), which becomes the input to the next readout at x_2 , namely,

$$M_2 = \int_{-\infty}^{\infty} Q[1-G(x-x_1)]G(x-x_2)dx. \quad (2.2)$$

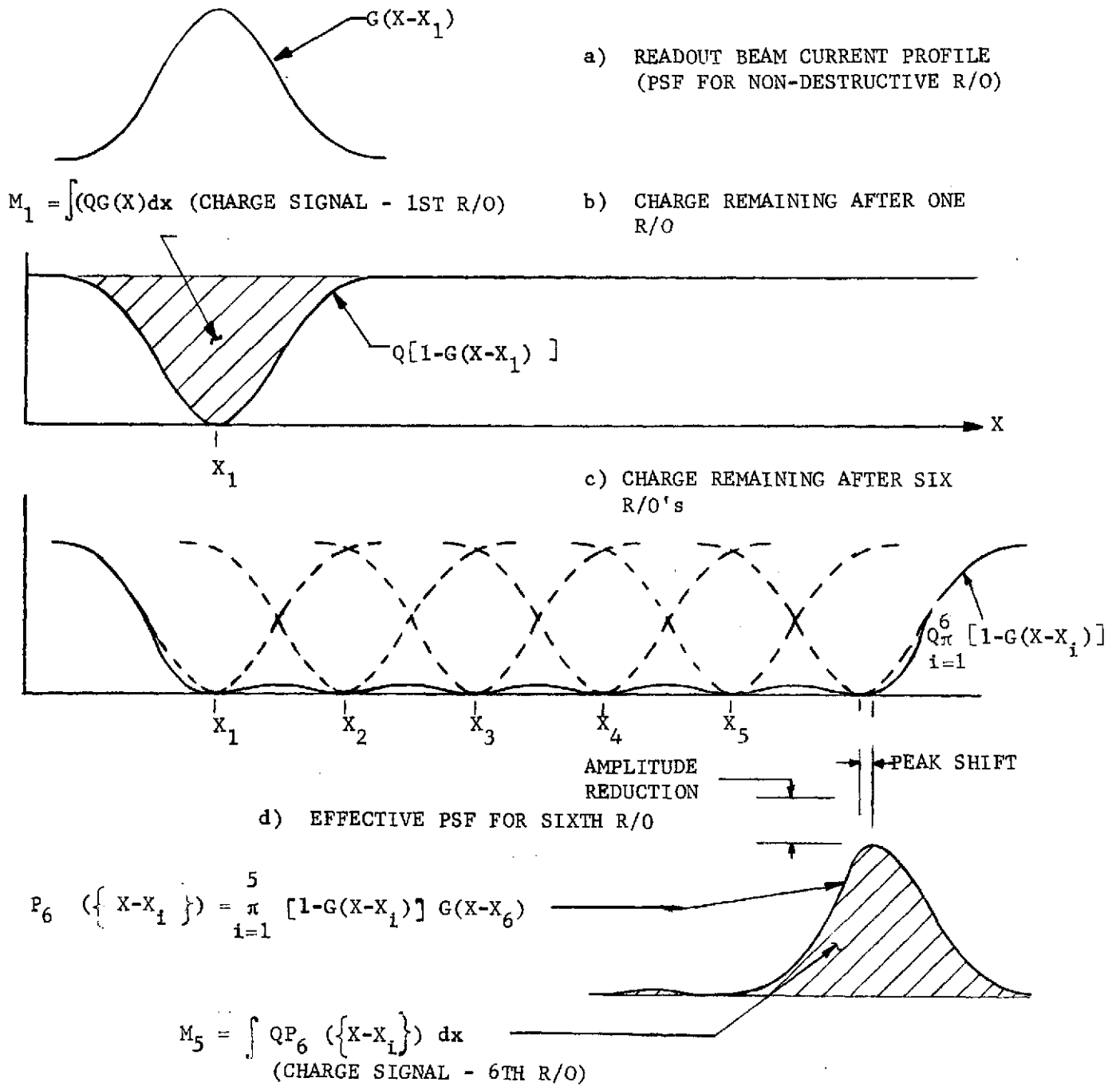


Figure 2. Destructive Readout of Uniformly Charged Target (1-dimensional Model)

Thus, at the k'th beam address, the charge readout is

$$M_k = \int_{-\infty}^{\infty} Q \pi \prod_{i=1}^{k-1} [1-G(x-x_i)] G(x-x_k) dx \quad (2.3)$$

2.2.2 Space-Invariant Approximation - Effective PSF

It should be apparent from the foregoing that, due to the finite extent of the readout beam, the previously read pixels more than a few addresses (3-4) removed from the current address make negligible contributions to the readout integral, Equation (2.3). For example, consider a pixel spacing of 1.5σ , where σ is the standard deviation width of the Gaussian function $G(x) = \exp(-x^2/2\sigma^2)$. The value of G four pixels removed from the current position ($x = 0$ in this example) is $\exp(-18) = 1.5 \times 10^{-8}$, giving $1-G \cong 1$ to one part in 10^8 .

Hence, only the $1-G$ factors corresponding to the nearest two or three previously read pixels need be retained in the readout integral, Equation (2.3).

Thus, we are able to make the following approximation to the readout integral, Equation (2.3):

$$M_k \cong \int_{-\infty}^{\infty} Q \pi \prod_{i=k-m}^{k-1} [1-G(x-x_i)] G(x-x_k) dx, \quad (2.4)$$

where we have dropped all pixel contributions more than m beam addresses removed from the current (k' th) one.

Next, we introduce the analytically convenient notion of an "effective PSF" for destructive readout by associating the product of $(1-G)$ factors with $G(x-x_k)$, the PSF of the current readout, rather than with the charge density Q . This has the computational advantage of allowing the calculation of the destructive readout PSF, or its Fourier transform (a complex optical transfer function [OTF]), independently of the input echellogram represented by the charge distribution Q . Hence, the effective PSF for destructive readout at beam address x_k is defined by (see Figure 2-d):

$$P_k (\{x-x_i\}) = \pi \prod_{i=k-m}^{k-1} [1-G(x-x_i)]G(x-x_k), \quad (2.5)$$

where the braces denote the set of $x-x_i$'s over the range of the products.

If the readout lattice is of uniform spacing, which is the case for the SEC vidicon in the IUE instrument, then the G functions are independent of k , and therefore, since m is a fixed constant, the expression (2.5) is space-invariant.

Finally, we rewrite the approximation (2.5) to the readout integral, using our new definition of effective PSF, and also generalizing to the case of a variable charge density $Q(x)$:

$$M_k \cong \int_{-\infty}^{\infty} Q(x) P_k (\{x-x_i\}) dx, \quad (2.6)$$

where the notation is to be understood from the definition of P in Equation (2.5). This last integral expression exhibits the form of a convolution, which, as we have already noted, is important for the purposes of computation.

2.2.3 Extension to Two Dimensions

The extension of Equations (2.5) and (2.6) to two dimensions is obvious: $Q(x)$ goes over to $Q(x,y)$, and the $(x-x_i)$ go over to $(x-x_i), (y-y_j)$ giving

$$P_{k,l} (\{x-x_i\}, \{y-y_j\}) = \pi \prod_{i,j} [1-G(x-x_i, y-y_j)]G(x-x_k, y-y_l) \quad (2.7)$$

and

$$M_{k,l} \cong \int_{-\infty}^{+\infty} \int Q(x,y) P_{k,l} (\{x-x_i\}, \{y-y_j\}) dx dy \quad (2.8)$$

for the two-dimensional effective PSF and charge readout expressions respectively. Since $G(x,y)$ is circular Gaussian, it may be factored into a product of the corresponding one-dimensional functions, i.e.,

$$G(x,y) = G(x) G(y)$$

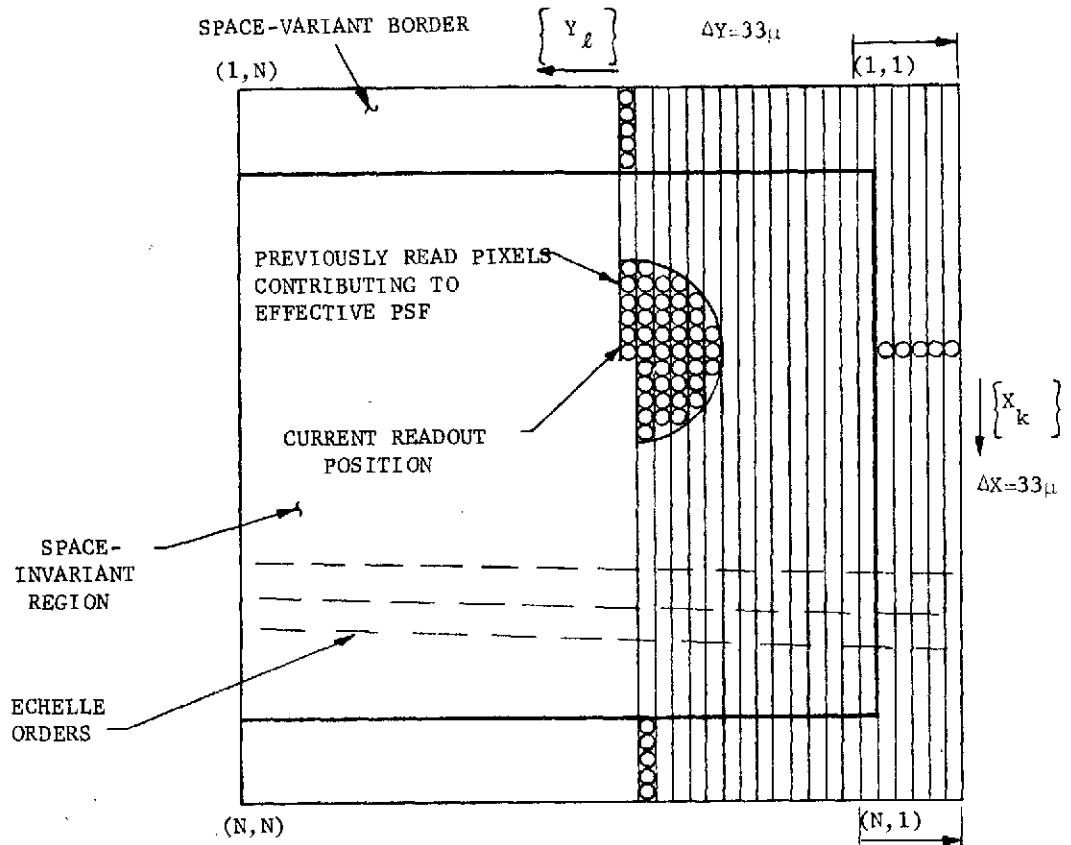
This will be convenient later on in the construction of the effective PSF computer algorithm. Note in Equation (2.7) that we have not specified the ranges of the product indices i, j . These will depend upon the particular sequence of readout beam addressing employed. In the case under study, a two-dimensional square lattice is digitally scanned in raster fashion with pixel spacings specified by NASA to be:

$$\Delta x = \Delta y = 33\mu \quad (2.9)$$

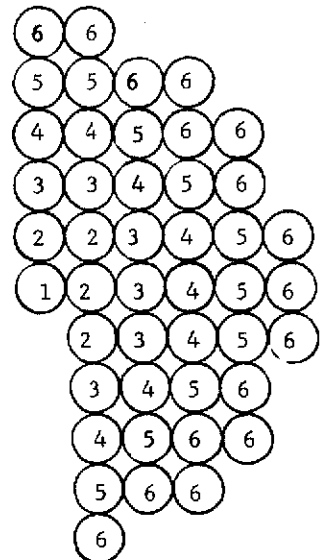
at the camera focal plane. Therefore, the beam addresses (x_k, y_ℓ) are given by

$$\begin{aligned} x_k &= k\Delta x \quad , \quad k = 0, 1, \dots, N-1 \\ y_\ell &= \ell\Delta y \quad , \quad \ell = 0, 1, \dots, N-1 \end{aligned} \quad (2.10)$$

where N is the dimension of the readout lattice. It seems most convenient to indicate the (1-G) factors retained in the product of Equation (2.7) diagrammatically, which we have done in Figure 3. Here we show the previously read pixels in the raster which are within a radius approximately $5\Delta x$ (or $5\Delta y$) of the current readout address (x_k, y_ℓ) . The numbers 1-6 indicate the degree of nearest neighbor, where 1 is the current beam position. This is helpful in keeping track of the (1-G) factors when writing the computer subroutine. The number assignments are somewhat arbitrary, but it does not matter, since the ordering of the factors in the product is immaterial. A border five pixels wide has been indicated in the diagram around three sides of the raster within which the effective PSF is not space-invariant, since (1-G) factors are progressively lost as the edges of the raster are approached (except for the left-hand side where there are no previously read pixels). However, very little information is lost by ignoring the edge regions, since they comprise a very small fraction of the total format. Moreover, the side edges are also where the blaze angle falloff of the spectrograph is greatest, so they are likely to be of little interest.



(a) SEC VIDICON DIGITAL READOUT RASTER



(b) LABELING SEQUENCE OF PREVIOUSLY READ PIXELS

Figure 3. Readout Raster and Pixel Labeling

2.2.4 Computer Algorithm for Destructive Readout

With the aid of the labeling sequence in Figure 3-b, the (1-G) factors may readily be determined and the effective PSF constructed. In the space-invariant region, $P_{k,\ell}$ is independent of the beam address (x_k, y_ℓ) . Hence, we take the current readout position to be (0,0), also setting $k = \ell = 0$. Then, the G functions for the current readout position and previously read neighboring pixels are given by (see Figure 3-b):

Programming Notation †

$G(x)G(y)$	→	GXPOS(1)*GY(1)	current readout position
$G(x+\Delta x)G(y)$	→	GXPOS(2)*GY(1)	} nearest neighbors
$G(x+\Delta x)G(y+\Delta y)$	→	GXPOS(2)*GY(2)	
$G(x)G(y+\Delta y)$	→	GXPOS(1)*GY(2)	
$G(x-\Delta x)G(y+\Delta y)$	→	GXNEG(1)*GY(2)	
$G(x+2\Delta x)G(y)$	→	GXPOS(3)*GY(1)	} second nearest neighbors
$G(x+2\Delta x)G(y+\Delta y)$	→	GXPOS(3)*GY(2)	
⋮		⋮	

where the nearest, second nearest, etc. neighbors have been written in clockwise sequence, starting at the top.

From this table, the zeroth, nearest neighbor, second nearest neighbor, etc. approximations to the effective PSF may be constructed as follows:

Zeroth approximation (equivalent to nondestructive readout):

$$\text{PSF}(1) = C * \text{GXPOS}(1) * \text{GY}(1)$$

Nearest neighbor approximation:

$$\begin{aligned} \text{PSF}(2) = \text{PSF}(1) * (1 - C * \text{GXPOS}(2) * \text{GY}(1)) * (1 - C * \text{GXPOS}(2) * \text{GY}(2)) \\ * (1 - C * \text{GXPOS}(1) * \text{GY}(2)) * (1 - C * \text{GXNEG}(2) * \text{GY}(2)) \end{aligned}$$

Second nearest neighbor approximation:

$$\begin{aligned} \text{PSF}(3) = \text{PSF}(2) * (1 - C * \text{GXPOS}(3) * \text{GY}(1)) * (1 - C * \text{GXPOS}(3) * \text{GY}(2)) \\ * \dots \end{aligned}$$

† The notations GXPOS, GXNEG refer to previously read pixels in the $x > 0$, $x < 0$ half-planes respectively. GY is not so distinguished since all pixels are in the $y < 0$ half-plane.

Note that a parameter C ($0 \leq C \leq 1$) has been introduced which takes account of the possibility of less than 100% target discharge at the center of the readout beam.

The above construction has been carried out to the fifth nearest neighbor approximation for the circular Gaussian case, and programmed as FORTRAN subroutine SECPSF. A listing can be found in Figure 4.

2.2.5 Effective PSF Features

Subroutine SECPSF was used to make perspective plots of the effective PSF on Perkin-Elmer's Calcomp plotter for two ratios of pixel spacing-to-beam sigma width: $\Delta x/\sigma = 1.551$, and 2.35 (FWHM spacing). For comparison, the circular Gaussian (nondestructive R/0) PSF was also plotted. These are shown in Figures 5 to 7. The x- and y-axes have been labelled in units of σ . The view is from the negative x, negative y quadrant. The PSF maxima relative to unit height for the nondestructive case are indicated in the graphs. Corresponding numerical printouts of the nondestructive and destructive readout processing arrays appear in Figures 8 and 9. These arrays are calculated from subroutine SECPSF at points on the computational sampling lattice which is interpolated 2:1 from the readout lattice. (See Section 2.7 for a discussion of the requirement for interpolation.)

The most obvious features to be noticed in the perspective plots are the shift of the PSF maximum relative to the center of the beam, and the two nearest neighbor holes located on the x- and y-axes. The "ripple", or residual charge, between these holes is also visible. The scale of the plots is not large enough to see the effects of the second and higher nearest neighbors; these can be seen in the processing array printouts. PSF profiles for the case $\Delta x/\sigma = 1.551$ at constant x and at constant y are plotted in Figure 10 from the array data in Figure 8.

The shift of the maximum and the ripple effects are most evident for the $\Delta x/\sigma = 1.551$ case, which corresponds to the greatest amount of beam overlap. This value is derived from the NASA-furnished parameter values of

```

SUBROUTINE SECPSF(X,Y,DX,DY,SIG,C,KNEAR,PSF)
DIMENSION PSF(1),GXPOS(6),GXNEG(6),GY(6)
DXX=DX/SIG
DYY=DY/SIG
XX=X/SIG
YY=Y/SIG
IMAX=KNEAR+1
DO 1 I=1,IMAX
XPSHF=XX+(I-1)*DXX
XXPSHF=XPSHF*XPSHF/2.
XNSHF=XX-(I-1)*DXX
XXNSHF=XNSHF*XNSHF/2.
YSHF=YY+(I-1)*DYY
YYSHF=YSHF*YSHF/2.
IF(XXPSHF.GT.25.)XXPSHF=25.
IF(XXNSHF.GT.25.)XXNSHF=25.
IF(YYSHF.GT.25.)YYSHF=25.
IF(XXPSHF.LT.-25.)XXPSHF=-25.
IF(XXNSHF.LT.-25.)XXNSHF=-25.
IF(YYSHF.LT.-25.)YYSHF=-25.
GXPOS(I)=EXP(-XXPSHF)
GXNEG(I)=EXP(-XXNSHF)
1 GY(I)=EXP(-YYSHF)
PSF(1)=C*GXPOS(1)*GY(1)
IF(KNEAR.LE.0)GO TO 2
PSF(2)=PSF(1)*(1.-C*GXPOS(2)*GY(1))*(1.-C*GXPOS(2)*GY(2))*(1.-C*GX
ZPOS(1)*GY(2))*(1.-C*GXNEG(2)*GY(2))
IF(KNEAR.EQ.1)GO TO 2
PSF(3)=PSF(2)*(1.-C*GXPOS(3)*GY(1))*(1.-C*GXPOS(3)*GY(2))*(1.-C*GX
ZPOS(2)*GY(3))
Z*(1.-C*GXPOS(1)*GY(3))*(1.-C*GXNEG(2)*GY(3))*(1.-C*GXNEG(3)*GY(2))
IF(KNEAR.EQ.2)GO TO 2
PSF(4)=PSF(3)*(1.-C*GXPOS(4)*GY(1))*(1.-C*GXPOS(4)*GY(2))*(1.-C*GX
ZPOS(3)*GY(3))*(1.-C*GXPOS(2)*GY(4))
Z*(1.-C*GXPOS(1)*GY(4))*(1.-C*GXNEG(2)*GY(4))*(1.-C*GXNEG(3)*GY(3))
Z*(1.-C*GXNEG(4)*GY(2))
IF(KNEAR.EQ.3)GO TO 2
PSF(5)=PSF(4)*(1.-C*GXPOS(5)*GY(1))*(1.-C*GXPOS(5)*GY(2))*(1.-C*GX
ZPOS(4)*GY(3))*(1.-C*GXPOS(3)*GY(4))
Z*(1.-C*GXPOS(2)*GY(5))*(1.-C*GXPOS(1)*GY(5))*(1.-C*GXNEG(2)*GY(
Z5))*(1.-C*GXNEG(3)*GY(4))
Z*(1.-C*GXNEG(4)*GY(3))*(1.-C*GXNEG(5)*GY(2))
IF(KNEAR.EQ.4)GO TO 2
PSF(6)=PSF(5)*(1.-C*GXPOS(6)*GY(1))*(1.-C*GXPOS(6)*GY(2))*(1.-C*GX
ZPOS(5)*GY(3))*(1.-C*GXPOS(5)*GY(4))*(1.-C*GXPOS(4)*GY(4))
Z*(1.-C*GXPOS(4)*GY(5))*(1.-C*GXPOS(3)*GY(5))*(1.-C*GXPOS(2)*GY(
Z6))*(1.-C*GXPOS(1)*GY(6))
Z*(1.-C*GXNEG(2)*GY(6))*(1.-C*GXNEG(3)*GY(5))*(1.-C*GXNEG(4)*GY(5))
Z*(1.-C*GXNEG(4)*GY(4))
Z*(1.-C*GXNEG(5)*GY(4))*(1.-C*GXNEG(5)*GY(3))*(1.-C*GXNEG(6)*GY(2))
2 RETURN
END

```

14:31:16

Figure 4. Computer Subroutine for Destructive
R/O of SEC Vidicon

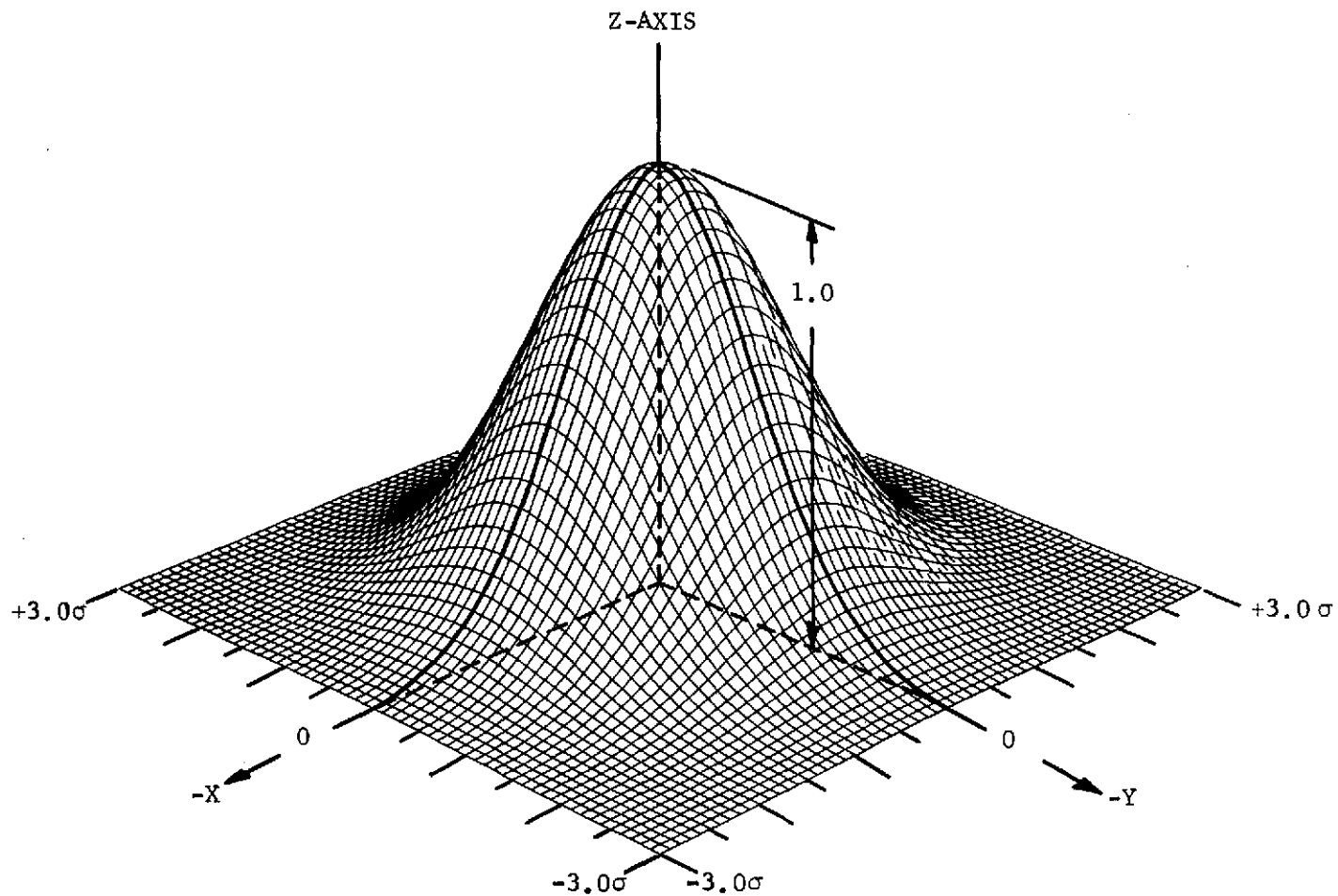


Figure 5. Gaussian Beam Current Distribution
(PSF For Non-Destructive R/O)

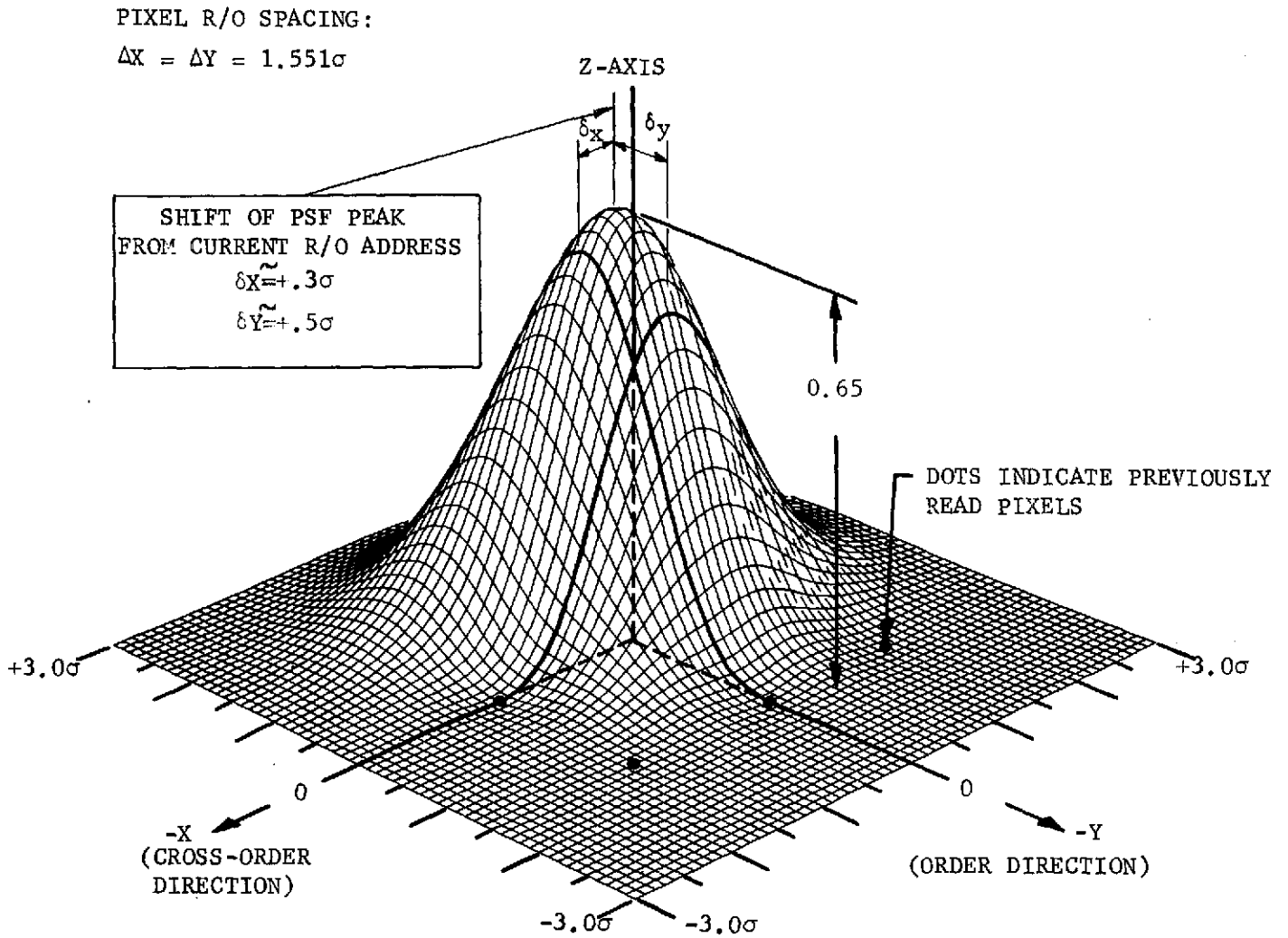


Figure 6. Effective PSF For SEC Vidicon Destructive R/O (100 Percent Discharge)

PIXEL R/O SPACING:

$$\Delta X = \Delta Y = 2.35\sigma$$

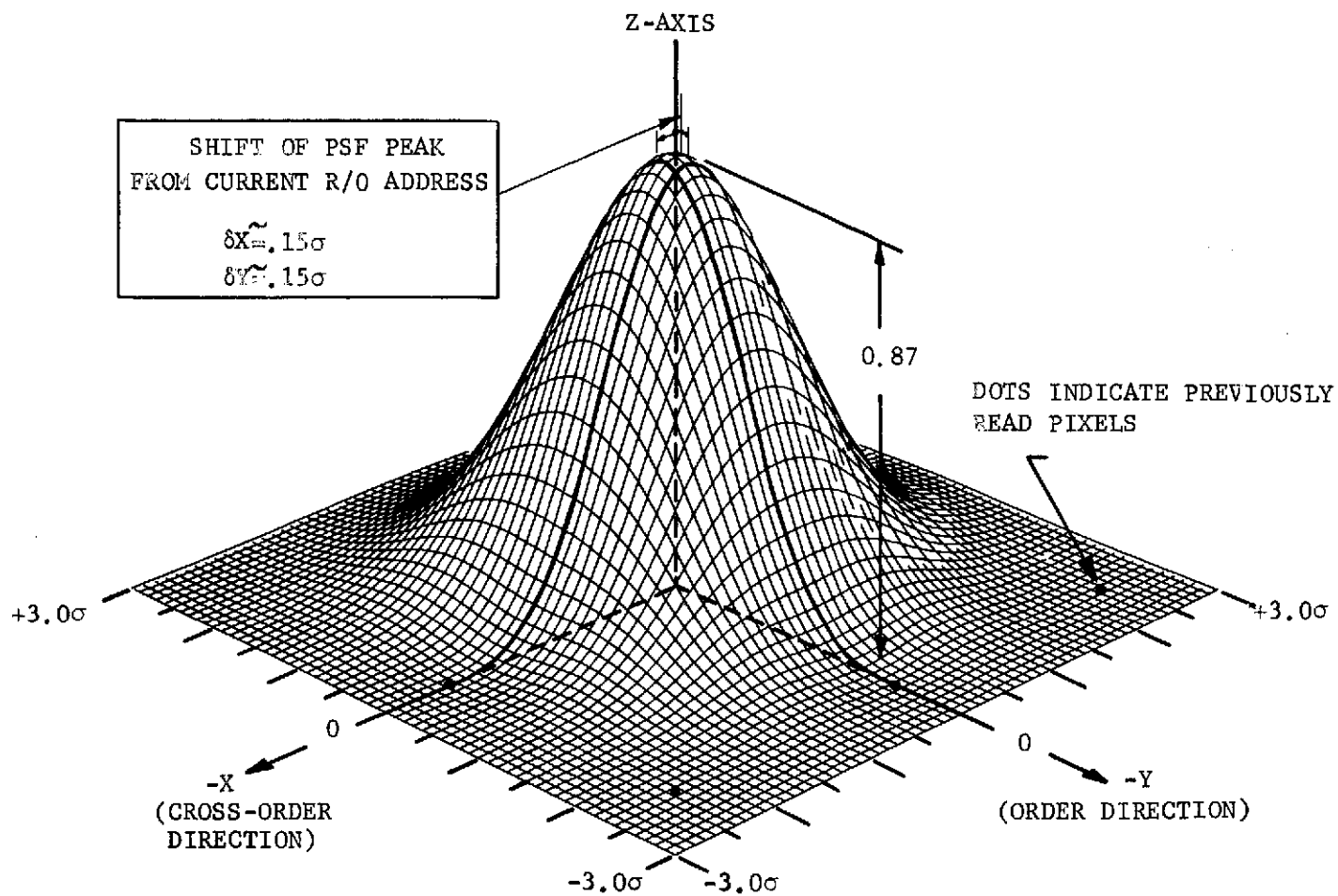


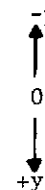
Figure 7. Effective PSF for SEC Vidicon Destructive R/O
(100 Percent Discharge)

SECPSF2D TEST

DX= 16.500000 DY= 16.500000 XMIN= -99.000000 XMAX= 99.000000 YMIN= -99.000000 YMAX= 99.000000
 DISCH FRACTION= 1.000000 DXSEC= 33.000000 DYSEC= 33.000000 SIG= 21.276993

DROPSF(P(6))

				-x ←	0	→ +x								
0.0	0.0000	0.0	0.0000	0.0	0.0000	0.0	0.0000	0.0	0.0000	0.0	0.0000	0.0	0.0000	0.0
0.0000	0.0000	0.0000	0.0000	0.0000	0.0000	0.0000	0.0000	0.0000	0.0000	0.0000	0.0000	0.0000	0.0000	0.0000
0.0	0.0000	0.0	0.0000	0.0	0.0001	0.0	0.0001	0.0	0.0000	0.0	0.0000	0.0	0.0000	0.0
0.0000	0.0000	0.0000	0.0001	0.0004	0.0014	0.0014	0.0015	0.0004	0.0001	0.0000	0.0000	0.0000	0.0000	0.0000
0.0	0.0000	0.0	0.0004	0.0	0.0057	0.0	0.0073	0.0	0.0007	0.0	0.0000	0.0	0.0000	0.0
0.0000	0.0000	0.0001	0.0016	0.0062	0.0388	0.0794	0.0859	0.0307	0.0082	0.0008	0.0001	0.0000	0.0000	0.0000
0.0	0.0000	0.0	0.0024	0.0	0.1027	0.3946	0.3956	0.1694	0.0382	0.0046	0.0003	0.0000	0.0000	0.0000
0.0000	0.0001	0.0008	0.0086	0.0399	0.2106	0.5118	0.4659	0.1977	0.0442	0.0054	0.0004	0.0000	0.0000	0.0000
0.0000	0.0001	0.0014	0.0117	0.0565	0.1672	0.2690	0.2150	0.0888	0.0198	0.0024	0.0002	0.0000	0.0000	0.0000
0.0000	0.0000	0.0005	0.0040	0.0183	0.0467	0.0654	0.0492	0.0200	0.0045	0.0005	0.0000	0.0000	0.0000	0.0000
0.0000	0.0000	0.0001	0.0005	0.0024	0.0060	0.0081	0.0060	0.0024	0.0005	0.0001	0.0000	0.0000	0.0000	0.0000
0.0000	0.0000	0.0000	0.0000	0.0002	0.0004	0.0005	0.0004	0.0002	0.0000	0.0000	0.0000	0.0000	0.0000	0.0000
0.0000	0.0000	0.0000	0.0000	0.0000	0.0000	0.0000	0.0000	0.0000	0.0000	0.0000	0.0000	0.0000	0.0000	0.0000



NDROPSF(P(1))

0.0000	0.0000	0.0000	0.0000	0.0000	0.0000	0.0000	0.0000	0.0000	0.0000	0.0000	0.0000	0.0000	0.0000	0.0000
0.0000	0.0000	0.0000	0.0000	0.0002	0.0004	0.0005	0.0004	0.0002	0.0000	0.0000	0.0000	0.0000	0.0000	0.0000
0.0000	0.0000	0.0001	0.0005	0.0024	0.0060	0.0081	0.0060	0.0024	0.0005	0.0001	0.0000	0.0000	0.0000	0.0000
0.0000	0.0000	0.0005	0.0045	0.0201	0.0494	0.0668	0.0494	0.0201	0.0045	0.0005	0.0000	0.0000	0.0000	0.0000
0.0000	0.0002	0.0024	0.0201	0.0902	0.2224	0.3004	0.2224	0.0902	0.0201	0.0024	0.0002	0.0000	0.0000	0.0000
0.0000	0.0004	0.0060	0.0494	0.2224	0.5481	0.7403	0.5481	0.2224	0.0494	0.0060	0.0004	0.0000	0.0000	0.0000
0.0000	0.0005	0.0081	0.0668	0.3004	0.7403	1.0000	0.7403	0.3004	0.0668	0.0081	0.0005	0.0000	0.0000	0.0000
0.0000	0.0004	0.0060	0.0494	0.2224	0.5481	0.7403	0.5481	0.2224	0.0494	0.0060	0.0004	0.0000	0.0000	0.0000
0.0000	0.0002	0.0024	0.0201	0.0902	0.2224	0.3004	0.2224	0.0902	0.0201	0.0024	0.0002	0.0000	0.0000	0.0000
0.0000	0.0000	0.0005	0.0045	0.0201	0.0494	0.0668	0.0494	0.0201	0.0045	0.0005	0.0000	0.0000	0.0000	0.0000
0.0000	0.0000	0.0001	0.0005	0.0024	0.0060	0.0081	0.0060	0.0024	0.0005	0.0001	0.0000	0.0000	0.0000	0.0000
0.0000	0.0000	0.0000	0.0000	0.0002	0.0004	0.0005	0.0004	0.0002	0.0000	0.0000	0.0000	0.0000	0.0000	0.0000
0.0000	0.0000	0.0000	0.0000	0.0000	0.0000	0.0000	0.0000	0.0000	0.0000	0.0000	0.0000	0.0000	0.0000	0.0000

2-15

Figure 8. Processing Spot for 100% Discharge $\Delta X = \Delta Y = 1.551\sigma$

1

SECPSF2D TEST

DX= 16.500000 DY= 16.500000 XMIN= -99.000000 XMAX= 99.000000 YMIN= -99.000000 YMAX= 99.000000
DISCH FRACTION= 1.000000 DXSEC= 33.000000 DYSEC= 33.000000 SIG= 14.042548

DROPSF(P(6))

				-x ←	0	→ +x							
0.0	0.0000	0.0	0.0000	0.0	0.0000	0.0	0.0000	0.0	0.0000	0.0	0.0000	0.0	0.0000
0.0000	0.0000	0.0000	0.0000	0.0000	0.0000	0.0000	0.0000	0.0000	0.0000	0.0000	0.0000	0.0000	0.0000
0.0	0.0000	0.0	0.0000	0.0	0.0000	0.0	0.0000	0.0	0.0000	0.0	0.0000	0.0	0.0000
0.0000	0.0000	0.0000	0.0000	0.0000	0.0003	0.0004	0.0003	0.0000	0.0000	0.0000	0.0000	0.0000	0.0000
0.0	0.0000	0.0	0.0000	0.0	0.0071	0.0	0.0074	0.0	0.0000	0.0	0.0000	0.0	0.0000
0.0000	0.0000	0.0000	0.0003	0.0071	0.1049	0.2265	0.1402	0.0148	0.0006	0.0000	0.0000	0.0000	0.0000
0.0	0.0000	0.0	0.0005	0.0	0.2339	0.8705	0.4691	0.0587	0.0019	0.0000	0.0000	0.0000	0.0000
0.0000	0.0000	0.0000	0.0006	0.0153	0.1876	0.4844	0.2507	0.0316	0.0010	0.0000	0.0000	0.0000	0.0000
0.0000	0.0000	0.0000	0.0001	0.0037	0.0307	0.0630	0.0317	0.0040	0.0001	0.0000	0.0000	0.0000	0.0000
0.0000	0.0000	0.0000	0.0000	0.0001	0.0010	0.0020	0.0010	0.0001	0.0000	0.0000	0.0000	0.0000	0.0000
0.0000	0.0000	0.0000	0.0000	0.0000	0.0000	0.0000	0.0000	0.0000	0.0000	0.0000	0.0000	0.0000	0.0000
0.0000	0.0000	0.0000	0.0000	0.0000	0.0000	0.0000	0.0000	0.0000	0.0000	0.0000	0.0000	0.0000	0.0000
0.0000	0.0000	0.0000	0.0000	0.0000	0.0000	0.0000	0.0000	0.0000	0.0000	0.0000	0.0000	0.0000	0.0000

-y ↑
0
↓ +y

NDROPSF(P(1))

0.0000	0.0000	0.0000	0.0000	0.0000	0.0000	0.0000	0.0000	0.0000	0.0000	0.0000	0.0000	0.0000	0.0000
0.0000	0.0000	0.0000	0.0000	0.0000	0.0000	0.0000	0.0000	0.0000	0.0000	0.0000	0.0000	0.0000	0.0000
0.0000	0.0000	0.0000	0.0000	0.0000	0.0000	0.0000	0.0000	0.0000	0.0000	0.0000	0.0000	0.0000	0.0000
0.0000	0.0000	0.0000	0.0001	0.0001	0.0010	0.0020	0.0010	0.0001	0.0000	0.0000	0.0000	0.0000	0.0000
0.0000	0.0000	0.0000	0.0001	0.0040	0.0317	0.0632	0.0317	0.0040	0.0001	0.0000	0.0000	0.0000	0.0000
0.0000	0.0000	0.0000	0.0010	0.0317	0.2514	0.5014	0.2514	0.0317	0.0010	0.0000	0.0000	0.0000	0.0000
0.0000	0.0000	0.0000	0.0020	0.0632	0.5014	1.0000	0.5014	0.0632	0.0020	0.0000	0.0000	0.0000	0.0000
0.0000	0.0000	0.0000	0.0010	0.0317	0.2514	0.5014	0.2514	0.0317	0.0010	0.0000	0.0000	0.0000	0.0000
0.0000	0.0000	0.0000	0.0001	0.0040	0.0317	0.0632	0.0317	0.0040	0.0001	0.0000	0.0000	0.0000	0.0000
0.0000	0.0000	0.0000	0.0000	0.0001	0.0010	0.0020	0.0010	0.0001	0.0000	0.0000	0.0000	0.0000	0.0000
0.0000	0.0000	0.0000	0.0000	0.0000	0.0000	0.0000	0.0000	0.0000	0.0000	0.0000	0.0000	0.0000	0.0000
0.0000	0.0000	0.0000	0.0000	0.0000	0.0000	0.0000	0.0000	0.0000	0.0000	0.0000	0.0000	0.0000	0.0000
0.0000	0.0000	0.0000	0.0000	0.0000	0.0000	0.0000	0.0000	0.0000	0.0000	0.0000	0.0000	0.0000	0.0000

2-16

09:09:13

Figure 9. Processing Spot for 100% Discharge $\Delta X = \Delta Y = 2.35\sigma$

ER-267

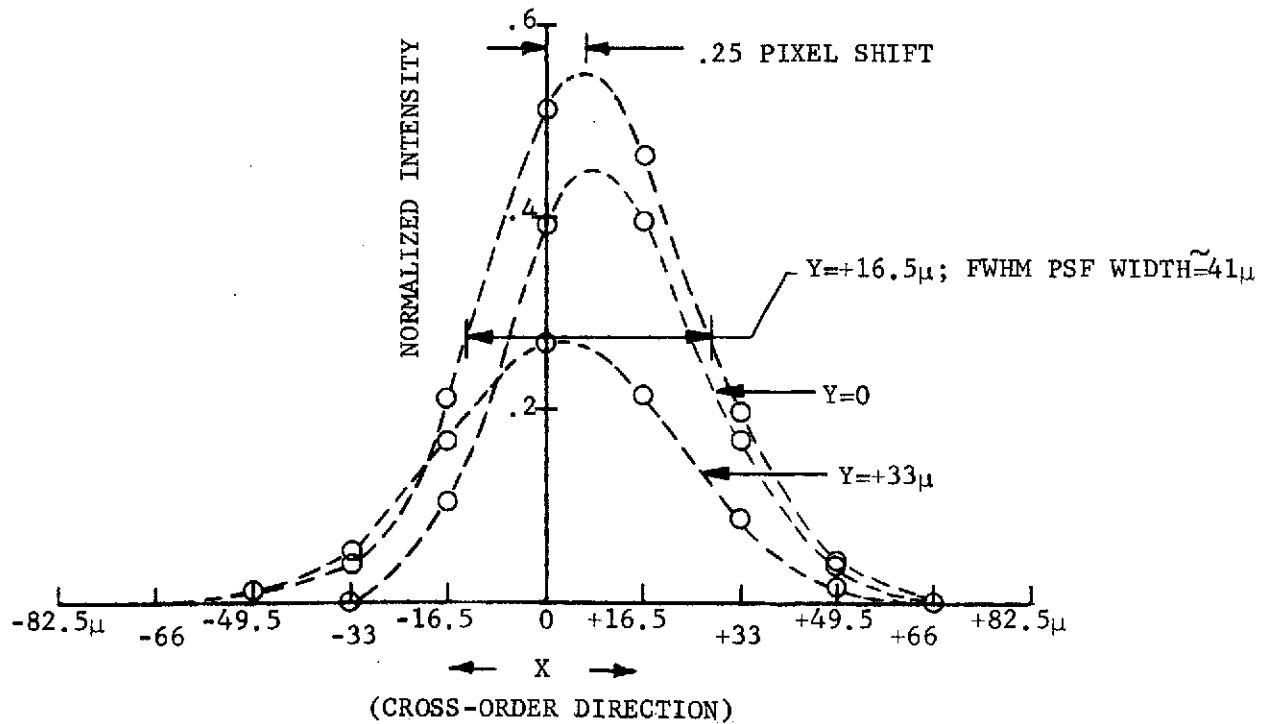
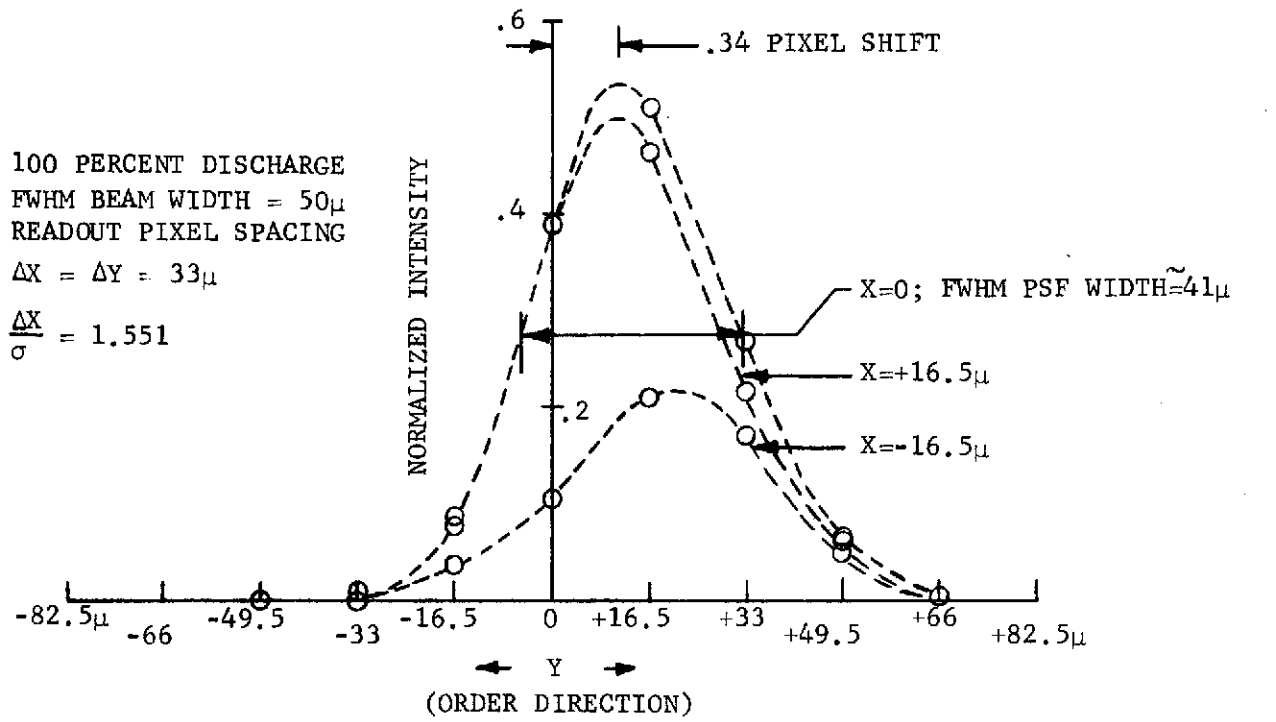


Figure 10. X - and Y - Profiles of Effective PSF

$\Delta x = 33\mu$ and FWHM beam width of 50μ ($\approx 2.35\sigma$), and is the value used for the first two destructive readout simulations performed in this study. From Figure 10 it can be seen that the shift of the peak is about 0.25 pixel in the +x direction and about 0.34 pixel in the +y direction. The y shift (along the order direction) would lead to an error of about 0.019\AA in wavelength determination, which would appear to be inconsequential, since it is about 1/5 the wavelength resolution requirement.

The relative amount of charge readout from a uniformly charged target in a single destructive read compared to a nondestructive read may be calculated from the ratio of the integral Equation (2.7) of the effective PSF for

destructive readout $\iint_{-\infty}^{\infty} P(\{x-x_1\}, \{y-y_1\}) dx dy$ to the integral of the non-destructive readout PSF $\iint_{-\infty}^{\infty} G(x,y) dx dy$.

This ratio can be approximated by the ratio of the sums of the respective PSF array elements in Figures 8 and 9. For 90% and 100% discharge and $\Delta x/\sigma = 1.551$, the ratios are 0.411 and 0.377 respectively.

It was belatedly realized that the ratio $\Delta x/\sigma = 1.551$ is in error, since the FWHM width of 50μ , which was given to us as a "measured beam width", should be interpreted as the effective PSF width in the context of our math model, not the readout beam width. (The measurement consisted of scanning across a very narrow line target, of the order of 5-10 μ in width, which gives the one-dimensional effective PSF.) The above value of $\Delta x/\sigma$ leads to an effective PSF FWHM width of approximately 41μ , about 20 % too narrow, as can be seen from the PSF profiles in Figure 10.

The correct value of beam width was found by computing PSF arrays, varying the beam width parameter. The results show that a FWHM readout beam width of 70.5μ yields an effective PSF FWHM width of approximately 50μ . The corresponding PSF profiles are shown in Figure 11. Note that the widths are different in the two directions, being wider in the x-direction, which can be explained by the fewer previous reads in the negative x half-plane than in the negative y half-plane (see Figure 3).

100 PERCENT DISCHARGE
 FWHM Beam Width = 70.5μ

$\Delta X = \Delta Y = 33\mu$

$\frac{\Delta X}{\sigma} = 1.10$

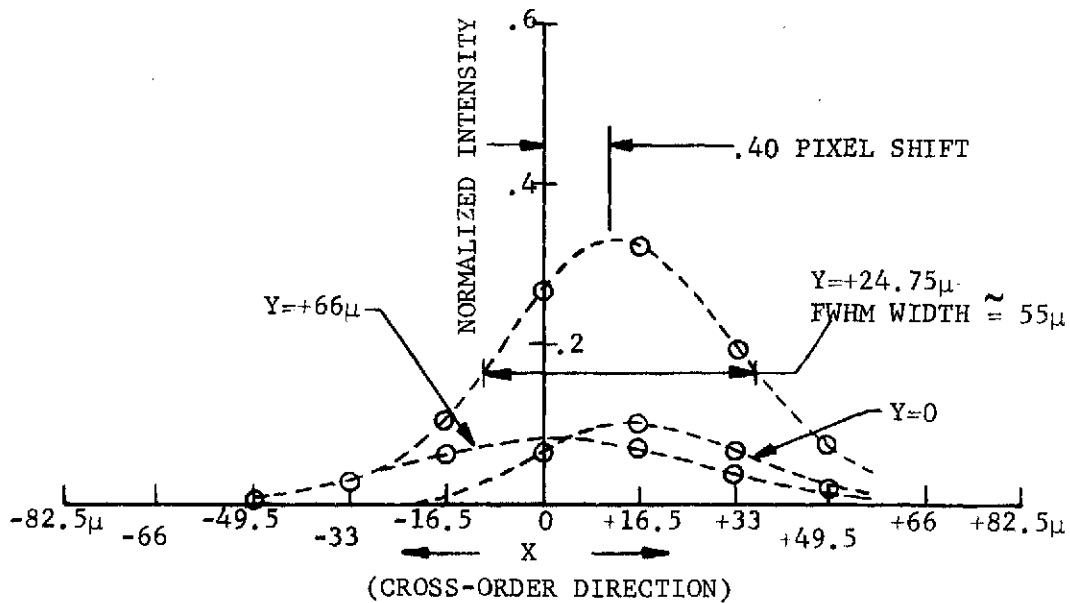
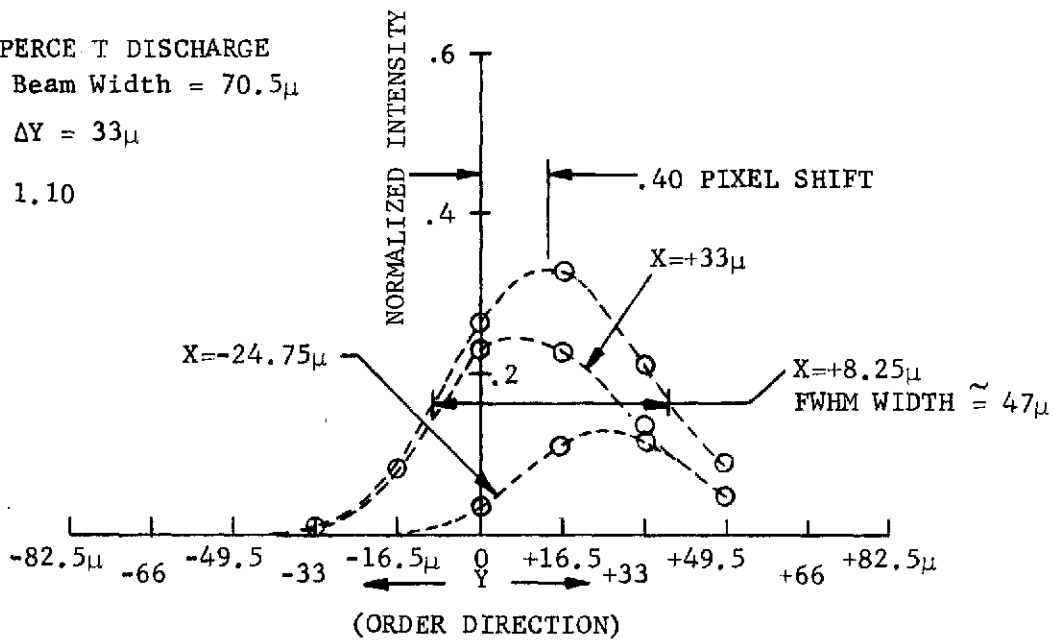


Figure 11. X - And Y - Profiles Of Effective PSF

The peak shift of 0.4 pixel in both directions is somewhat greater and the peak amplitude lower than in the previous case because of the increased discharge overlap. This PSF was used to rerun the destructive readout simulation at $\lambda = 2000\text{\AA}$.

At the request of NASA, a simulation was also done for an effective readout PSF width of 100μ . (This actually prompted the reexamination of the proper definition of PSF width discussed in the preceding.) The profiles for this width (in the x-direction) are illustrated in Figure 12. The width asymmetry, peak shift and reduction in peak amplitude are even more pronounced. Most of the increased width is in the order direction, which may lead to slightly reduced resolution within an order. This would be most noticeable at $\lambda = 1216\text{\AA}$ where the UV converter performance is best. The increased spread in the cross-order direction is not enough to significantly increase the order overlap, or, indeed, alter the results of the simulations with the 41μ width. This is borne out by the simulation results (see Section 5.). Again, the shift is mostly in the cross-order direction which does not affect the accuracy of wavelength determination.

2.3 UV CONVERTER

2.3.1 Introduction

The NASA-furnished converter data was provided in the form of a square wave response (SQR) measurements at four wavelengths: $\lambda = 1216\text{\AA}$, 1608\AA , 2000\AA and 2500\AA . Sine wave response (SWR), or MTF, which is necessary for the performance calculations, was not directly given but was contained in the "Detector MTF" data of Data Sheet 1 of Reference 2, which consists of the cascaded converter and SEC vidicon MTF's. Since the latter had been computed assuming nondestructive readout of the SEC target, it was necessary to redo the detector MTF calculations.

The calculation of the converter MTF was accomplished in several steps:

- a. Conversion of SQR to SWR via the Coltman formula (Reference 3).
- b. Fitting the resulting SWR curves to an empirical formula

90 PERCENT DISCHARGE

FWHM BEAM WIDTH = 112.8μ

$\Delta X = \Delta Y = 33\mu$

$\frac{\Delta X}{\sigma} = .6875$

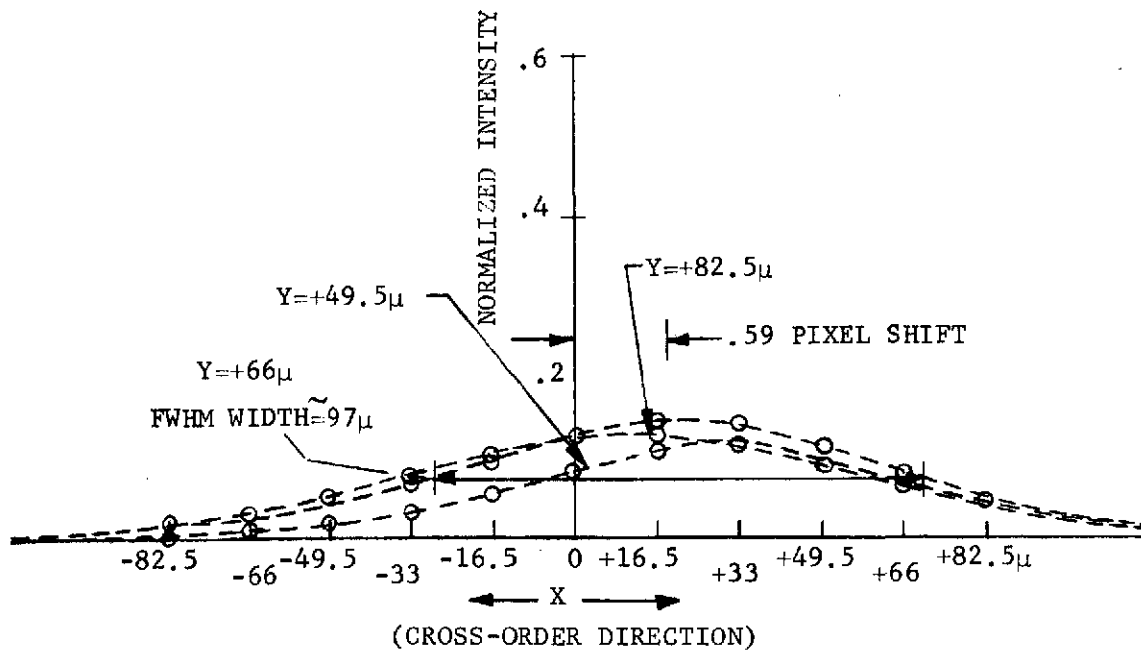
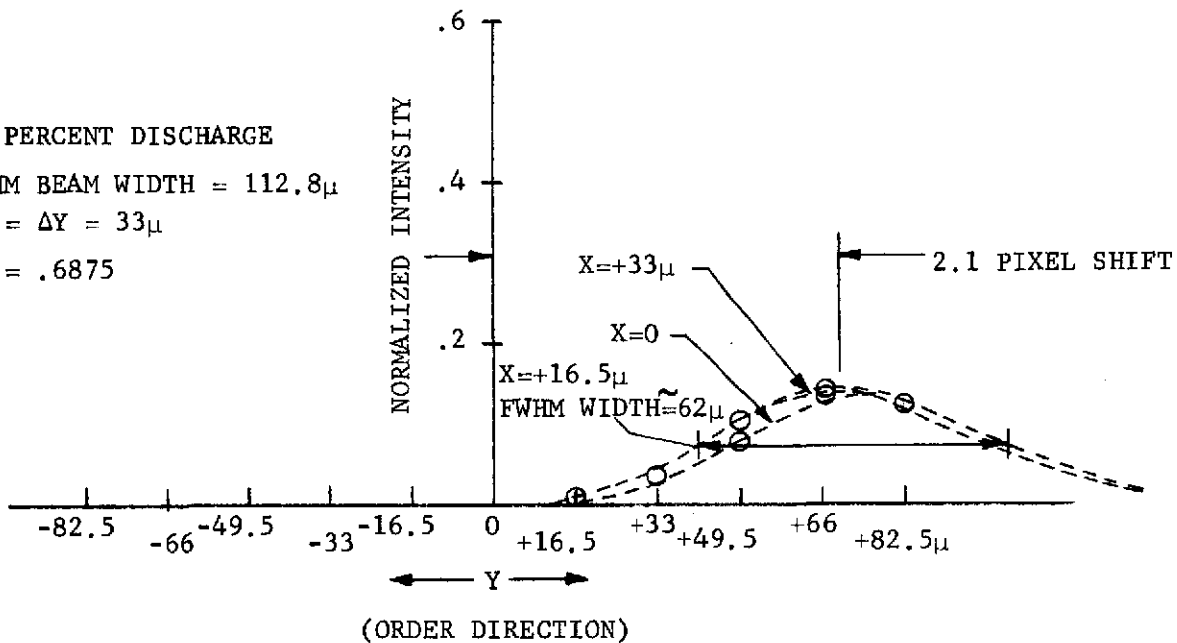


Figure 12. X - And Y - Profiles Of Effective PSF

$$M(s) = \exp [-(s/s_c)^n] \quad (2.11)$$

which has been shown by Johnson (Reference 4) to represent the MTF's of a wide variety of optical and electro-optical imaging devices by suitable choice of the "MTF index" n and "frequency constant" s_c , and

c. Re-inverting the best fitting "Johnson-formula" MTF curves back to SQR as a comparison check with the original SQR data.

2.3.2 MTF Derivation from Square Wave Response Data

The NASA-furnished SQR curves for the UV converter at the four wavelengths of interest are shown in Figure 13. The dotted portions are extrapolations for the purpose of calculating SWR's via the Coltman formula, which is given by

$$M(s) = \frac{\pi}{4} \left[N(s) + N(3s)/3 - N(5s)/5 + N(7s)/7 + N(11s)/11 - N(13s)/13 - N(15s)/15 - N(17s)/17 + N(19s)/19 \dots \right] \quad (2.12)$$

where M is the SWR at spatial frequency s , and N is the SQR. At low spatial frequencies, the higher square wave harmonics contribute more than at high frequencies - hence the need for extrapolation of the SQR data. The SWR's thus calculated are shown in Figure 14. (These are the "best fitting" curves to the Johnson formula; the corresponding modulation indices and frequency constants are also noted in the figure.)

2.3.3 Best Fit to Johnson Formula

The calculated SWR curves were plotted on log-log paper as $-\ln M(s)$ versus s . Equation (2.11) thus plotted appears as a straight line. The intercept $-\ln M=0$ yields the frequency constant s_c , the $1/e$ point on the SWR curve, while the slope is proportional to the modulation index n . "Best fitting" (in the sense of matching by eye) straight lines were superimposed on the data and s_c and n determined in the above manner.

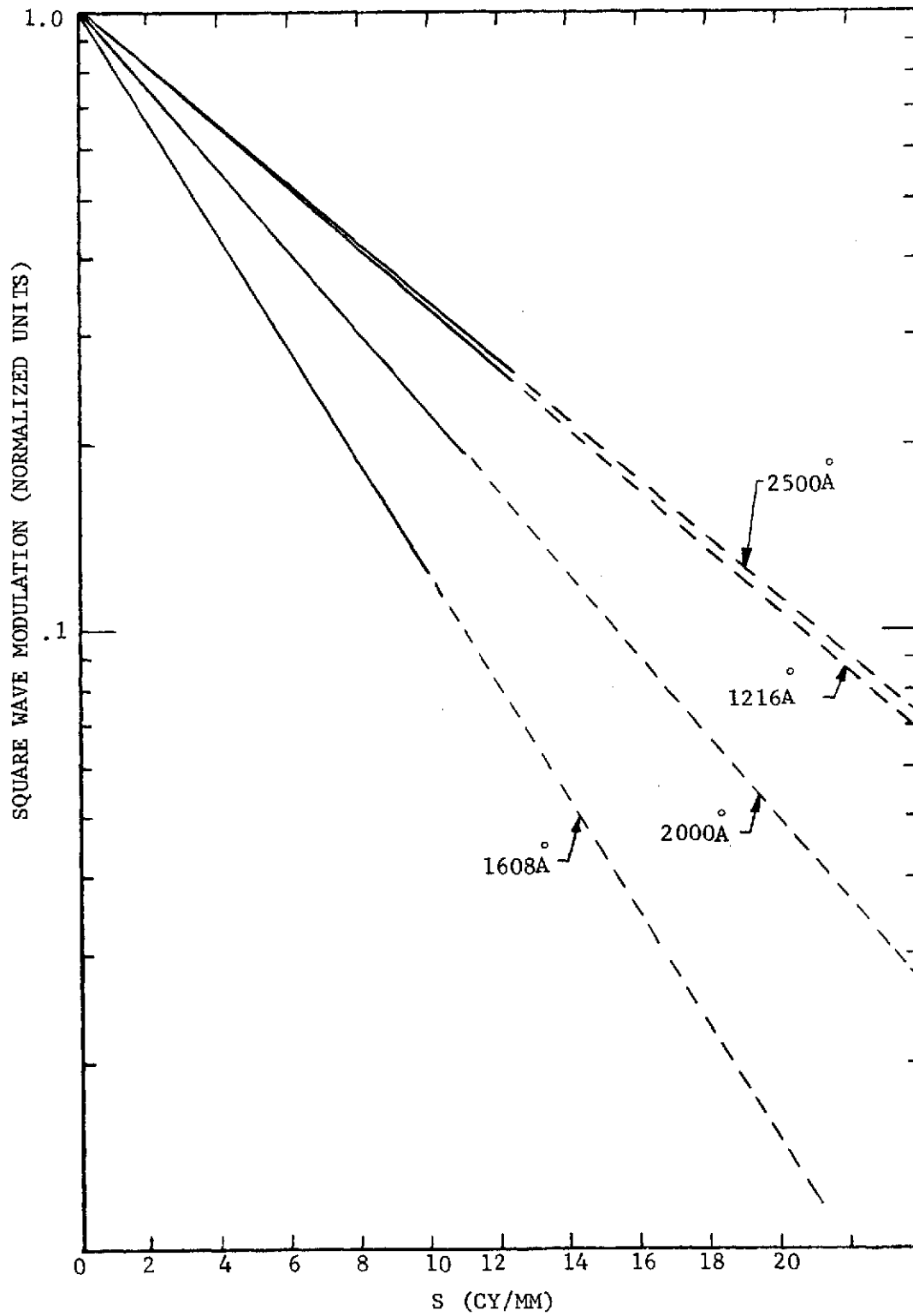


Figure 13. Square Wave Response of Proximity Focussed Converters
Average of Bendix Tubes #401, 402, 403-25, 407X

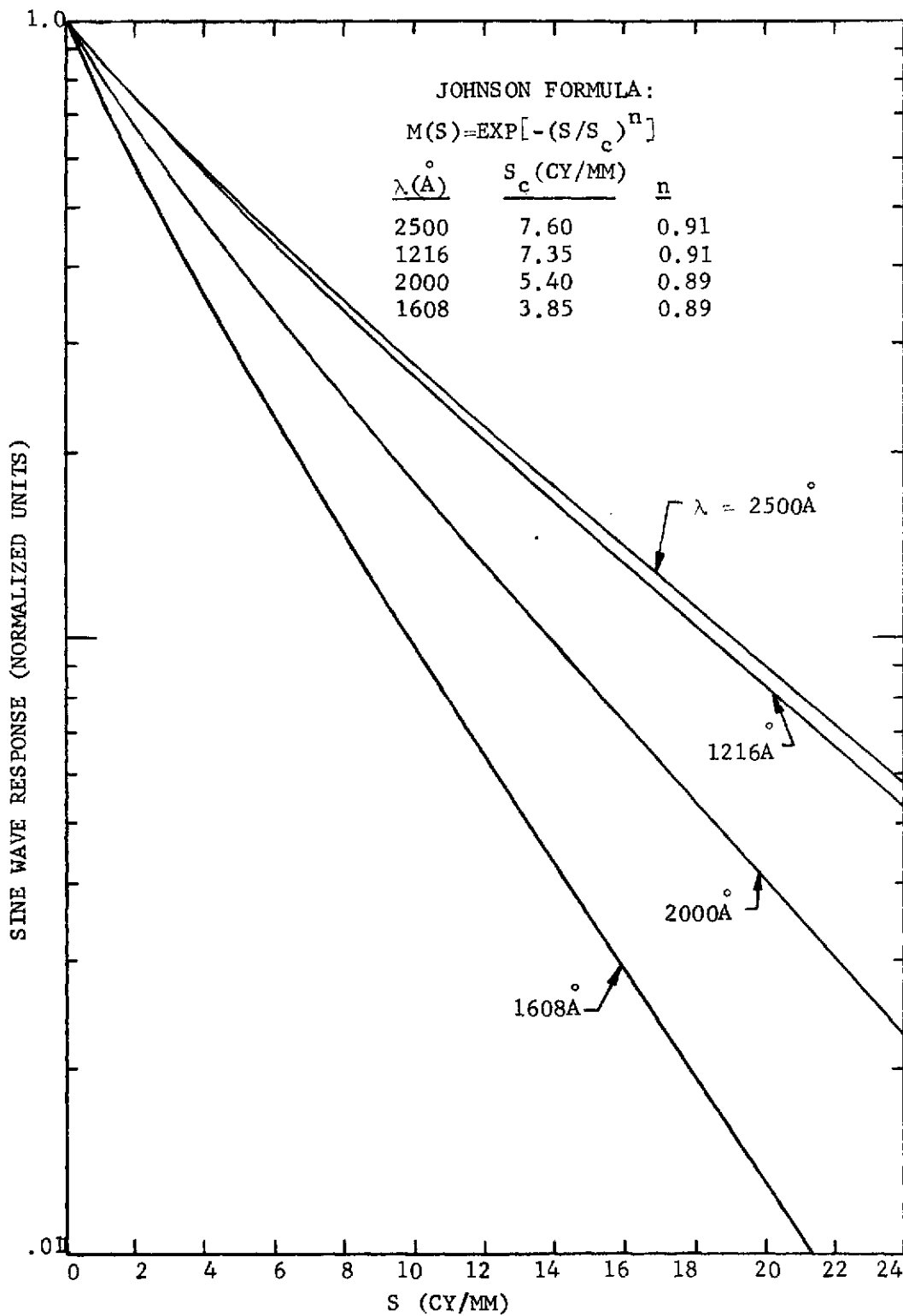


Figure 14. Sine Wave Response of Proximity Focussed UV Converter (Calculated from Square Wave Response Data and Fitted to Johnson Formula)

2.3.4 Re-Inversion to SQR - Comparison with Original Data

The "best fitting" Johnson formula representations of the SWR data shown in Figure 14 were re-inverted to SQR data using the familiar sine wave expansion of a square wave:

$$N(s) = \frac{4}{\pi} \left[M(s) - M(3s)/3 + M(5s)/5 - M(7s)/7 + \dots \right] \quad (2.13)$$

and compared with the original SQR data of Figure 13. Agreement was within 1% over the unextrapolated frequency range.

2.4 GUIDANCE PSF

2.4.1 NASA-Furnished Specification of Truncated Gaussian Servo Jitter PSF

The guidance PSF arising from a stellar point source smeared by servo jitter has been specified by NASA to be circular Gaussian with $\sigma = 0.5 \widehat{\text{sec}}$. This is truncated at the entrance aperture of the spectrograph. The circular aperture of radius $r_0 = 1.5 \widehat{\text{sec}}$ was chosen for study.

At the camera focal plane, the above parameters become $\sigma = 70.7\mu$ and $r_0 = 212.1\mu$.

2.4.2 MTF Derivation

Bogges (Reference 2) calculated the one-dimensional line spread function in the order direction for the truncated Gaussian PSF, which is an error function, and also the corresponding MTF. However, the image at the SEC faceplate is smeared by the two-dimensional PSF; hence, we redid the calculation.

It turned out that our result differed only slightly from those of Bogges - less than 1% - in the spatial frequency range 0-14 cy/mm (the system MTF is dominated by the converter MTF, and drops below 0.01 above 14 cy/mm). Indeed, both calculations differ from the Gaussian MTF (no truncation) by less than 1% in this frequency range. Above approximately 40 cy/mm, the truncated Gaussian MTF begins to depart significantly from the Gaussian function, reaching zero at 51.75 cy/mm, with "side lobes" above this frequency. (Remember that the MTF is equivalent to the Fraunhofer diffraction pattern modulus.) Hence, our derivation by Hankel transform is of academic interest

only. The work done is briefly summarized below. Additional material is given in Appendix A.

Since the guidance PSF is radially symmetric, the MTF may be calculated by the finite Hankel transform

$$M_g(s) = \frac{1}{2} \int_0^{r_0} J_0(2\pi r_0 s) r \exp(-r^2/2\sigma^2) \quad (2.14)$$

where J_0 is the Bessel function of the first kind and zero order.

This integral was evaluated by partial integration (Appendix A) obtaining the asymptotic expansion

$$M_g(s) \cong \exp(-2\pi^2 \sigma^2 s^2) - \exp(-r_0^2/2\sigma^2) \sum_{n=0}^{\infty} (-4\pi^2 \sigma^2 s^2)^n \frac{J_n(2\pi r_0 s)}{(2\pi r_0 s)^n} \quad (2.15a)$$

which gives explicitly the expected Gaussian MTF in the limit $r_0/\sigma \gg 1$.

An alternative derivation found in the literature (Reference 4) gives the result

$$M_g(s) \cong \frac{(r_0/\sigma)^2}{\exp(r_0^2/2\sigma^2) - 1} \sum_{n=0}^{\infty} (r_0/\sigma)^{2n} \frac{J_{n+1}(2\pi r_0 s)}{(2\pi r_0 s)^{n+1}}, \quad (2.15b)$$

which yields the Fraunhofer diffraction pattern of a clear circular aperture in the limit $r_0/\sigma \ll 1$. The latter asymptotic expansion is obtained also by partial integration but with the u and dv factors interchanged with respect to those chosen in this author's derivation (see Appendix B).

Both expressions were programmed for numerical evaluation. However, due to limitations in the accuracy of the IBM SSP subroutine employed to calculate the J_n in the small argument region, this effort was abandoned, and direct numerical integration of Equation (2.14) using Simpson's rule was programmed. The resulting radial MTF for guidance smear is illustrated in Figure 15.

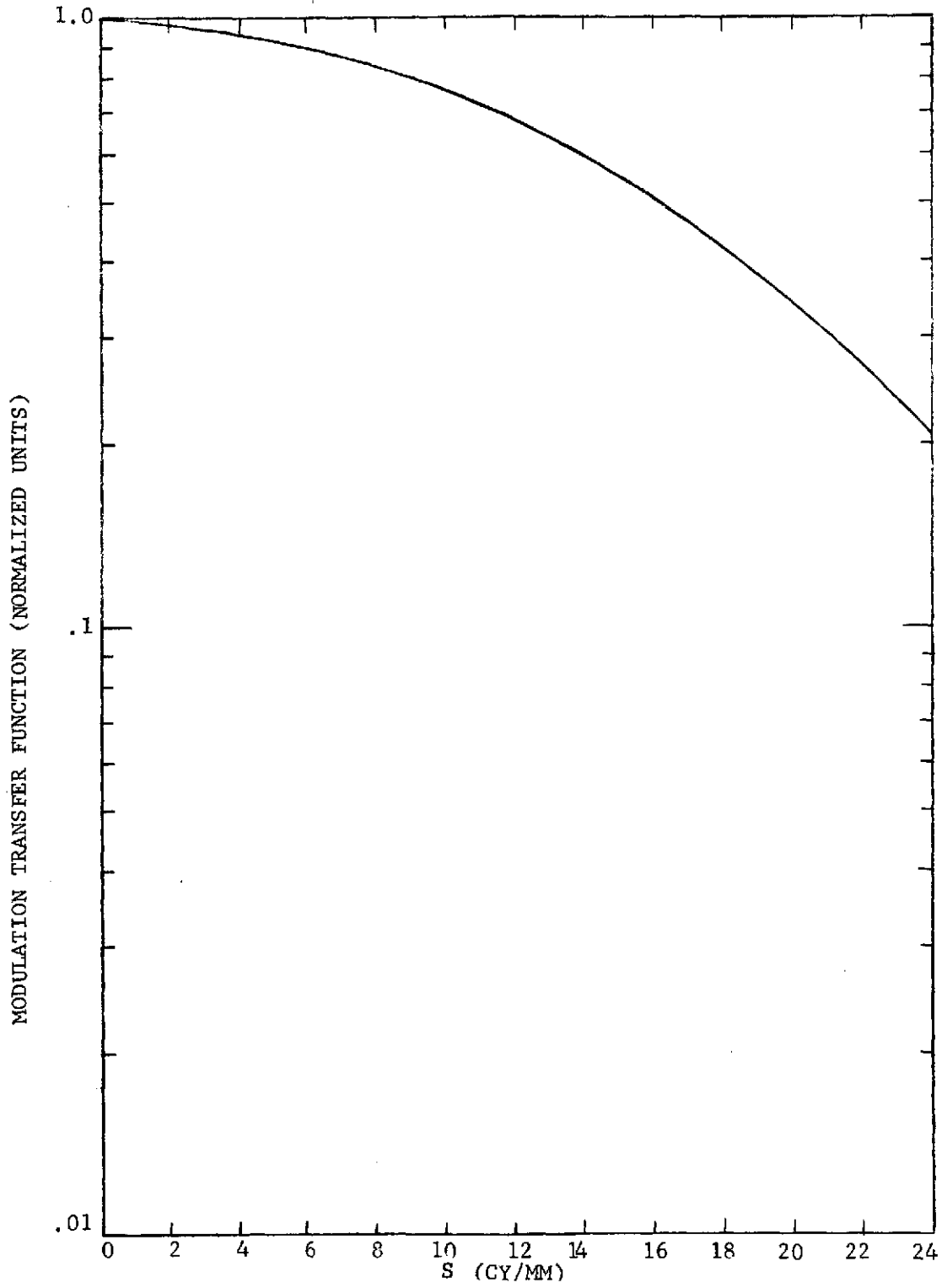


Figure 15. Point Source Guidance MTF

2.5 UV SPECTROGRAPH

The UV spectrograph consists of crossed echelle and concave spherical gratings. In this study, the spectrograph optical performance degradations were assumed to be negligible. NASA-generated spot diagrams indicate that geometrical aberrations in the spectrograph result in image smear that is small compared to smear from the other system components, in particular, the guidance and UV converter smear. Our experience at Perkin-Elmer with the design and fabrication of instruments employing similar grating spectrographs, suggests that the off-axis geometrical aberrations may be more serious than indicated by the NASA spot diagrams. However, Perkin-Elmer has not investigated the particular case of the IUE spectrograph design, since it is beyond the scope of this study.

"Blaze angle falloff" or "ripple", the single slit intensity (sinc^2) function, was also to be included in the math model. However, the NASA-furnished unsmearred echellogram data includes this in the order direction already, making it unnecessary to add to the Perkin-Elmer model. However, the NASA data does not include the ripple factor for the cross-order direction. The sinc function squared reaches its half-maximum value at $\pi sp/\lambda \cong 0.463\pi$, where s here is the slit width, and $p = \sin\theta - \sin\theta_0$ with θ_0 and θ being the angle of incidence and diffraction angle respectively. Thus, at the half-maximum point $p_{1/2} \approx 0.463\lambda/s$. For the spherical grating $\lambda/s \approx \lambda/d$, where $1/d$ is the grating frequency ($3.3802 \times 10^3 \text{ cm}^{-1}$ for the short wavelength grating and $2.3314 \times 10^3 \text{ cm}^{-1}$ for the long wavelength grating). At the short and long wavelengths of $\lambda = 1400\text{\AA}$, and 2500\AA , $p_{1/2} \approx 0.0219$ radians and 0.0271 radians, which correspond to half-maximum widths at the camera focal plane of 14.9mm and 18.4mm .

Hence, the falloff in the cross-order direction is not negligible, and should be included in a calibration subsystem for the operating IUE hardware (or software). We have not included it in the Perkin-Elmer simulation model since it is not of central concern in this study.

2.6 SYSTEM MTF AND PSF

The component MTF's discussed in the preceding paragraphs, with the exception of the destructive readout MTF (actually the complex optical

transfer function, or OTF, since the PSF is asymmetric in this case), were cascaded together for input to the simulation program. They are illustrated in Figure 16 for the four converter wavelengths.

The destructive readout OTF (or PSF, depending on the method of simulation) was used as input in an intermediate simulation in a two-step process consisting of the smear due to the readout process alone, followed by the additional smear of the cascaded converter and guidance components. This is discussed more fully in the following subsection (Paragraph 2.7).

The system PSF (again minus the SEC readout) was obtained by Hankel transforming the cascaded converter and guidance MTF's. These are shown in Figure 17 for the four converter wavelengths. These were calculated for the purpose of simulation by the direct convolution method but were not used, since the frequency domain method was alternatively used, as discussed in Paragraph 2.7.

2.7 COMPUTER IMPLEMENTATION

The simulations can be carried out by either direct convolution in the spatial domain or by linear filtering via Fast Fourier Transform (FFT) in the spatial frequency domain, followed by inverse FFT. (The latter process is also referred to as "FFT convolution.") Spatial domain simulation was the method initially chosen. However, the cost per simulation proved to be greater than anticipated to the point of being prohibitive ($\leq \$250$ per simulation). Overlooked in the original decision was the need to interpolate the data and also the processing spot to be convolved which approximately doubled the array dimensions of each. The input echellogram data points had been generated on the SEC readout sampling lattice. At all previously read sample points, the processing array amplitudes were zero, for 100% discharge. The SEC readout effective PSF (see Equation (2.7)) is non-zero between the sampling points, but this information is lost in the digital approximation to the continuous convolution integral, unless one samples the PSF between the zeroes. This means, since the echellogram and PSF must be defined on the same sampling lattice, that the echellogram must be interpolated to whatever density

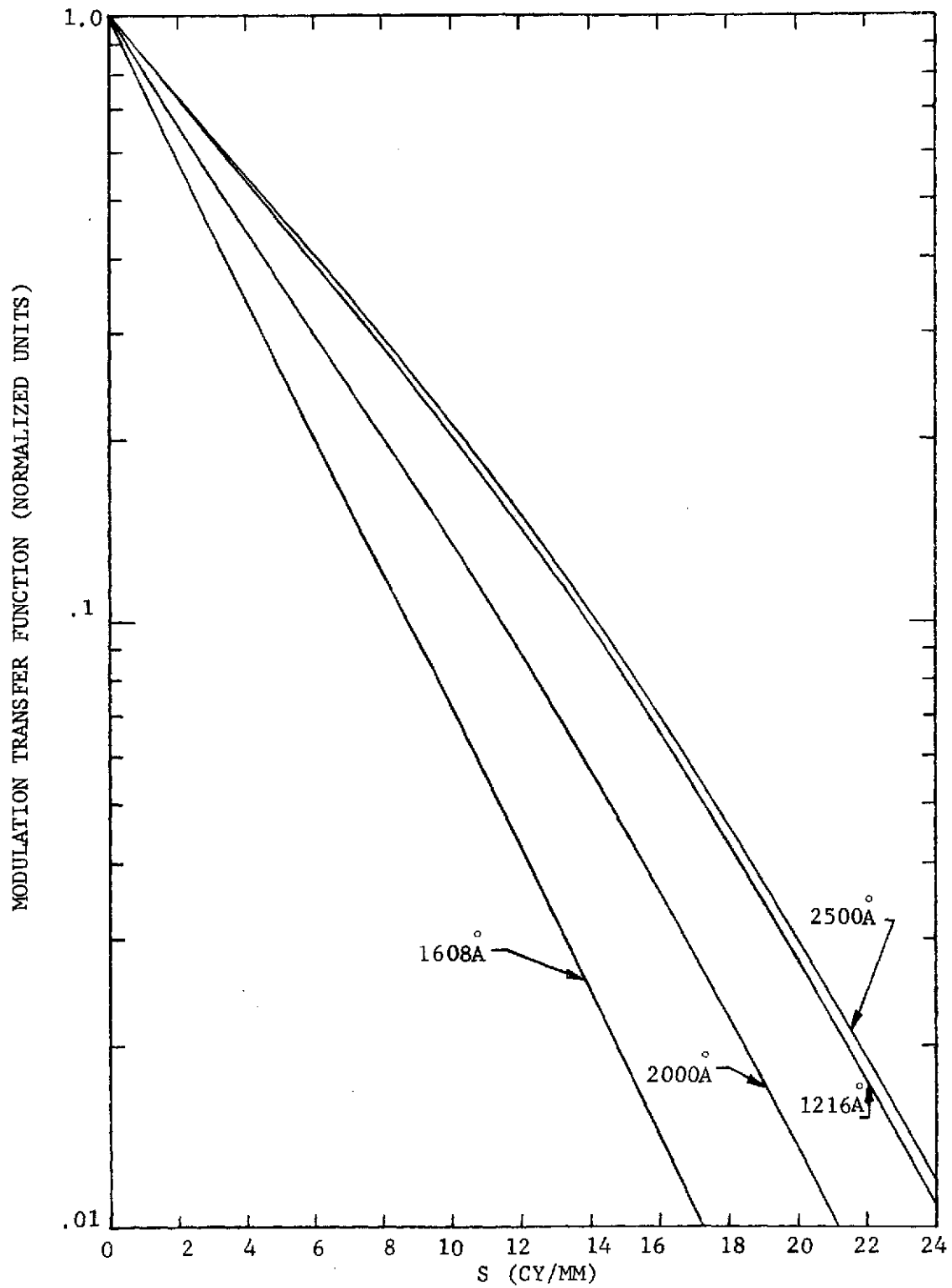


Figure 16. Cascaded Point Source Guidance And UV Converter MTF's

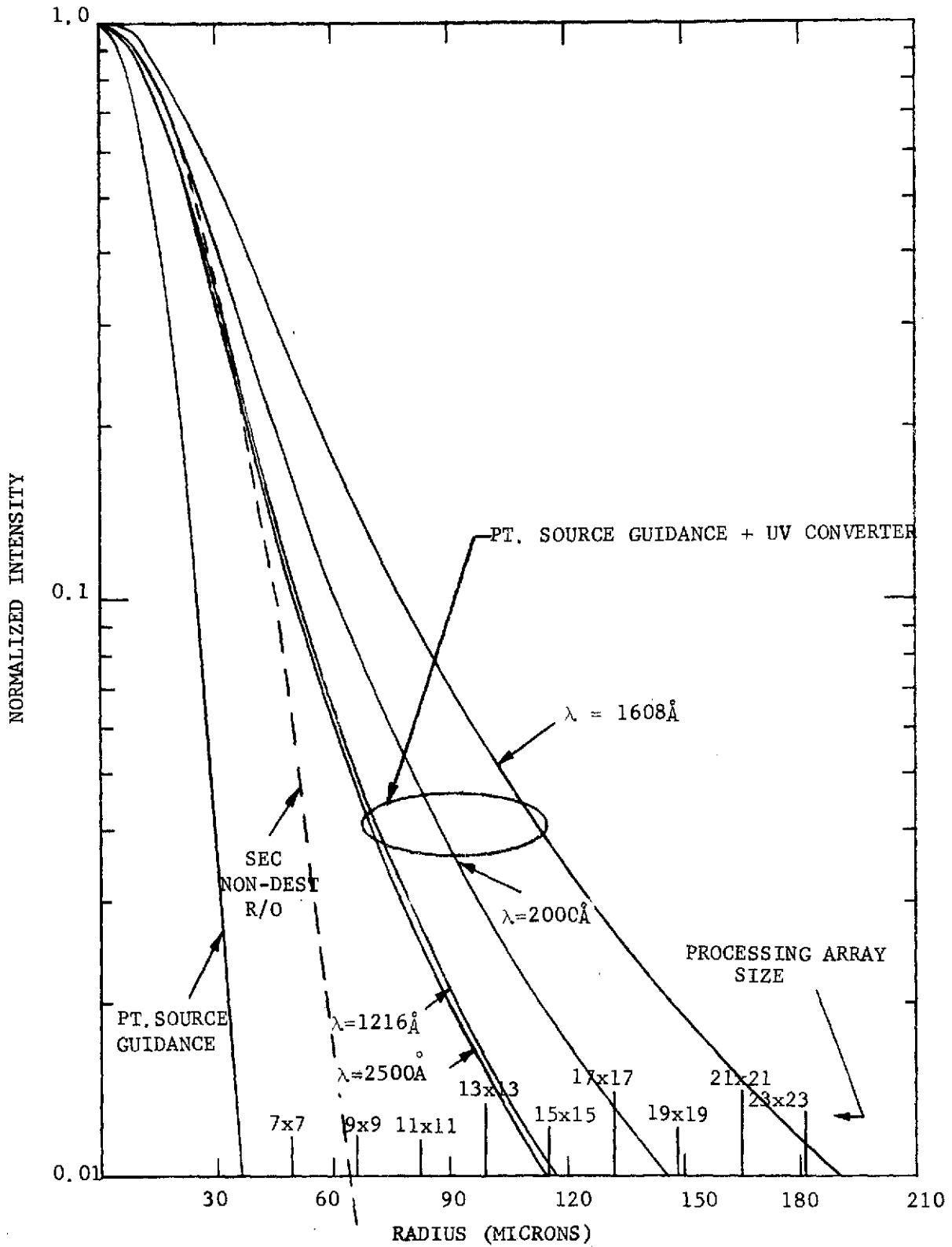


Figure 17. Instrument PSF's (not including destructive R/O)

desired for the sampling of the PSF. Thus, for example, at $\lambda = 1216\text{\AA}$ the processing array size, requirement (truncating the PSF array at $\approx 2\%$ of the peak value) went from 7×7 to 13×13 (see Figure 17). At $\lambda = 2000\text{\AA}$, the required size for comparable accuracy becomes 17×17 .

Essentially, the digital computation process introduces a sampling in addition to that of the readout. (Again, for convenience, we discuss the one-dimensional case. Generalization to two dimensions is straightforward as in Section 2.2.3.) The convolution integral Equation (2.6) is replaced by a sum, i.e., at the k 'th beam address

$$\int_{-\infty}^{\infty} Q(x) P_k(\{x-x_i\}) dx \cong \Delta x \sum_{m=0}^{M-1} Q(x_m) P_k(\{x_m-x_i\})$$

where the x_m are the M points on the computational lattice ($M = 2N-1$, where N is the dimension of the readout lattice).

The two-dimensional form of this discrete convolution was performed using program "CONVOL" from Perkin-Elmer's Digital Image Processing Programs (DIPP) library for the spatial domain computations giving the result of the destructive readout process alone, without the other contributions to smear. The latter, namely the guidance and converter smear, were simulated by FFT convolution of these with the echellogram smeared by destructive readout.

In the frequency domain, the Fourier transform of the above integral is given by the product of the Fourier transforms of $Q(x)$ and $P(x)$, i.e., $Q(s)$ and $P(s)$. The discrete transforms are equal to the values of $Q(s)$ and $P(s)$ at the points s_m ($m=0, 1, \dots, M-1$) on the frequency sampling lattice of spacing Δs which is related to the spatial sampling lattice by $\Delta s = 1/M\Delta x$.

The discrete Fourier transform of $Q(x_i)$, denoted as $\hat{Q}(s_i)$, is

$$\hat{Q}(s_i) = \Delta s \sum_{m=0}^{M-1} Q(x_m) \left[\exp\left(-\frac{2\pi s_i x_m}{M}\right) \right]^m$$

and similarly for $\hat{P}(s_i)$.

In this study, the system PSF was constructed by cascading the component MTF's (Fourier transforms of the PSF's) and then inverse transforming this result to obtain the PSF. Hence, the switch to frequency domain processing required only the calculation of the echellogram transform.

Another program package in the DIPP library called "XFORM" was used for the frequency domain processing. It consists of a set of subroutines which reads the input "scene" (echellogram in our case), performs the two-dimensional discrete Fourier transform via FFT, multiplies this by the processing OTF (system OTF), which is complex in this case because of the asymmetrical destructive readout PSF, performs the inverse transform of the result and outputs to LSIG magnetic tape. Optionally, the echellogram transform may be saved on tape or disk in case it is desired to process the same scene with more than one OTF, which was the case here. To satisfy the discrete Fourier transform requirement of periodicity and continuity of the scene at the edges (the points x_0 and x_{M-1}), a raised cosine rolloff to zero intensity was applied to the echellogram borders extending nine samples in from each edge.

The echellograms 256×400 were processed in 256×256 "chunks," overlapping by 112 records (order direction) in the center. The spatial frequency sampling interval and maximum spatial frequency for an $N \times N$ image are given by $\Delta F = 1/N \cdot \Delta X$ and $F_{\max} = (N/2) \cdot \Delta F$, where ΔX is the spatial sampling interval. In the case of $N = 256$, $\Delta X = 16.5 \mu$, $\Delta F = 0.23674$ cy/mm, and $F_{\max} = 30.30303$ cy/mm.

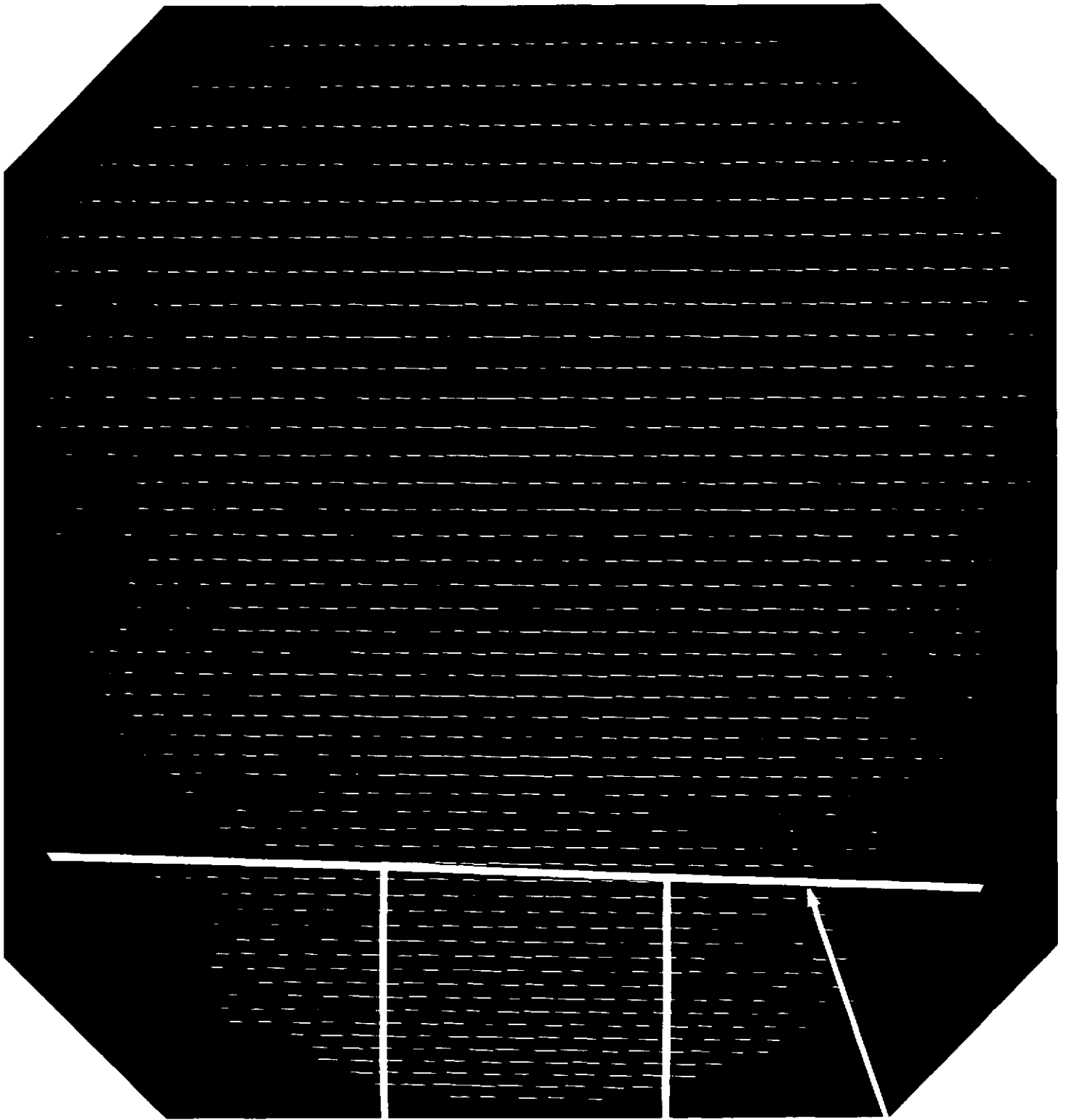
SECTION 3

PREPARATION OF INPUT ECHELLOGRAM

The NASA furnished tape used in the subsequent simulations contains three files: the first two consisting of slit scan spectra, "crowded" and "uncrowded" absorption spectra in the UV, and the third a simulated "un-smearred" echellogram made from the former slit scan spectrum by geometrically transforming the various orders into the echelle format, but without smear due to IUE system degradations.

The echellogram tape was in VICAR format, i.e., each data point was written as one byte. Some problems were encountered in the process of writing a program to read this unfamiliar format. These were eventually solved and a section of the tape was rewritten in LSIG-compatible format (two 6-bit bytes, reversed) and the amplitudes were multiplied by a factor of 32 to provide sufficient grey level amplitude for the LSIG. A 150 x 200 section from the bottom of the format was taken where the orders are most closely spaced. This is illustrated in Figure 18 which is an LSIG reproduction of the NASA echellogram.

The echellogram subsection was next linearly interpolated two-to-one in both dimensions to obtain sufficient sample density for the digital convolution purposes as discussed in Section 2.6, yielding an array almost four times as large, 299 points x 397 records. (One would expect dimensions of $(2M-1) \times (2N-1)$ in an array generated by linear interpolation from an $M \times N$ array -- in this case, 299 x 399.) However, the interpolation program terminated after 397 records due to a system bug.)



RECORD NO. 275

RECORD NO. 475

POINT NO. 600

Figure 18. NASA Echellogram "REDPSF" (750 x 750) Reproduced on LSIG, Showing Subsection Used for Simulations

the relevant parameters of wavelength, spatial sampling intervals for the SEC readout and for computation, PSF and R/O beam widths, spatial frequency sampling interval, etc.

Negative transparencies of all simulations were made on the LSIG using a clear square writing mask.

The simulation outputs are shown in the deliverable photographs and positive transparencies which accompany the report in a separate package. Tape dumps of selected subsections of the simulated echellograms are given in Figures A-1 to A-7 of Appendix A.

SECTION 5

DISCUSSION OF RESULTS

5.1 EFFECTS OF DESTRUCTIVE READOUT

The major results to be noted here are, first, that the wavelength error introduced by the pixel shift due to PSF asymmetry is small for the case of the 50 micron width. As discussed in Paragraph 2.2.5, the shift of the peak of the effective PSF is less than 1/2 pixel in both the order and cross-order directions. However, this does not give the whole story. In Figure 19 a portion of a single order, smeared by the SEC readout alone (Simulation 2) and integrated across the width of the order (simulating a slit scan) taken near the bottom of the echelle format, was plotted in the order direction. For comparison, the corresponding portion of the unsmeared input (Simulation 1) was also plotted. The abscissa units are pixel numbers for the interpolated echellogram (remember that 2 interpolated pixels = 1 readout pixel) and the ordinate is grey level (x32 relative to the NASA-furnished data). It is evident from this comparison plot that the spectra are nearly identical. The SEC readout spectrum is shifted by approximately one readout pixel with respect to the input, whereas the shift of the PSF peak was less than 1/2 pixels as noted above. In addition, there is some smoothing of the data. The peaks and valleys agree in amplitude to better than one percent. Indeed, it appears that if the shift were taken out, the two spectra would agree within one percent throughout. We remind the reader that the normalized OTF for SEC readout was used for the simulations, and that a gain reduction factor of 0.411 (see Paragraph 2.2.5) should be applied to the curve for SEC readout. However, this is not a loss of modulation, but merely gain.

Hence, the only significant result of the destructive readout process for spectroradiometric data analysis as predicted by our linear model (assuming sufficient noise-free gain elsewhere in the system chain) is the shift of one

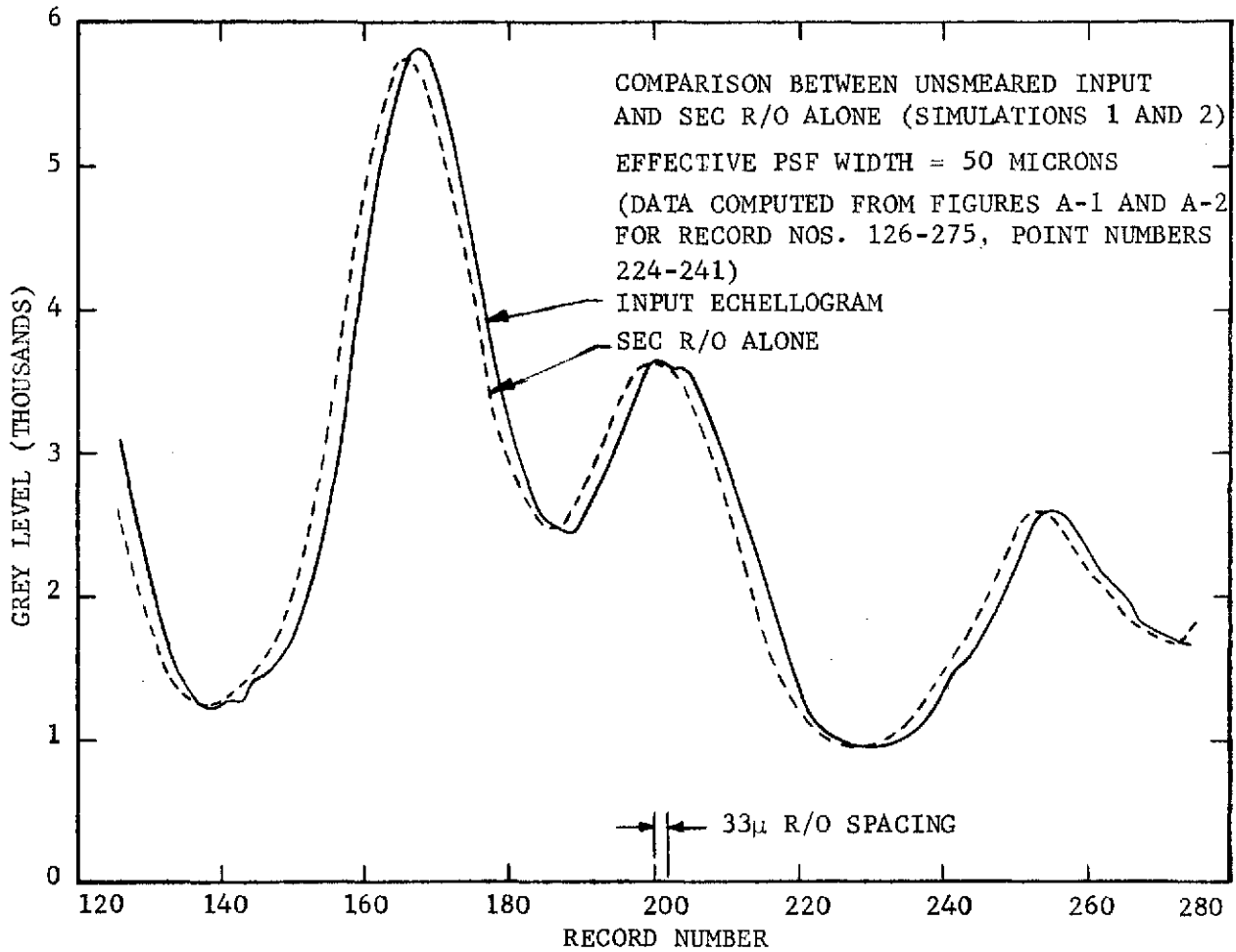


Figure 19. Simulated Slit Scan of Echelle Order Along Order Direction

readout pixel. The smear resulting from the SEC readout does not appreciably affect the resolution along the order direction, if the energy spread in the cross-order direction is integrated by slit scanning. For the case of the 100 microns PSF width, the smear has increased enough in the cross-order direction to cause a small degree of order overlap in simulation of the SEC readout alone (see the printout in Figure A-3). Because of this, and because of insufficient time remaining in the contract, the slit scan calculation done to obtain Figure 19 was not repeated. However, in this case, one would expect a result similar to the 50 microns case, since the overlap is not serious. Some loss in modulation should be expected since the PSF width in the order direction is doubled.

5.2 EFFECTS OF GUIDANCE AND UV CONVERTER SMEAR

These components, when convolved with the echellogram data smeared by the SEC vidicon, give rise to the greater part of the total smear, with resulting order overlap, which can be seen in both the photographs and the computer printouts of Appendix A. We have also plotted representative profiles in the cross-order direction near the bottom center of the format. These are shown in Figure 20.

The wavelength dependence can be observed by comparing simulations 8 and 9 (reference Table 4-1). As one would expect, the greatest smear occurs for the $\lambda = 2000\text{\AA}$ case, where the converter performance is worst.

The result of doubling the SEC readout PSF width from 50 to 100 microns is largely masked by the converter and guidance smear contributions, as can be seen by comparing Simulations 4 and 5.

A peak shift of approximately one readout pixel in the cross-order direction can also be observed in Figure 20.

Order overlap in the complete system simulations is significant enough that one would expect a slit scan calculation similar to that done for the SEC readout alone (Figure 19) to be in error, particularly for a case integrating

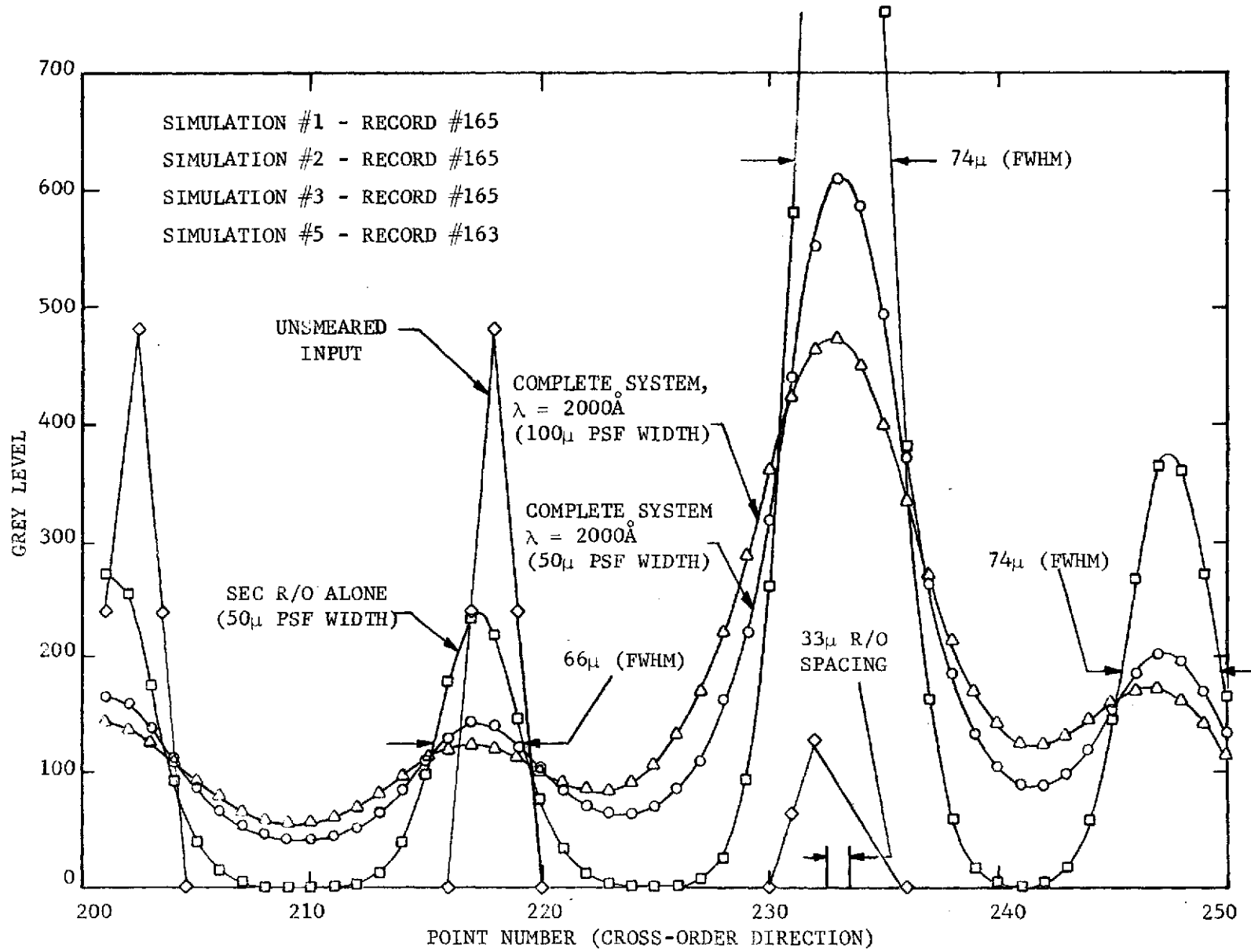


Figure 20. Simulation Profiles in Cross-Order Direction at Bottom Center of Echelle Format

a weak profile adjacent to a strong one. A suggested approach would be to try enhancement filtering in the cross-order direction, wherever the overlap is serious.

SECTION 6

SUMMARY AND CONCLUSIONS

This study program has resulted in the generation of a linear mathematical model for computer simulation of the optical performance of the IUE Scientific-Instrument imaging chain. A series of computer programs has been written to implement the model, and a number of simulated echellograms were generated demonstrating the major effects of performance degradations due to the several imaging components. In particular, an algorithm was developed to represent the two-dimensional destructive readout process in the SEC vidicon camera by an effective PSF which, to a good approximation, is space-invariant.

The major conclusions of this program are:

- a. Wavelength determination error due to the pixel shift arising from destructive readout is predicted to be approximately one readout pixel (33 micron width), or approximately 0.06\AA in wavelength, for the case where the effective PSF FWHM width is taken to be 50 microns.
- b. Order overlap is principally due to the smear of the guidance and converter components, and may be a significant problem at the bottom of the echelle format, particularly for the case of a weak order profile adjacent to a strong one. Enhancement filtering in the cross-order direction may provide help in this instance.
- c. Radiometric error due to the discharge overlap of the destructive readout is predicted to be negligible, provided that the assumption of a linear readout process is a good approximation to reality, and also that there is sufficient noise-free gain in the system chain to overcome the loss in gain due to destructive readout. Radiometric error may result from aberrations in the spectrograph (which were ignored in this study) and also in the electron beam focus of the SEC vidicon.

REFERENCES

1. System Design Report for International Ultraviolet Explorer, Volume 1, Scientific Instrument, NASA/Goddard Space Flight Center, Greenbelt, Maryland, June, 1973.
2. NASA/GSFC Memorandum to D. Fischel from A. Boggess, "IUE Resolution", dated January 3, 1973.
3. Coltman, J. W., J.O.S.A. 44, page 468 (1954).
4. Johnson, C. B., Developments in Electronic Imaging Techniques, Volume 32, pp. 25-28, October 16, 1972. (An SPIE Conference in San Mateo, California).
5. Wortendyke, D. R., "The Far Field Patterns of a Circular Gaussian Field Distribution Restricted by a Circular Aperture", Report 1641-11, Ohio State Univ. Research Foundation, Columbus, Ohio, dated June 15, 1965, pp. 4-5.

6-2

APPENDIX A

COMPUTER PRINTOUTS OF SIMULATIONS 1-7

Figures A-1 through A-7 are dumps of selected portions of the echellogram simulation tapes for simulations 1 through 7 (of Table 4-1) near the bottom center of the echelle format.

The point and record numbers are those of the computational lattice which has dimensions of 256 points x 400 records. The lattice spacing in both directions is 16.5 microns. The point numbers increase horizontally (cross-order direction) from left to right, while the record numbers increase vertically (order direction) from top to bottom.

The simulated slit scan discussed in Paragraph 5.1 and shown in Figure 19 was hand calculated from swaths of data in Figures A-1 and A-2 between point numbers 224-241, records 126-275.

ECHHELLOGRAM SUBSECTION

TAPE 812 - NASA INTERPOLATED ECHHELLOGRAM REDPSF,32X (SIMULATION INPUT)

PTS: 201 TO 225 TOTAL PIXELS = 102400 SUM = 0.1170E 08
 RECS: 126 TO 275 AVG = 0.1142E 03

768	1536	840	144	72	0	0	0	0	0	0	0	0	0	0	576	1152	632	112	56	0	0	0	0
832	1664	896	128	64	0	0	0	0	0	0	0	0	0	0	624	1248	672	96	48	0	0	0	0
864	1728	928	128	64	0	0	0	0	0	0	0	0	0	0	672	1344	720	96	48	0	0	0	0
896	1792	960	128	64	0	0	0	0	0	0	0	0	0	0	720	1440	768	96	48	0	0	0	0
896	1792	952	112	56	0	0	0	0	0	0	0	0	0	0	760	1520	808	96	48	0	0	0	0
896	1792	944	96	48	0	0	0	0	0	0	0	0	0	0	800	1600	848	96	48	0	0	0	0
864	1728	912	96	48	0	0	0	0	0	0	0	0	0	0	808	1616	856	96	48	0	0	0	0
832	1664	880	96	48	0	0	0	0	0	0	0	0	0	0	816	1632	864	96	48	0	0	0	0
784	1568	824	80	40	0	0	0	0	0	0	0	0	0	0	792	1584	832	80	40	0	0	0	0
736	1472	768	64	32	0	0	0	0	0	0	0	0	0	0	768	1536	800	64	32	0	0	0	0
688	1376	720	64	32	0	0	0	0	0	0	0	0	0	0	736	1472	768	64	32	0	0	0	0
640	1280	672	64	32	0	0	0	0	0	0	0	0	0	0	704	1408	736	64	32	0	0	0	0
584	1168	608	48	24	0	0	0	0	0	0	0	0	0	0	648	1296	680	64	32	0	0	0	0
528	1056	544	32	16	0	0	0	0	0	0	0	0	0	0	592	1184	624	64	32	0	0	0	0
472	944	488	32	16	0	0	0	0	0	0	0	0	0	0	536	1072	560	48	24	0	0	0	0
416	832	432	32	16	0	0	0	0	0	0	0	0	0	0	480	960	496	32	16	0	0	0	0
368	736	384	32	16	0	0	0	0	0	0	0	0	0	0	432	864	448	32	16	0	0	0	0
320	640	336	32	16	0	0	0	0	0	0	0	0	0	0	384	768	400	32	16	0	0	0	0
280	560	288	16	8	0	0	0	0	0	0	0	0	0	0	360	720	376	32	16	0	0	0	0
240	480	240	0	0	0	0	0	0	0	0	0	0	0	0	336	672	352	32	16	0	0	0	0
224	448	224	0	0	0	0	0	0	0	0	0	0	0	0	312	624	320	16	8	0	0	0	0
208	416	208	0	0	0	0	0	0	0	0	0	0	0	0	288	576	288	0	0	0	0	0	0
192	384	192	0	0	0	0	0	0	0	0	0	0	0	0	272	544	272	0	0	0	0	0	0
176	352	176	0	0	0	0	0	0	0	0	0	0	0	0	256	512	256	0	0	0	0	0	0
168	336	168	0	0	0	0	0	0	0	0	0	0	0	0	248	496	248	0	0	0	0	0	0
160	320	160	0	0	0	0	0	0	0	0	0	0	0	0	240	480	240	0	0	0	0	0	0
160	320	160	0	0	0	0	0	0	0	0	0	0	0	0	232	464	232	0	0	0	0	0	0
160	320	160	0	0	0	0	0	0	0	0	0	0	0	0	224	448	224	0	0	0	0	0	0
160	320	160	0	0	0	0	0	0	0	0	0	0	0	0	216	432	216	0	0	0	0	0	0
160	320	160	0	0	0	0	0	0	0	0	0	0	0	0	208	416	208	0	0	0	0	0	0
160	320	160	0	0	0	0	0	0	0	0	0	0	0	0	200	400	200	0	0	0	0	0	0
160	320	160	0	0	0	0	0	0	0	0	0	0	0	0	192	384	192	0	0	0	0	0	0
160	320	160	0	0	0	0	0	0	0	0	0	0	0	0	192	384	192	0	0	0	0	0	0
168	336	168	0	0	0	0	0	0	0	0	0	0	0	0	200	400	200	0	0	0	0	0	0
176	352	176	0	0	0	0	0	0	0	0	0	0	0	0	208	416	208	0	0	0	0	0	0
184	368	184	0	0	0	0	0	0	0	0	0	0	0	0	208	416	208	0	0	0	0	0	0
192	384	192	0	0	0	0	0	0	0	0	0	0	0	0	208	416	208	0	0	0	0	0	0
216	432	216	0	0	0	0	0	0	0	0	0	0	0	0	224	448	224	0	0	0	0	0	0
240	480	240	0	0	0	0	0	0	0	0	0	0	0	0	240	480	240	0	0	0	0	0	0
272	544	272	0	0	0	0	0	0	0	0	0	0	0	0	248	496	248	0	0	0	0	0	0
304	608	304	0	0	0	0	0	0	0	0	0	0	0	0	256	512	256	0	0	0	0	0	0
352	688	344	0	0	0	0	0	0	0	0	0	0	0	0	280	560	280	0	0	0	0	0	0
400	768	384	0	0	0	0	0	0	0	0	0	0	0	0	304	608	304	0	0	0	0	0	0
448	864	432	0	0	0	0	0	0	0	0	0	0	0	8	16	336	656	328	0	0	0	0	0
496	960	480	0	0	0	0	0	0	0	0	0	0	16	32	368	704	352	0	0	0	0	0	0
544	1056	528	0	0	0	0	0	0	0	0	0	0	16	32	400	768	384	0	0	0	0	0	0
592	1152	576	0	0	0	0	0	0	0	0	0	0	16	32	432	832	416	0	0	0	0	0	0
648	1248	624	0	0	0	0	0	0	0	0	0	0	16	32	464	896	448	0	0	0	0	0	0
704	1344	672	0	0	0	0	0	0	0	0	0	0	16	32	496	960	480	0	0	0	0	0	0
736	1408	704	0	0	0	0	0	0	0	0	0	0	16	32	520	1008	504	0	0	0	0	0	0
768	1472	736	0	0	0	0	0	0	0	0	0	0	16	32	544	1056	528	0	0	0	0	0	0

Figure A-1. Echellogram Subsection - Tape No. 812

A-2 ORIGINAL PAGE IS OF POOR QUALITY

SECTION 4

SIMULATIONS

The interpolated echellogram made in Task II was first convolved with the effective PSF for destructive readout yielding an intermediate echellogram on LSIG magnetic tape. At this point, it was decided to switch to FFT convolution processing to save money on computer time, which, as we have noted in Section 2, was prohibitively expensive for direct convolution because of the large size of the PSF processing array required.

Destructive readout simulations at converter wavelengths of $\lambda = 1216\text{\AA}$ and 2000\AA were completed via FFT convolution using the cascaded MTF's for the converter, and guidance components as inputs.

This was followed by a nondestructive readout simulation at $\lambda = 2000\text{\AA}$ which was done entirely by FFT convolution.

At a meeting with NASA, the above results were presented, and plans for modifying and limiting the schedule of further simulations were made. It was requested by NASA that we do a destructive readout simulation using an effective PSF width of 100 microns (double the width used previously) because the order overlap appeared from the photographs to be less than expected. In the course of selecting the appropriate beam width parameter, it was realized that the effective PSF width and the readout beam width are not the same, as already discussed in Paragraph 2.2.5. After determining the correct beam width parameter for the 100 microns PSF width, it was decided to redo the 50 micron case. This was accomplished by FFT convolution which required the calculation the complex OTF for the SEC readout, due to the asymmetry of the PSF.

A table of simulation data appears in Table 4-1, including the intermediate simulations of SEC readout alone and giving titles, figure numbers, and

TABLE 4-1
SIMULATION DATA

Simulation No.	Tape No.	Fig. No. (Computer Printout)	Title	Sim Type	Eff. Sec. PSF Width (μ)	R/O Beam Width (μ)	Type of Convolution	Conv. Wavel. (\AA)	Sec R/O Spacing (μ)	Comput. Lattice Spacing (μ)	Spatial Freq. Sampling Interval (cy/mm)
1	812	A-1	Interpolated NASA Echellogram, "REDPSF," 32X (Simulation Input)	-	-	-	-	-	33	16.5	-
2	518	A-2	Destructive R/O Simulation (SEC Alone)	DRO	50	70.5	FFT	-	33	16.5	0.23674
3	255	A-3	Destructive R/O Simulation (SEC Alone)	DRO	100	112.8	FFT	-	33	16.5	0.23674
4	422	A-4	Destructive R/O Simulation (Complete System)	DRO	50	70.5	FFT	2000	33	16.5	0.23674
5	275	A-5	Destructive R/O Simulation (Complete System)	DRO	100	112.8	FFT	2000	33	16.5	0.23674
6	813	A-6	Non-Destructive R/O Simulation (Complete System)	NDRO	50	50	FFT	2000	33	16.5	0.23674
7	170	-	Destructive R/O Simulation (SEC Alone)	DRO	41	50	Direct	-	33	16.5	0.23674
8	888	-	Destructive R/O Simulation (Complete System)	DRO	41	50	Direct + FFT	2000	33	16.5	0.23674
9	1107	A-7	Destructive R/O Simulation (Complete System)	DRO	41	50	Direct + FFT	1216	33	16.5	0.23674

4-2

ORIGINAL PAGE IS
OF POOR QUALITY

A-4

240	0	0	0	0	0	0	0	0	0	0	0	0	0	112	224	112	0	0	0	0	0	0	0	0	0
240	0	0	0	0	0	0	0	0	0	0	0	0	0	0	112	224	112	0	0	0	0	0	0	0	0
248	0	0	0	0	0	0	0	0	0	0	0	0	0	0	120	240	120	0	0	0	0	0	0	0	0
256	0	0	0	0	0	0	0	0	0	0	0	0	0	0	128	256	128	0	0	0	0	0	0	0	0
264	0	0	0	0	0	0	0	0	0	0	0	0	0	0	128	256	128	0	0	0	0	0	0	0	0
272	0	0	0	0	0	0	0	0	0	0	0	0	0	0	128	256	128	0	0	0	0	0	0	0	0
288	0	0	0	0	0	0	0	0	0	0	0	0	0	0	136	272	136	0	0	0	0	0	0	0	0
304	0	0	0	0	0	0	0	0	0	0	0	0	0	0	144	288	144	0	0	0	0	0	0	0	0
320	0	0	0	0	0	0	0	0	0	0	0	0	0	0	152	304	152	0	0	0	0	0	0	0	0
336	0	0	0	0	0	0	0	0	0	0	0	0	0	0	160	320	160	0	0	0	0	0	0	0	0
352	0	0	0	0	0	0	0	0	0	0	0	0	0	0	176	352	176	0	0	0	0	0	0	0	0
368	0	0	0	0	0	0	0	0	0	0	0	0	0	0	192	384	192	0	0	0	0	0	0	0	0
400	0	0	0	0	0	0	0	0	0	0	0	0	0	0	216	432	216	0	0	0	0	0	0	0	0
432	0	0	0	0	0	0	0	0	0	0	0	0	0	0	240	480	240	0	0	0	0	0	0	0	0
480	0	0	0	0	0	0	0	0	0	0	0	0	0	0	264	528	264	0	0	0	0	0	0	0	0
528	0	0	0	0	0	0	0	0	0	0	0	0	0	0	288	576	288	0	0	0	0	0	0	0	0
576	0	0	0	0	0	0	0	0	0	0	0	8	16	320	624	312	0	0	0	0	0	0	0	0	0
624	0	0	0	0	0	0	0	0	0	0	0	16	32	352	672	336	0	0	0	0	0	0	0	0	0
672	0	0	0	0	0	0	0	0	0	0	0	16	32	384	736	368	0	0	0	0	0	0	0	0	0
720	0	0	0	0	0	0	0	0	0	0	0	16	32	416	800	400	0	0	0	0	0	0	0	0	0
760	0	0	0	0	0	0	0	0	0	0	0	16	32	456	880	440	0	0	0	0	0	0	0	0	0
800	0	0	0	0	0	0	0	0	0	0	0	16	32	496	960	480	0	0	0	0	0	0	0	0	0
808	0	0	0	0	0	0	0	0	0	0	0	24	48	536	1024	512	0	0	0	0	0	0	0	0	0
816	0	0	0	0	0	0	0	0	0	0	0	32	64	576	1088	544	0	0	0	0	0	0	0	0	0
792	0	0	0	0	0	0	0	0	0	0	0	32	64	592	1120	560	0	0	0	0	0	0	0	0	0
768	0	0	0	0	0	0	0	0	0	0	0	32	64	608	1152	576	0	0	0	0	0	0	0	0	0
736	0	0	0	0	0	0	0	0	0	0	0	40	80	608	1136	568	0	0	0	0	0	0	0	0	0
704	0	0	0	0	0	0	0	0	0	0	0	48	96	608	1120	560	0	0	0	0	0	0	0	0	0
656	0	0	0	0	0	0	0	0	0	0	0	48	96	592	1088	544	0	0	0	0	0	0	0	0	0
608	0	0	0	0	0	0	0	0	0	0	0	48	96	576	1056	528	0	0	0	0	0	0	0	0	0
568	0	0	0	0	0	0	0	0	0	0	0	56	112	552	992	496	0	0	0	0	0	0	0	0	0
528	0	0	0	0	0	0	0	0	0	0	0	64	128	528	928	464	0	0	0	0	0	0	0	0	0

ER-267

Figure A-1 (Sheet 3 of 6)

ECHHELLOGRAM SUBSECTION

TAPE B12 - NASA INTERPOLATED ECHHELLOGRAM REDPSF,32X (SIMULATION INPUT)

PTS: 226 TO 250 TOTAL PIXELS = 102400 SUM = 0.1170E 08
 RECS: 126 TO 275 AVG = 0.1142E 03

0	0	0	0	0	0	0	736	1472	768	64	32	0	0	0	0	0	0	0	8	16	368	720
0	0	0	0	0	0	0	672	1344	704	64	32	0	0	0	0	0	0	0	16	32	400	768
0	0	0	0	0	0	0	616	1232	640	48	24	0	0	0	0	0	0	0	16	32	440	848
0	0	0	0	0	0	0	560	1120	576	32	16	0	0	0	0	0	0	0	16	32	480	928
0	0	0	0	0	0	0	520	1040	536	32	16	0	0	0	0	0	0	0	16	32	528	1024
0	0	0	0	0	0	0	480	960	496	32	16	0	0	0	0	0	0	0	16	32	576	1120
0	0	0	0	0	0	0	440	880	456	32	16	0	0	0	0	0	0	0	24	48	624	1200
0	0	0	0	0	0	0	400	800	416	32	16	0	0	0	0	0	0	0	32	64	672	1280
0	0	0	0	0	0	0	376	752	384	16	8	0	0	0	0	0	0	0	32	64	696	1328
0	0	0	0	0	0	0	352	704	352	0	0	0	0	0	0	0	0	0	32	64	720	1376
0	0	0	0	0	0	0	336	672	336	0	0	0	0	0	0	0	0	0	32	64	720	1376
0	0	0	0	0	0	0	320	640	320	0	0	0	0	0	0	0	0	0	32	64	720	1376
0	0	0	0	0	0	0	312	624	312	0	0	0	0	0	0	0	0	0	32	64	712	1360
0	0	0	0	0	0	0	304	608	304	0	0	0	0	0	0	0	0	0	32	64	704	1344
0	0	0	0	0	0	0	312	624	312	0	0	0	0	0	0	0	0	0	32	64	688	1312
0	0	0	0	0	0	0	320	640	320	0	0	0	0	0	0	0	0	0	32	64	672	1280
0	0	0	0	0	0	0	320	640	320	0	0	0	0	0	0	0	0	0	32	64	656	1248
0	0	0	0	0	0	0	320	640	320	0	0	0	0	0	0	0	0	0	32	64	640	1216
0	0	0	0	0	0	0	336	672	336	0	0	0	0	0	0	0	0	0	40	80	632	1184
0	0	0	0	0	0	0	352	704	352	0	0	0	0	0	0	0	0	0	48	96	624	1152
0	0	0	0	0	0	0	360	720	360	0	0	0	0	0	0	0	0	0	56	112	600	1088
0	0	0	0	0	0	0	368	736	368	0	0	0	0	0	0	0	0	0	64	128	576	1024
0	0	0	0	0	0	0	384	768	384	0	0	0	0	0	0	0	0	0	64	128	544	960
0	0	0	0	0	0	0	400	800	400	0	0	0	0	0	0	0	0	0	64	128	512	896
0	0	0	0	0	8	16	432	848	424	0	0	0	0	0	0	0	0	0	72	144	480	816
0	0	0	0	0	16	32	464	896	448	0	0	0	0	0	0	0	0	0	80	160	448	736
0	0	0	0	0	16	32	504	976	488	0	0	0	0	0	0	0	0	0	88	176	424	672
0	0	0	0	0	16	32	544	1056	528	0	0	0	0	0	0	0	0	0	96	192	400	608
0	0	0	0	0	24	48	600	1152	576	0	0	0	0	0	0	0	0	0	104	208	384	560
0	0	0	0	0	32	64	656	1248	624	0	0	0	0	0	0	0	0	0	112	224	368	512
0	0	0	0	0	32	64	728	1392	696	0	0	0	0	0	0	0	0	0	120	240	352	464
0	0	0	0	0	32	64	800	1536	768	0	0	0	0	0	0	0	0	0	128	256	336	416
0	0	0	0	0	40	80	888	1696	848	0	0	0	0	0	0	0	0	0	144	288	328	368
0	0	0	0	0	48	96	976	1856	928	0	0	0	0	0	0	0	0	0	160	320	320	320
0	0	0	0	0	48	96	1056	2016	1008	0	0	0	0	0	0	0	0	0	184	368	336	304
0	0	0	0	0	48	96	1136	2176	1088	0	0	0	0	0	0	0	0	0	208	416	352	288
0	0	0	0	0	56	112	1208	2304	1152	0	0	0	0	0	0	0	0	0	232	464	368	272
0	0	0	0	0	64	128	1280	2432	1216	0	0	0	0	0	0	0	0	0	256	512	384	256
0	0	0	0	0	64	128	1336	2544	1272	0	0	0	0	0	0	0	0	0	288	576	408	240
0	0	0	0	0	64	128	1392	2656	1328	0	0	0	0	0	0	0	0	0	320	640	432	224
0	0	0	0	0	72	144	1424	2704	1352	0	0	0	0	0	0	0	0	0	360	720	464	208
0	0	0	0	0	80	160	1456	2752	1376	0	0	0	0	0	0	0	0	0	400	800	496	192
0	0	0	0	0	80	160	1448	2736	1368	0	0	0	0	0	0	0	0	0	432	864	520	176
0	0	0	0	0	80	160	1440	2720	1360	0	0	0	0	0	0	0	0	0	464	928	544	160
0	0	0	0	0	88	176	1408	2640	1320	0	0	0	0	0	0	0	0	0	496	992	568	144
0	0	0	0	0	96	192	1376	2560	1280	0	0	0	0	0	0	0	0	0	528	1056	592	128
0	0	0	0	0	104	208	1320	2432	1216	0	0	0	0	0	0	0	0	0	560	1120	616	112
0	0	0	0	0	112	224	1264	2304	1152	0	0	0	0	0	0	0	0	0	592	1184	640	96
0	0	0	0	0	120	240	1192	2144	1072	0	0	0	0	0	0	0	0	0	616	1232	664	96
0	0	0	0	0	128	256	1120	1984	992	0	0	0	0	0	0	0	0	0	640	1280	688	96
0	0	0	0	0	144	288	1064	1840	920	0	0	0	0	0	0	0	0	0	648	1296	688	80
0	0	0	0	0	160	320	1008	1696	848	0	0	0	0	0	0	0	0	0	656	1312	688	64

A-5

Figure A-1 (Sheet 4 of 6)

ER-267

0	0	0	16	32	400	768	384	0	0	0	0	0	0	0	0	0	0	0	192	384	512	640	320	0
0	0	0	16	32	416	800	400	0	0	0	0	0	0	0	0	0	0	0	208	416	496	576	288	0
0	0	0	16	32	440	848	424	0	0	0	0	0	0	0	0	0	0	0	224	448	488	528	264	0
0	0	0	16	32	464	896	448	0	0	0	0	0	0	0	0	0	0	0	240	480	480	480	240	0
0	0	0	16	32	496	960	480	0	0	0	0	0	0	0	0	0	0	0	264	528	480	432	216	0
0	0	0	16	32	528	1024	512	0	0	0	0	0	0	0	0	0	0	0	288	576	480	384	192	0
0	0	0	24	48	560	1072	536	0	0	0	0	0	0	0	0	0	0	0	312	624	488	352	176	0
0	0	0	32	64	592	1120	560	0	0	0	0	0	0	0	0	0	0	0	336	672	496	320	160	0
0	0	0	32	64	616	1168	584	0	0	0	0	0	0	0	0	0	0	0	376	752	520	288	144	0
0	0	0	32	64	640	1216	608	0	0	0	0	0	0	0	0	0	0	0	416	832	544	256	128	0
0	0	0	32	64	648	1232	616	0	0	0	0	0	0	0	0	0	0	0	456	912	576	240	120	0
0	0	0	32	64	656	1248	624	0	0	0	0	0	0	0	0	0	0	0	496	992	608	224	112	0
0	0	0	32	64	648	1232	616	0	0	0	0	0	0	0	0	0	0	0	536	1072	640	208	104	0
0	0	0	32	64	640	1216	608	0	0	0	0	0	0	0	0	0	0	0	576	1152	672	192	96	0
0	0	0	40	80	624	1168	584	0	0	0	0	0	0	0	0	0	0	0	616	1232	704	176	88	0
0	0	0	48	96	608	1120	560	0	0	0	0	0	0	0	0	0	0	0	656	1312	736	160	80	0
0	0	0	48	96	584	1072	536	0	0	0	0	0	0	0	0	0	0	0	688	1376	760	144	72	0
0	0	0	48	96	560	1024	512	0	0	0	0	0	0	0	0	0	0	0	720	1440	784	128	64	0
0	0	0	56	112	544	976	488	0	0	0	0	0	0	0	0	0	0	0	744	1488	800	112	56	0
0	0	0	64	128	528	928	464	0	0	0	0	0	0	0	0	0	0	0	768	1536	816	96	48	0
0	0	0	80	160	520	880	440	0	0	0	0	0	0	0	0	0	0	0	776	1552	824	96	48	0
0	0	0	96	192	512	832	416	0	0	0	0	0	0	0	0	0	0	0	784	1568	832	96	48	0
0	0	0	104	208	488	768	384	0	0	0	0	0	0	0	0	0	0	0	784	1568	824	80	40	0
0	0	0	112	224	464	704	352	0	0	0	0	0	0	0	0	0	0	0	784	1568	816	64	32	0
0	0	0	128	256	456	656	328	0	0	0	0	0	0	0	0	0	0	0	760	1520	792	64	32	0
0	0	0	144	288	448	608	304	0	0	0	0	0	0	0	0	0	0	0	736	1472	768	64	32	0
0	0	0	160	320	440	560	280	0	0	0	0	0	0	0	0	0	0	0	704	1408	736	64	32	0
0	0	0	176	352	432	512	256	0	0	0	0	0	0	0	0	0	0	0	672	1344	704	64	32	0
0	0	0	192	384	424	464	232	0	0	0	0	0	0	0	0	0	0	0	632	1264	664	64	32	0
0	0	0	208	416	416	416	208	0	0	0	0	0	0	0	0	0	0	0	592	1184	624	64	32	0
0	0	0	224	448	416	384	192	0	0	0	0	0	0	0	0	0	0	0	552	1104	576	48	24	0
0	0	0	240	480	416	352	176	0	0	0	0	0	0	0	0	0	0	0	512	1024	528	32	16	0

A-7

Figure A-1 (Sheet 6 of 6)

ECHELLOGRAM SUBSECTION

TAPE 518 - DESTRUCTIVE R/O SIMULATION (SEC ALGNE), SEC PSF FWHM WIDTH = 50 MICR ONS

PTS: 201 TO 225 TOTAL PIXELS = 102400 SUM = 0.1113E 08
 RECS: 126 TO 275 AVG = 0.1087E 03

783	750	530	295	138	55	18	5	1	0	1	7	31	102	251	458	610	587	417	233	110	44	14	4	1
806	768	538	297	138	54	18	5	1	0	1	8	33	109	268	489	650	623	440	245	114	45	15	4	1
814	772	537	293	135	53	17	5	1	0	1	8	35	115	283	517	686	655	460	254	118	47	15	4	1
808	763	527	285	130	51	16	5	1	0	2	9	37	120	296	539	714	679	475	260	121	47	16	4	1
789	742	510	274	125	49	16	4	1	0	2	9	38	123	303	552	730	692	481	262	121	47	15	4	1
759	713	488	261	118	46	15	4	1	0	2	9	38	124	305	555	732	692	478	258	118	46	15	4	1
721	676	450	245	110	42	14	4	1	0	2	9	37	123	301	548	721	679	466	249	113	43	14	4	1
678	634	430	228	102	39	13	3	1	0	2	8	36	119	293	532	700	656	448	238	107	41	13	4	1
634	591	400	211	95	36	12	3	1	0	1	8	35	115	282	511	671	628	427	226	102	39	13	3	1
588	547	369	194	86	33	10	3	1	0	1	8	33	109	268	486	637	595	403	213	96	37	12	3	1
539	501	336	175	77	29	9	2	1	0	1	7	31	102	251	455	596	556	376	198	89	34	11	3	1
489	452	302	156	68	26	8	2	0	0	1	7	29	94	231	419	549	511	344	181	81	31	10	3	1
438	404	269	139	61	23	7	2	0	0	1	6	26	86	210	381	498	463	311	162	72	27	9	2	1
390	360	239	123	54	21	7	2	0	0	1	6	24	77	190	344	449	416	278	145	64	24	8	2	0
344	318	211	109	48	18	6	2	0	0	1	5	21	70	171	309	404	374	250	130	57	22	7	2	0
302	279	185	95	41	15	5	1	0	0	1	4	19	63	154	280	365	339	227	119	53	20	6	2	0
264	243	160	81	35	13	4	1	0	0	1	4	18	57	141	256	335	311	210	110	49	19	6	2	0
231	212	139	70	29	10	3	1	0	0	1	4	16	53	131	237	310	288	194	101	44	17	5	1	0
207	189	124	62	26	9	3	1	0	0	1	4	15	49	121	220	287	266	178	91	39	14	4	1	0
189	173	113	56	24	8	2	1	0	0	1	3	14	46	113	204	266	245	162	82	35	12	4	1	0
175	160	104	52	22	8	2	1	0	0	1	3	13	43	105	191	248	228	150	75	32	11	3	1	0
163	149	98	49	20	7	2	0	0	0	1	3	12	41	100	180	234	215	141	71	30	11	3	1	0
153	141	93	46	20	7	2	0	0	0	0	3	12	39	95	172	224	206	136	68	29	10	3	1	0
147	136	90	45	19	7	2	0	0	0	0	3	11	37	92	166	216	199	131	66	28	10	3	1	0
144	133	88	45	19	7	2	0	0	0	0	3	11	36	89	160	209	192	126	64	27	10	3	1	0
143	132	88	45	19	7	2	0	0	0	0	2	11	35	86	155	201	185	122	61	26	9	3	1	0
143	132	88	45	19	7	2	0	0	0	0	2	10	34	82	149	194	179	118	59	25	9	3	1	0
143	132	88	45	19	7	2	0	0	0	0	2	10	32	80	144	187	172	113	57	24	9	3	1	0
143	132	88	45	19	7	2	0	0	0	0	2	10	31	77	139	181	166	110	55	23	8	2	1	0
143	132	88	45	19	7	2	0	0	0	0	2	9	30	75	135	176	162	107	54	23	8	2	1	0
144	133	89	45	19	7	2	0	0	0	0	2	9	30	73	133	173	161	107	54	23	8	2	1	0
146	135	90	46	20	7	2	0	0	0	0	2	9	30	74	133	174	162	108	55	24	9	2	1	0
150	140	94	48	21	7	2	0	0	0	0	2	9	31	75	136	178	165	110	56	24	9	3	1	0
156	146	98	50	22	8	2	1	0	0	0	2	10	31	77	139	182	169	113	58	25	9	3	1	0
165	154	104	53	23	8	2	1	0	0	0	2	10	32	79	143	186	173	115	59	25	9	3	1	0
176	165	112	58	25	9	3	1	0	0	0	2	10	33	81	146	191	178	119	61	26	9	3	1	0
192	181	123	64	28	10	3	1	0	0	0	2	10	34	84	152	199	186	125	64	28	10	3	1	0
214	201	137	72	31	11	3	1	0	0	0	3	11	36	88	160	210	196	131	68	29	11	3	1	0
241	226	154	81	35	13	4	1	0	0	0	3	12	38	93	169	221	206	138	71	31	11	3	1	0
272	255	174	91	40	14	4	1	0	0	1	3	12	40	98	178	233	218	146	76	33	12	3	1	0
308	288	196	102	44	16	5	1	0	0	1	3	13	43	105	190	249	233	157	82	35	13	4	1	0
347	323	219	115	50	18	5	1	0	0	1	4	15	48	115	207	271	253	170	88	38	14	4	1	0
388	361	245	128	55	20	6	1	0	0	1	4	18	54	128	227	295	274	185	96	41	15	4	1	0
430	400	271	141	61	22	6	1	0	0	1	6	21	61	142	249	321	297	200	103	45	16	5	1	0
473	440	297	154	67	24	7	2	0	0	1	6	23	68	155	270	347	322	216	112	48	18	5	1	0
518	480	323	167	72	26	8	2	0	0	2	7	25	73	168	292	375	347	233	121	52	19	5	1	0
562	520	349	180	78	28	8	2	0	0	2	7	27	78	180	313	403	373	250	129	56	20	6	1	0
602	556	372	191	82	30	9	2	0	0	2	8	28	83	191	334	430	397	266	137	59	21	6	1	1
637	586	391	200	86	31	9	2	0	0	2	8	30	88	202	353	454	419	280	144	62	22	6	2	1
663	609	405	207	88	32	9	2	0	0	2	9	31	93	213	371	476	438	292	149	64	23	7	2	1
682	626	415	211	90	32	9	2	0	0	2	9	34	98	223	387	495	454	302	154	66	24	7	2	1
694	635	419	212	90	33	9	2	0	0	2	10	36	104	233	401	510	467	309	157	67	24	7	2	1

A-8

Figure A-2. Echellogram Subsection - Tape No. 518

ER-267

137	70	30	11	3	1	0	0	0	0	1	6	18	45	81	106	99	66	34	15	5	2	0	0	0	2
142	73	31	11	3	1	0	0	0	0	1	6	19	47	84	111	103	69	35	15	5	2	0	0	0	2
147	75	32	12	3	1	0	0	0	0	1	6	20	48	87	114	106	71	36	15	6	2	0	0	0	2
153	78	34	12	4	1	0	0	0	0	1	6	20	49	89	117	109	73	37	16	6	2	0	0	0	2
160	83	35	13	4	1	0	0	0	0	1	6	21	51	93	121	113	76	39	17	6	2	0	0	0	2
169	87	37	14	4	1	0	0	0	0	2	7	22	54	97	128	119	80	41	18	6	2	0	0	0	2
179	92	39	14	4	1	0	0	0	0	2	7	23	57	103	135	126	85	44	19	7	2	0	0	1	3
188	97	41	15	4	1	0	0	0	0	2	8	25	61	110	145	135	91	47	20	7	2	1	0	1	3
198	102	44	16	5	1	0	0	0	0	2	8	27	66	119	157	147	100	52	22	8	2	1	0	1	3
211	109	47	17	5	1	0	0	0	0	2	9	29	72	131	172	161	110	57	25	9	3	1	0	1	3
227	118	51	18	5	1	0	0	0	0	2	10	32	80	145	190	179	122	63	28	10	3	1	0	1	3
248	129	56	20	6	1	0	0	0	0	3	11	36	88	160	211	198	134	70	30	11	3	1	0	1	3
272	141	61	22	6	1	0	0	1	3	12	40	98	177	233	218	148	77	33	12	4	1	0	1	3	3
298	154	67	24	7	2	0	0	1	3	14	45	109	196	256	239	162	84	36	13	4	1	0	1	3	3
324	168	72	26	8	2	0	0	1	4	17	52	122	216	281	261	176	91	39	14	4	1	0	1	3	3
351	181	78	28	8	2	0	0	1	5	20	59	136	238	306	284	191	99	43	16	5	1	0	1	3	3
377	194	84	30	9	2	0	0	1	6	23	66	150	260	334	309	208	108	47	17	5	1	0	1	4	4
401	206	89	32	9	2	0	0	2	7	25	71	163	283	364	337	227	118	51	18	5	1	0	1	4	4
422	216	93	33	10	2	0	0	2	7	27	77	177	308	396	367	247	128	55	20	6	1	0	1	4	4
438	223	95	34	10	2	0	0	2	8	29	84	193	335	430	398	267	138	59	22	6	1	0	1	5	5
445	225	96	34	10	2	0	0	2	9	32	92	209	362	463	427	285	147	63	23	7	2	0	1	6	6
444	224	95	34	10	2	0	0	2	10	35	100	224	386	490	450	300	153	66	24	7	2	1	1	6	6
436	219	92	33	10	2	0	1	3	11	38	106	236	403	511	467	309	158	67	24	7	2	1	1	7	7
423	212	89	32	9	2	0	1	3	11	40	110	244	414	523	476	314	159	67	24	7	2	1	2	7	7
407	203	85	30	9	2	0	1	3	12	41	113	248	419	527	478	314	158	67	24	7	2	1	2	8	8
388	192	80	29	8	2	0	1	3	13	43	116	250	419	523	472	309	155	65	23	7	2	1	2	9	9
366	181	75	27	8	2	0	1	3	13	44	117	249	413	512	461	300	150	63	23	7	2	1	2	9	9
343	169	70	25	7	2	0	1	3	14	44	116	245	403	497	446	289	144	60	22	6	1	1	2	10	10
322	158	66	23	7	2	0	1	4	14	45	116	241	391	480	427	276	137	57	20	6	1	1	3	11	11
302	149	62	22	6	1	0	1	4	15	47	118	238	380	461	408	262	130	54	19	6	1	1	3	12	12
285	139	58	21	6	1	0	1	4	17	50	121	239	372	443	389	253	123	51	18	5	1	1	3	13	13
267	130	54	19	5	1	0	1	5	18	54	126	241	365	428	372	238	117	49	17	5	1	1	3	14	14

Figure A-2 (Sheet 3 of 6)

ECHFLLOGRAM SUBSECTION

TAPE 518 - DESTRUCTIVE R/O SIMULATION (SEC ALONE), SEC PSF FWHM WIDTH = 50 MICRONS

PTS: 226 TO 250 TOTAL PIXELS = 102400 SUM = 0.1113E 08
 RECS: 126 TO 275 AVG = 0.1087E 03

C	1	7	30	98	241	437	572	531	356	185	82	31	10	3	1	0	1	6	22	62	138	234	290	259
O	1	6	28	90	221	400	523	485	324	168	74	28	9	2	1	0	2	7	24	68	151	256	317	283
O	1	6	25	83	203	367	480	445	297	154	68	26	8	2	0	0	2	7	26	74	165	280	347	310
O	1	5	23	76	187	338	442	409	274	142	62	24	7	2	0	0	2	8	28	81	180	305	378	337
O	1	5	21	70	172	312	407	377	252	131	57	22	7	2	0	0	2	9	31	88	196	331	409	363
O	1	5	20	65	158	287	375	347	232	120	52	19	6	1	0	0	2	10	34	96	211	354	435	385
O	1	4	18	60	147	265	347	321	213	109	47	17	5	1	0	1	3	11	37	102	223	371	455	401
O	1	4	17	56	137	248	324	298	197	100	42	15	4	1	0	1	3	11	38	106	230	383	468	412
O	1	4	16	53	130	235	305	281	185	93	39	14	4	1	0	1	3	11	39	107	233	388	475	416
O	1	4	15	51	124	224	292	269	177	89	38	14	4	1	0	1	3	11	39	107	234	389	475	416
O	1	3	15	49	120	217	283	261	172	87	37	13	4	1	0	1	3	11	38	107	233	387	472	413
O	1	3	15	48	118	213	279	258	171	87	37	13	4	1	0	1	3	11	38	106	230	382	466	407
O	1	3	15	48	118	213	279	259	172	88	37	14	4	1	0	1	3	11	38	104	226	375	458	399
O	1	3	15	49	119	216	282	262	174	89	38	14	4	1	0	1	3	11	37	102	222	368	448	391
O	1	4	15	49	121	219	286	265	177	90	38	14	4	1	0	1	3	11	37	101	218	360	438	381
O	1	4	15	50	123	223	291	270	180	92	39	14	4	1	0	1	3	11	37	100	215	353	428	373
O	1	4	16	51	126	228	299	278	186	95	41	15	4	1	0	1	3	11	38	101	214	348	420	364
O	1	4	16	53	130	236	310	288	193	99	42	15	4	1	0	1	3	12	39	103	213	343	409	353
O	1	4	17	55	135	245	320	297	199	102	44	16	5	1	0	1	3	13	41	105	212	335	396	339
O	1	4	17	57	139	253	330	307	205	105	45	16	5	1	0	1	4	14	42	105	208	324	378	322
O	1	4	18	59	145	262	343	319	214	110	47	17	5	1	0	1	4	14	43	104	202	309	358	303
O	1	5	20	63	153	276	361	335	225	116	50	18	5	1	0	1	4	14	42	101	195	294	338	284
O	1	6	22	69	165	294	383	356	239	123	53	19	6	1	0	1	4	15	43	100	188	279	316	264
O	1	7	25	77	179	317	410	380	256	132	57	21	6	1	0	1	4	15	44	100	183	265	296	244
O	2	8	28	84	195	343	442	410	276	143	62	22	7	2	0	1	5	16	45	101	179	253	277	226
O	2	9	31	93	213	373	480	445	300	155	67	24	7	2	0	1	5	17	47	102	177	243	260	210
O	2	10	35	102	234	408	524	486	327	170	73	27	8	2	1	1	5	18	49	104	175	234	246	196
O	2	11	39	114	259	448	575	533	359	187	81	29	9	2	1	1	6	19	51	106	174	227	233	183
1	3	12	44	126	285	493	632	586	396	206	89	32	9	2	1	1	6	20	53	109	175	222	222	171
1	3	14	48	139	315	544	698	647	437	227	98	36	10	2	1	2	6	21	56	113	177	217	212	161
1	3	15	53	153	347	600	768	711	479	249	107	39	11	3	1	2	7	23	60	119	181	216	205	151
1	4	17	59	169	381	657	841	777	523	271	117	42	12	3	1	2	8	26	65	127	190	220	201	145
1	4	18	64	184	414	714	912	843	566	292	126	46	13	3	1	2	9	28	72	139	203	228	202	143
1	4	19	69	198	445	769	982	905	607	313	134	49	14	3	1	2	10	32	80	153	219	241	208	143
1	5	21	74	211	476	820	1047	964	644	331	142	51	15	3	1	3	11	35	89	168	238	256	215	145
1	5	22	79	224	504	868	1106	1016	678	348	149	54	16	4	1	3	12	39	98	184	258	273	224	148
1	5	23	83	236	529	910	1158	1063	708	362	155	56	16	4	1	3	13	44	108	203	281	292	234	151
1	6	24	86	246	551	946	1202	1102	732	373	159	58	17	4	1	4	15	48	120	223	307	314	246	155
1	6	26	90	254	560	974	1236	1130	748	380	162	58	17	4	1	4	16	54	133	246	335	338	260	160
1	6	26	92	261	580	991	1255	1144	755	382	162	59	17	4	1	4	18	59	146	269	364	362	273	165
1	6	27	94	264	585	997	1259	1146	754	380	161	58	17	4	1	5	20	65	159	292	392	385	285	169
1	7	28	95	265	584	992	1250	1134	744	374	158	57	16	4	2	5	21	69	171	313	418	407	297	172
1	7	28	95	264	578	978	1228	1111	726	364	153	55	16	4	2	5	23	74	183	333	443	428	308	176
1	7	29	96	262	569	955	1194	1076	701	350	147	53	15	4	2	6	24	79	194	353	468	448	319	179
1	7	29	96	259	556	925	1149	1032	670	333	140	50	14	3	2	6	26	84	205	373	492	469	330	183
2	7	30	97	255	549	888	1096	980	634	314	131	47	14	3	2	6	27	88	216	392	516	488	340	187
2	8	30	96	250	520	846	1036	922	594	293	122	44	13	3	2	7	28	92	225	409	537	505	350	190
2	8	31	97	245	500	803	975	863	554	273	114	41	12	3	2	7	29	95	233	422	553	519	356	192
2	8	32	97	241	482	761	914	804	514	253	105	37	11	3	2	7	30	97	238	430	562	524	358	191
2	9	33	99	239	465	720	854	745	475	232	96	34	10	2	2	7	30	98	238	430	561	521	352	186
2	9	34	100	235	448	678	793	686	434	212	87	31	9	2	2	7	30	96	235	423	550	509	342	179
2	10	35	101	232	430	637	733	629	396	192	79	28	8	2	2	7	29	93	227	408	530	489	327	170

II-V

Figure A-2 (Sheet 4 of 6)

7	26	76	173	301	386	356	238	123	53	19	6	1	1	3	11	37	96	192	299	366	357	273	162	76
7	27	79	182	318	408	377	253	130	56	20	6	1	1	3	12	39	101	201	306	365	346	260	152	70
8	29	84	193	337	433	401	269	138	59	22	6	1	1	3	13	42	108	211	316	366	338	248	143	66
8	31	90	206	359	461	425	284	146	63	23	7	2	1	3	14	46	116	224	328	371	332	238	135	61
9	33	97	220	381	487	449	299	153	66	24	7	2	1	3	15	49	124	238	344	380	330	230	129	58
10	36	104	233	402	512	470	313	160	69	25	7	2	1	4	16	53	134	255	363	392	332	226	124	55
11	39	110	245	420	533	489	325	166	71	26	7	2	1	4	18	58	146	275	387	410	338	224	121	53
11	40	113	253	434	551	504	334	170	73	26	8	2	1	5	19	64	159	298	415	433	348	225	119	52
12	41	116	259	443	562	514	340	173	73	26	8	2	1	5	21	70	174	324	447	458	360	227	119	51
12	41	117	261	448	567	518	341	173	73	26	8	2	1	5	23	76	188	350	479	485	374	232	119	51
12	41	117	261	447	566	515	338	170	72	26	8	2	1	6	25	82	203	376	512	512	389	236	119	50
12	42	117	260	442	558	507	332	167	70	25	7	2	1	6	27	88	218	402	544	540	404	241	120	50
12	42	117	257	435	546	493	322	161	68	24	7	2	1	7	29	94	232	427	576	567	418	245	120	49
13	43	117	253	424	529	476	310	155	65	23	7	2	2	7	30	100	246	452	607	592	431	249	120	49
13	44	116	248	411	509	457	297	148	62	22	6	2	2	7	32	105	259	475	635	615	443	252	120	48
14	44	115	242	397	490	439	285	142	59	21	6	2	2	8	33	110	270	495	659	634	452	253	119	47
14	44	115	238	386	473	421	273	135	57	20	6	2	2	8	35	114	280	512	680	650	459	254	118	46
15	47	117	237	377	457	404	261	129	54	19	6	1	2	8	36	117	288	525	696	662	463	254	117	46
17	50	121	238	370	441	387	248	123	51	18	5	1	2	9	36	119	293	534	706	670	466	254	117	45
18	53	126	240	363	425	369	235	115	48	17	5	1	2	9	37	120	296	539	712	674	466	252	115	44
20	57	130	240	354	406	349	221	108	45	16	5	1	2	9	37	121	297	540	712	672	462	248	112	43
21	60	133	239	344	387	329	207	101	41	15	4	1	2	9	37	120	295	536	705	663	453	241	108	41
23	63	138	240	336	370	311	194	94	39	14	4	1	2	8	36	118	289	526	691	647	440	233	105	40
25	67	144	244	331	356	294	183	88	36	13	4	1	2	8	35	114	281	510	670	626	426	225	101	39
27	72	151	249	328	344	279	171	82	33	12	3	1	2	8	34	110	270	490	644	602	409	216	97	37
29	77	158	254	325	331	264	160	76	31	11	3	1	1	7	32	105	258	468	614	574	390	206	93	36
31	82	166	260	322	319	249	149	71	28	10	3	1	1	7	30	99	244	443	581	543	368	195	87	34
34	87	173	266	320	309	236	140	66	26	9	3	1	1	7	29	93	229	416	546	510	345	182	81	31
36	93	182	274	322	302	226	132	62	25	8	2	1	1	6	27	87	214	389	509	474	320	167	74	28
39	100	193	286	328	299	219	126	58	23	8	2	1	1	6	25	81	199	360	471	438	294	153	67	25
43	108	208	304	340	301	214	122	56	22	7	2	1	1	5	23	75	184	333	434	403	269	139	61	23
47	127	228	327	357	307	213	119	54	21	7	2	1	1	5	21	69	168	305	398	369	246	128	56	21

A-13

Figure A-2 (Sheet 6 of 6)

ECHHELLOGRAM SUBSECTION

TAPE 255 - DESTRUCTIVE R/O SIMULATION (SEC ALCNE), SEC PSF WIDTH = 100 MICRONS

PTS: 201 TO 225 TOTAL PIXELS = 102400 SUM = 0.1113E 08
 RECS: 125 TO 275 AVG = 0.1087E 03

515	474	389	290	199	127	76	45	31	32	50	90	155	242	334	406	430	399	330	248	172	110	67	40	27
513	471	384	285	195	124	75	44	31	33	52	94	162	253	350	424	447	414	341	256	176	113	68	40	26
503	460	374	276	189	120	72	43	30	33	54	97	168	261	360	436	459	423	347	259	178	114	68	40	26
486	443	359	265	180	114	69	41	30	33	55	99	170	265	365	440	462	425	347	258	177	113	67	39	25
463	421	341	250	170	108	65	39	29	33	55	99	170	264	364	437	458	419	341	252	172	109	65	38	24
437	397	320	234	159	101	61	37	27	32	54	97	167	259	356	427	446	407	330	243	165	105	62	36	23
409	370	298	218	147	93	56	34	26	31	52	94	162	251	344	412	429	390	315	232	157	100	59	34	21
380	343	275	201	136	86	52	32	24	29	50	90	155	240	328	393	408	370	298	219	148	94	56	32	20
349	315	252	183	124	78	47	29	22	28	47	85	146	226	310	370	383	347	279	204	138	87	52	30	19
318	285	228	165	111	70	42	26	21	26	44	80	136	211	288	343	355	320	257	187	127	80	48	27	18
286	256	204	147	99	62	38	23	19	24	40	73	125	194	264	315	325	292	234	170	115	72	43	25	16
255	228	181	131	88	55	34	21	17	21	37	67	114	176	240	285	294	264	211	153	103	65	38	22	15
226	202	160	116	78	49	30	19	15	19	33	60	103	159	217	257	265	238	190	136	93	58	35	20	14
199	178	141	102	68	43	26	16	13	17	30	55	93	144	196	233	240	215	172	125	84	53	32	19	13
175	156	123	88	59	37	22	14	12	16	27	49	85	130	178	212	218	196	157	114	77	49	29	17	12
153	136	108	77	51	32	19	12	10	14	25	45	77	120	163	194	201	181	145	105	71	45	27	16	12
136	121	95	68	45	28	17	11	9	13	23	42	72	111	151	180	186	167	134	97	65	41	24	15	11
122	109	86	62	41	26	16	10	9	12	21	39	66	103	140	167	172	154	123	89	60	37	22	14	11
112	100	79	57	38	24	15	9	8	11	20	36	62	96	130	155	160	143	114	82	55	34	21	13	10
104	93	74	53	36	23	14	9	7	10	18	34	58	90	122	145	150	134	107	77	52	33	20	12	10
98	88	70	51	34	21	13	8	7	10	17	32	55	85	116	138	142	127	102	74	50	31	19	12	11
94	84	67	49	33	21	13	8	7	9	17	31	53	81	111	132	136	122	98	71	48	30	18	12	11
91	82	66	48	32	20	12	8	7	9	16	29	51	78	107	127	131	118	94	69	46	29	18	12	11
90	81	65	48	32	20	12	8	6	9	15	28	49	75	103	123	127	114	91	66	45	28	17	12	12
89	81	65	48	32	20	12	8	6	8	15	27	47	73	100	119	122	110	88	64	43	27	17	12	13
89	81	65	48	32	20	12	8	6	8	14	27	46	70	96	114	118	106	85	62	42	26	17	12	13
89	81	65	48	32	20	12	8	6	8	14	26	44	68	93	111	114	103	82	60	40	26	16	12	14
90	81	65	48	32	20	12	8	6	8	14	25	43	66	90	108	111	100	80	59	40	25	16	12	15
90	82	66	48	33	21	12	8	6	8	13	24	42	65	89	106	109	99	80	58	39	25	16	13	16
91	83	67	49	33	21	13	8	6	8	13	24	41	64	88	105	109	99	80	59	40	26	17	14	18
94	85	69	51	35	22	13	8	6	8	13	24	42	65	89	106	111	101	81	60	41	26	17	14	19
97	89	72	53	36	23	14	8	6	8	13	25	42	66	91	109	113	103	83	61	42	27	18	15	20
103	94	77	57	39	24	15	9	7	8	14	25	44	68	93	111	116	106	85	63	43	28	18	16	22
110	101	82	61	42	26	16	9	7	8	14	26	45	69	95	114	119	109	88	65	44	29	19	17	23
119	110	90	67	46	29	17	10	7	9	15	27	46	72	99	118	124	113	92	68	46	30	20	18	25
132	122	100	75	51	33	19	11	8	9	15	28	48	75	103	124	129	118	96	71	49	32	21	19	26
148	136	112	84	58	37	22	13	9	10	16	29	51	79	109	131	137	125	102	75	52	34	23	20	27
166	154	127	94	65	41	24	14	10	11	17	31	54	84	115	138	145	133	108	80	55	36	24	21	28
188	174	143	106	73	46	27	16	11	11	18	33	57	89	123	147	154	142	116	86	59	38	25	22	29
212	195	160	119	82	52	31	18	12	13	20	36	62	96	132	159	167	153	125	93	64	41	27	23	30
237	218	179	133	91	58	34	20	13	14	22	40	68	105	144	173	181	166	136	101	69	45	29	24	31
263	242	198	147	100	64	38	22	15	15	25	44	75	115	157	189	197	180	147	109	75	48	32	25	31
290	266	217	161	110	70	41	24	16	17	27	48	82	126	171	205	214	195	159	118	81	52	34	26	32
317	290	237	175	120	75	45	26	18	19	30	53	89	136	186	221	231	211	172	127	87	56	36	27	32
344	314	256	189	129	81	48	28	19	20	32	57	96	147	200	238	248	226	184	136	93	60	38	29	32
369	337	273	202	137	86	51	30	20	22	34	61	103	157	213	254	264	241	196	144	98	63	40	30	33
391	356	288	212	144	90	53	31	21	23	36	64	109	166	226	269	280	255	206	152	104	66	42	30	33
409	371	300	220	149	94	55	32	22	24	38	68	115	175	238	283	294	267	216	159	108	69	43	31	33
422	382	308	225	152	96	56	33	23	25	40	71	120	184	249	295	306	277	224	164	111	71	45	32	33
431	389	312	228	154	96	57	34	24	26	42	75	126	191	258	306	316	286	230	168	114	73	46	32	33
434	391	313	228	153	96	57	34	24	27	44	78	130	197	265	314	323	291	234	171	116	74	46	32	33
433	388	310	225	151	94	56	33	24	28	45	79	133	201	270	318	326	294	235	172	116	74	46	32	33

A-14

ER-267

Figure A-3. Echellogram Subsection - Tape No. 255

108	80	54	34	20	11	7	6	9	16	27	41	56	68	71	64	52	38	26	17	11	8	10	17	33
113	83	56	35	21	12	7	6	9	16	27	43	58	70	73	67	54	40	27	17	11	9	10	16	35
118	87	59	37	22	12	8	7	10	17	28	44	60	72	76	69	56	41	28	18	12	9	11	19	37
125	92	62	39	23	13	8	7	10	17	28	46	63	76	79	72	59	44	30	19	12	10	12	20	40
132	97	66	41	24	14	8	7	11	18	31	48	67	80	84	77	63	46	32	20	13	10	12	22	42
140	103	70	44	26	14	9	8	11	19	33	52	71	86	90	82	67	50	34	22	14	11	13	23	44
148	109	74	46	27	15	9	8	12	21	36	55	76	92	97	89	73	54	37	24	15	12	14	24	45
157	116	79	50	29	16	10	9	13	23	39	60	83	101	106	98	80	60	41	26	17	13	14	24	46
169	125	85	53	31	18	11	10	14	25	43	66	92	111	117	108	88	66	45	29	18	13	15	25	47
183	135	92	58	34	19	12	11	16	28	47	73	101	122	129	119	98	73	50	32	20	14	15	25	47
200	148	101	64	37	21	13	12	17	31	52	81	112	135	142	131	108	80	55	35	22	15	16	25	47
218	162	110	70	41	23	14	13	19	34	58	90	124	149	157	144	118	88	60	38	24	16	17	26	47
238	176	120	76	45	25	16	15	22	38	64	100	137	164	172	158	129	96	66	42	26	18	17	26	46
258	191	130	82	48	27	17	16	24	42	71	110	150	180	188	173	141	104	71	46	28	19	18	26	46
278	205	139	88	52	29	19	18	27	47	79	121	165	197	206	188	154	114	78	50	30	20	18	26	46
296	218	148	93	55	31	20	20	30	51	87	132	180	215	224	205	167	124	85	54	33	21	19	26	46
312	229	155	97	57	33	21	21	32	56	94	144	196	234	243	223	182	134	92	58	36	23	20	27	46
324	237	160	101	59	34	22	23	35	61	102	156	212	253	264	241	196	145	99	63	38	24	21	28	47
331	242	163	102	60	35	23	24	37	66	111	169	229	273	283	258	210	155	105	67	40	26	22	29	48
333	242	163	102	60	35	24	25	40	71	119	181	245	291	301	274	221	163	110	70	42	27	23	30	49
330	239	160	100	59	35	24	27	43	75	126	191	258	305	315	285	230	168	114	72	44	28	23	31	50
322	233	156	97	57	34	24	28	45	79	132	199	267	315	324	292	234	171	115	73	44	28	24	31	51
312	225	150	93	55	33	24	28	46	81	135	203	272	320	328	295	236	171	115	73	44	28	25	32	53
299	215	143	89	53	32	24	28	47	82	137	205	274	321	328	293	234	169	114	72	44	28	25	33	54
285	204	135	84	50	30	23	28	47	83	137	205	272	317	323	288	229	165	111	70	43	28	25	34	56
269	192	128	79	47	29	23	28	47	83	136	202	267	311	315	280	222	160	107	67	41	28	26	36	58
254	182	120	75	44	27	22	28	47	82	134	198	261	302	305	271	214	154	103	65	40	27	26	37	60
241	172	113	70	42	26	21	28	47	81	132	194	254	293	295	260	205	147	98	62	38	27	27	38	63
229	162	107	66	40	25	21	28	47	81	131	191	248	284	285	250	196	141	94	59	37	26	27	40	67
217	154	101	63	37	24	21	28	47	81	130	189	243	276	275	241	189	135	90	56	35	26	28	43	72
206	145	95	59	35	23	20	28	48	82	130	187	239	269	266	232	181	129	86	54	34	26	30	46	78
195	137	90	55	33	22	20	29	49	83	131	186	235	262	258	224	174	124	82	52	33	26	31	50	85
186	130	85	52	31	21	20	29	50	84	131	185	231	256	250	216	167	118	78	49	32	27	33	54	92

Figure A-3 (Sheet 3 of 6)

ECHTELLOGRAM SUBSECTION

TAPE 255 - DESTRUCTIVE R/O SIMULATION (SFC ALONE), SEC PSF WIDTH = 100 MICRONS

PTS: 226 TO 250 TOTAL PIXELS = 102400 SUM = 0.1113E 08
 RECS: 125 TO 275 AVG = 0.1087E 03

27	41	71	121	186	254	302	312	280	224	163	109	69	41	24	17	18	29	51	86	130	174	205	211	191
25	33	66	111	171	233	277	286	257	206	149	101	63	38	23	17	19	32	56	93	141	190	223	229	207
24	35	61	102	157	215	255	263	237	189	138	93	58	35	21	16	20	34	61	101	153	205	241	247	223
23	33	56	94	145	198	236	243	218	174	127	85	54	32	20	16	21	36	65	109	165	220	258	264	237
21	30	52	87	134	183	218	224	202	161	117	78	49	30	19	16	22	39	70	116	175	233	272	277	249
20	28	48	81	125	170	202	209	187	149	108	73	46	28	18	16	23	41	73	121	182	242	282	287	256
19	27	45	76	117	163	190	196	176	140	102	68	43	26	17	16	23	42	75	124	186	248	288	292	260
18	25	43	72	111	151	180	186	167	133	97	65	41	25	17	16	23	42	76	126	188	250	290	294	261
17	24	41	69	107	146	174	179	162	129	94	63	40	25	16	16	23	42	76	126	188	249	289	293	260
16	23	40	68	104	142	170	176	159	127	93	63	40	24	16	16	23	42	75	125	187	247	287	289	257
15	23	39	67	103	141	168	175	158	128	93	63	40	25	16	16	23	41	74	123	184	244	282	285	253
15	22	39	67	103	141	169	176	160	129	95	64	41	25	17	16	23	41	73	121	181	240	277	280	248
14	22	40	68	105	143	172	178	162	131	96	65	41	25	17	16	23	40	72	119	178	235	272	274	243
14	22	40	69	106	146	175	182	165	134	98	67	42	26	17	16	22	40	71	117	175	230	266	268	238
14	23	41	70	109	149	178	186	169	137	101	68	44	27	17	16	22	40	70	116	172	226	261	262	232
14	23	42	72	112	153	184	192	175	142	104	71	45	27	18	16	23	40	70	115	170	223	256	256	227
14	24	43	74	115	158	190	198	181	147	106	73	47	28	18	16	23	40	70	114	167	218	249	249	219
14	24	45	77	119	164	197	205	187	152	112	76	48	29	19	17	23	40	70	112	164	212	241	240	210
14	25	46	80	124	171	205	214	195	158	116	79	50	31	20	17	23	40	68	110	159	205	231	229	200
14	26	49	84	130	179	215	224	205	166	123	83	53	32	21	18	23	39	67	106	153	196	220	216	189
15	28	52	89	138	189	227	237	217	176	130	89	56	34	22	18	23	38	65	103	147	186	208	204	177
16	30	56	96	148	203	243	254	232	189	140	95	60	37	23	19	23	38	63	99	141	177	197	192	166
18	33	61	104	161	219	262	274	250	204	151	103	65	39	24	19	23	38	62	97	136	169	187	181	156
19	36	66	114	175	238	284	297	272	222	164	112	71	43	26	20	24	38	62	95	131	162	177	171	146
21	39	73	124	191	260	310	324	296	242	179	122	78	47	28	21	25	38	61	93	128	157	170	162	138
22	43	80	136	209	285	340	355	325	265	197	134	85	51	31	23	25	38	61	92	126	152	163	154	131
25	47	88	150	230	313	373	390	357	292	216	148	94	56	34	24	26	39	62	92	124	148	157	148	125
27	52	97	166	254	344	411	429	393	321	238	163	103	62	37	26	28	40	63	93	123	146	153	143	119
29	57	107	182	279	379	452	471	432	352	261	178	113	67	40	28	29	42	65	94	124	145	151	139	115
32	63	117	200	306	415	495	516	472	385	285	194	123	73	43	30	31	44	68	97	127	147	150	137	113
35	69	128	218	333	452	538	560	512	416	308	210	132	79	47	33	33	47	72	103	132	151	153	139	113
38	75	139	236	360	488	581	603	550	447	330	224	142	84	50	35	36	51	77	110	140	158	159	142	115
41	80	149	253	386	523	621	644	586	476	350	238	150	89	53	38	39	55	84	118	150	168	167	148	119
43	85	158	269	410	555	658	682	620	502	369	250	158	94	56	40	42	60	91	128	161	179	176	155	124
46	90	167	283	432	584	691	715	649	524	385	261	164	98	59	43	46	66	99	139	173	192	187	163	129
48	94	175	296	451	608	720	743	673	543	398	269	170	101	61	45	50	72	108	151	188	206	199	173	135
50	98	181	307	466	628	743	765	692	556	407	275	173	104	63	48	54	78	118	164	203	221	213	183	142
52	101	186	315	478	643	758	780	703	564	411	277	175	105	65	50	58	85	128	178	219	237	227	193	149
53	103	190	319	484	650	765	785	706	565	411	277	174	105	65	52	62	92	139	192	235	253	240	203	156
54	104	191	321	485	650	764	782	701	560	407	273	172	104	66	54	65	99	149	206	251	269	253	213	162
54	104	191	319	482	644	755	771	689	549	398	267	168	102	65	55	69	105	159	219	266	283	265	222	168
55	104	189	315	474	632	739	752	671	533	385	258	162	99	64	56	72	111	168	231	280	297	277	231	174
54	103	186	309	463	615	716	727	647	512	369	247	155	95	63	57	75	117	177	243	294	311	289	239	180
54	101	181	300	448	593	689	697	618	487	350	234	147	90	61	57	78	122	186	255	308	324	300	248	186
53	99	176	291	431	568	657	662	585	460	330	220	139	86	59	57	80	127	194	265	320	336	310	255	190
53	96	171	280	413	541	623	626	551	432	309	206	130	81	57	57	82	131	200	274	329	345	317	260	193
52	94	165	269	394	514	588	589	516	404	289	192	121	76	55	57	83	134	204	280	336	351	321	262	194
51	92	160	258	376	487	554	552	482	376	268	178	112	71	52	56	84	135	206	282	337	351	320	260	192
51	90	155	248	358	460	520	515	448	349	247	164	103	66	50	55	83	134	205	279	333	346	314	254	186
50	88	150	238	341	434	487	480	415	322	228	150	95	61	47	53	80	131	200	272	324	335	303	244	178
49	86	146	229	324	410	456	446	385	297	210	138	87	56	44	50	77	126	192	260	310	320	288	231	168
49	84	142	221	311	388	429	417	357	275	193	127	80	51	40	47	73	119	181	246	292	301	270	216	157

A-17

Figure A-3 (Sheet 4 of 6)

61	104	159	216	258	268	244	198	146	100	64	40	28	29	42	69	111	162	211	245	251	229	187	139	95
65	110	169	230	273	284	259	210	155	105	67	42	30	30	44	73	115	167	216	247	251	227	184	136	92
69	117	180	244	290	301	273	221	163	111	71	45	32	32	46	76	121	174	223	253	254	227	183	134	90
73	124	190	257	305	316	287	232	171	116	74	47	33	34	49	81	128	182	232	260	259	230	183	133	89
77	131	200	269	319	330	299	241	177	120	77	48	35	36	53	86	136	193	243	271	267	235	186	135	90
81	136	207	280	330	341	308	248	182	123	79	50	36	38	56	93	145	205	258	285	278	242	191	137	91
83	140	213	287	339	349	315	253	185	125	80	51	38	40	61	100	156	220	274	301	291	252	197	141	93
85	143	217	291	343	353	318	255	186	126	81	51	39	43	65	107	167	235	292	318	306	263	204	145	95
85	144	219	293	344	353	318	254	185	125	80	52	40	45	69	115	179	251	310	336	322	274	212	150	98
85	143	217	291	342	350	314	250	182	123	79	51	40	47	74	123	191	267	329	355	337	286	220	155	101
85	142	215	287	336	344	307	244	177	119	77	50	41	49	78	131	203	283	347	373	353	297	227	159	103
84	147	211	281	329	335	298	237	171	115	74	49	41	51	82	138	215	298	365	390	367	308	234	163	105
83	139	206	274	319	324	288	228	165	111	72	48	41	53	86	145	225	313	381	406	380	317	240	167	107
82	135	201	266	309	312	277	219	158	107	69	47	41	54	90	151	235	326	396	420	392	325	245	169	109
81	132	196	258	299	302	267	211	152	102	66	46	41	56	93	157	243	337	408	432	401	332	249	171	109
80	137	192	252	290	292	258	203	146	98	64	44	41	57	96	161	250	346	418	441	408	336	251	173	110
80	129	189	246	282	282	248	195	140	94	61	43	41	57	98	165	255	352	425	448	413	339	252	173	110
81	129	187	241	274	273	239	187	134	90	59	42	40	58	99	167	259	356	429	451	415	339	252	173	110
82	129	185	236	266	263	229	178	127	85	56	40	40	58	99	168	260	357	430	451	413	337	250	171	108
83	129	183	231	257	252	218	169	120	80	53	38	39	57	99	167	259	355	427	447	408	332	245	167	106
83	129	180	226	249	243	209	161	114	76	50	37	37	56	97	165	255	350	420	438	400	324	239	162	103
84	129	179	221	242	234	200	154	109	72	47	35	36	55	95	161	249	341	409	426	388	314	231	157	99
86	131	179	219	237	227	193	147	104	69	45	33	35	53	92	156	241	330	395	411	373	302	222	150	95
88	133	180	217	232	220	186	141	99	65	42	31	33	51	88	150	231	316	378	393	357	288	211	143	90
91	135	181	216	228	214	179	135	94	62	40	30	31	48	84	142	220	301	359	373	338	273	200	135	85
94	138	183	215	225	209	173	130	90	59	38	28	30	45	79	134	207	284	339	351	318	256	187	127	80
97	142	185	216	223	205	169	126	87	57	36	27	28	43	75	126	194	266	317	328	297	238	174	117	74
101	146	190	219	224	204	167	124	85	55	35	25	26	40	70	117	181	247	295	305	275	220	160	108	68
106	154	198	226	229	206	167	124	84	54	34	24	25	37	64	109	167	229	272	281	253	202	147	99	62
114	163	209	236	237	212	170	125	85	54	34	24	23	35	59	100	154	210	250	258	232	185	134	90	57
123	175	223	249	248	220	175	128	86	55	34	23	22	32	55	92	141	192	228	235	211	168	122	82	51
133	197	239	266	262	230	182	132	88	56	34	23	21	29	50	84	128	175	208	214	191	152	110	74	46
145	206	258	284	277	241	190	137	91	57	34	22	20	27	45	76	116	158	187	192	172	137	98	66	41

A-19

Figure A-3 (Sheet 6 of 6)

ER-267

ECHTELLOGRAM SUBSECTION

TAPE 422 - DESTRUCTIVE R/O SIMULATION (COMPLETE SYSTEM), LAMBDA = 2000 ANGST, SEC PSF WIDTH = 50 MICRONS

PTS: 201 TO 225 TOTAL PIXELS = 102400 SUM = 0.1098E 08
 RECS: 125 TO 275 AVG = 0.1072E 03

374	371	324	255	198	135	100	78	68	66	71	86	113	156	211	267	301	299	263	209	157	116	88	72	66
387	383	333	261	191	137	101	80	69	67	73	89	118	164	223	282	318	315	275	218	162	119	90	73	65
395	390	338	264	193	138	101	80	70	68	74	91	122	171	233	295	333	329	287	226	167	122	91	73	65
398	392	339	264	192	138	101	80	70	69	76	93	126	177	242	307	346	342	297	233	171	124	92	73	64
395	389	335	261	190	136	100	80	70	69	76	95	128	181	249	316	356	350	304	237	174	125	93	73	64
387	380	328	255	185	133	99	79	69	69	77	95	130	184	253	321	361	355	307	239	174	125	92	73	63
375	368	317	246	179	129	96	77	68	68	76	95	130	184	253	321	361	355	306	238	173	124	91	72	62
360	352	303	236	172	124	93	75	67	67	75	94	129	182	251	318	357	350	301	234	170	122	90	71	60
341	334	288	224	164	119	89	73	65	66	74	92	126	178	245	310	348	341	293	227	165	119	87	69	59
322	315	271	211	155	113	86	70	63	64	72	90	123	173	237	300	336	328	282	219	160	115	85	67	58
300	294	253	197	145	106	81	67	61	62	70	87	118	166	227	286	321	313	269	209	153	110	82	65	56
278	272	234	183	135	100	77	64	59	60	67	84	113	158	215	271	303	296	254	197	145	105	79	63	55
256	250	215	169	125	93	73	61	56	57	64	80	107	149	202	254	283	276	237	185	136	100	75	61	53
234	228	197	154	116	87	68	58	54	55	62	76	101	139	188	235	262	256	220	172	128	94	72	58	52
212	207	179	141	106	81	64	55	51	52	59	72	95	130	174	217	242	236	203	160	119	88	68	56	50
192	187	162	128	98	75	60	52	49	50	56	68	89	121	161	200	222	217	187	148	111	83	65	54	49
173	168	146	116	89	69	56	49	47	48	53	64	83	113	149	185	205	200	173	137	104	79	62	52	48
156	152	132	106	82	64	53	47	44	46	51	61	78	105	139	171	190	185	161	128	97	74	59	51	47
141	137	120	96	75	59	50	44	42	44	48	58	74	99	130	160	176	172	150	120	92	71	57	49	46
129	125	110	89	70	56	47	42	41	42	46	55	70	93	122	149	165	161	140	112	86	67	55	48	45
119	116	101	82	65	52	45	40	39	40	44	53	67	88	115	140	155	151	132	106	82	64	53	47	45
111	108	95	77	62	50	43	39	38	39	43	50	64	84	109	133	146	143	124	100	78	62	52	46	45
105	102	90	74	59	48	41	37	36	38	41	49	61	80	104	126	139	136	118	96	75	60	51	46	45
100	98	86	71	57	46	40	36	35	37	40	47	59	77	99	121	133	130	114	92	73	58	50	46	45
97	95	83	69	55	45	39	36	35	36	39	46	57	74	96	117	128	125	110	89	71	57	49	46	46
95	92	82	67	54	44	38	35	34	35	38	45	56	72	93	113	124	121	107	87	69	57	49	46	47
94	91	80	66	53	44	38	35	34	34	38	44	54	70	90	110	121	118	104	85	68	56	49	47	48
93	91	80	66	53	43	37	34	33	34	37	43	53	69	88	107	117	115	101	83	67	56	49	47	49
93	91	80	66	53	43	37	34	33	34	37	42	52	67	86	104	114	112	99	82	66	56	50	48	50
93	91	80	66	53	43	37	34	33	34	37	42	52	66	85	102	112	110	98	81	66	56	50	49	52
94	92	81	66	53	44	38	34	33	34	36	42	51	66	84	101	111	109	97	80	66	56	51	50	53
95	93	82	67	54	44	38	35	33	34	37	42	51	65	83	100	110	108	97	81	66	57	52	51	55
97	95	84	69	55	45	39	35	34	34	37	42	52	66	84	101	111	109	97	81	67	57	53	53	57
100	98	86	71	57	46	39	36	34	35	37	43	52	66	84	102	112	110	99	82	68	59	54	54	59
104	102	90	74	59	48	41	37	35	35	38	43	53	67	86	104	114	113	100	84	69	60	55	56	61
109	107	94	77	61	50	42	38	36	36	39	44	54	69	88	106	117	115	103	86	71	61	57	57	63
116	113	100	82	65	52	44	39	37	37	40	45	55	71	90	109	120	119	106	88	73	63	58	59	64
125	122	107	87	69	55	46	40	38	38	41	47	57	73	93	113	124	123	109	91	75	64	60	60	66
135	132	116	94	74	58	48	42	39	39	42	48	59	76	97	118	130	128	114	95	78	66	61	62	68
148	145	127	102	79	62	50	44	41	41	43	50	61	79	101	123	136	134	119	99	81	68	63	63	69
163	159	138	111	85	66	53	46	42	42	45	52	64	83	106	129	143	141	125	103	84	71	64	64	70
179	174	152	121	92	70	56	48	44	44	47	54	67	87	112	137	151	149	132	108	88	73	66	66	71
197	191	166	131	99	75	59	50	46	46	49	57	71	92	119	146	161	158	139	114	92	76	68	67	72
215	209	181	143	107	80	63	53	48	47	51	59	75	98	127	156	172	168	148	121	96	79	70	68	73
234	228	196	154	115	85	66	55	50	49	53	62	79	104	136	166	183	179	157	127	100	82	71	69	74
254	246	212	165	122	90	70	58	52	51	55	65	83	110	145	177	195	191	167	134	105	85	73	70	74
273	265	227	176	130	95	73	60	54	53	57	68	87	117	153	188	208	203	176	141	110	87	75	71	74
291	282	241	187	137	100	76	62	56	55	59	71	91	123	162	199	220	214	186	148	114	90	76	71	74
308	298	254	197	143	104	79	64	57	56	61	73	95	128	170	209	231	225	195	155	119	93	78	72	74
323	312	266	205	149	108	81	66	59	58	63	76	99	134	178	219	242	235	203	161	122	95	79	72	74
334	323	274	211	153	110	83	67	60	59	65	78	102	139	185	228	251	244	210	166	125	97	80	73	74
343	331	281	215	156	112	84	68	61	60	66	80	105	143	191	235	259	251	216	170	128	98	80	73	74

A-20

Figure A-4. Echellogram Subsection - Tape No. 422

111	89	68	53	43	36	33	31	32	34	39	46	56	66	71	70	63	53	44	38	35	34	36	40	47
112	90	69	53	43	37	33	32	32	34	39	47	57	67	73	72	64	54	45	39	36	35	36	41	48
115	92	71	54	44	37	34	32	32	35	40	48	59	69	75	73	66	55	46	40	36	36	37	42	50
118	94	72	56	45	38	34	33	33	35	41	49	60	71	77	76	68	57	47	41	37	36	38	43	51
122	98	75	57	46	39	35	33	34	36	42	50	62	73	79	78	70	59	49	42	38	37	39	44	53
127	101	77	59	47	40	36	34	34	37	43	52	64	75	82	81	72	61	50	43	39	38	40	45	55
133	106	80	61	49	41	37	35	35	38	44	54	66	79	86	84	75	63	52	44	40	39	41	46	56
139	110	84	64	50	42	38	36	36	40	46	56	70	83	90	88	79	66	54	46	41	40	42	47	58
146	116	88	66	52	44	39	37	38	41	48	59	73	87	95	94	83	69	57	48	43	41	43	49	59
154	122	92	69	54	45	40	38	39	43	50	62	78	93	102	100	89	74	60	50	44	42	44	49	60
163	129	97	73	57	47	42	40	41	45	53	66	83	100	109	107	95	78	63	52	46	44	45	50	61
174	137	103	77	60	49	44	41	42	47	56	70	89	107	118	116	102	84	67	55	48	45	46	51	62
186	146	109	81	62	51	45	43	44	49	59	75	96	116	127	125	110	90	71	57	49	46	47	52	62
200	156	116	86	66	54	47	45	46	52	63	81	103	125	138	135	119	96	75	60	51	47	48	53	63
214	167	123	91	69	56	49	47	49	55	67	87	112	136	149	146	128	103	80	63	53	49	49	53	63
229	178	131	96	72	58	51	49	51	58	72	93	120	147	161	157	137	110	85	67	55	50	50	54	64
245	190	139	101	76	61	53	51	53	61	76	100	130	158	174	169	147	117	90	70	58	52	51	54	64
259	200	146	105	79	63	55	53	56	65	81	107	139	170	187	182	158	125	95	73	60	53	51	55	64
273	210	152	109	81	65	57	55	58	68	86	114	149	183	201	195	169	133	101	77	62	54	52	56	65
284	218	158	113	84	67	59	56	60	71	91	121	159	195	215	209	180	141	106	80	64	56	53	56	65
293	224	162	116	86	68	60	58	62	74	95	128	169	208	229	222	191	149	112	84	66	57	54	57	66
298	228	164	117	87	70	61	59	64	77	100	135	179	220	242	234	200	156	116	87	68	58	55	58	67
300	229	165	118	88	70	62	61	66	79	104	141	187	230	253	244	209	162	120	89	70	59	56	59	67
298	227	164	118	88	71	63	62	67	82	107	146	194	238	262	252	215	167	123	91	71	60	57	59	68
293	224	162	116	87	71	63	62	69	83	110	150	199	244	267	257	219	169	125	92	72	61	57	60	69
286	219	158	114	86	70	63	63	69	85	112	152	201	247	270	259	220	170	125	93	72	62	58	61	70
277	212	154	112	85	70	63	63	70	85	113	153	202	247	270	258	219	169	125	93	72	62	59	61	71
267	205	149	109	83	69	63	63	70	86	113	153	202	246	267	255	216	167	124	92	72	62	59	62	72
257	197	144	106	82	68	62	63	70	86	113	153	200	242	262	250	212	164	122	91	72	62	59	63	74
246	189	139	103	80	67	62	63	70	86	113	152	197	238	257	244	207	160	119	90	71	62	60	64	76
236	181	134	100	78	66	61	63	70	86	113	151	195	233	250	238	201	156	116	88	71	62	61	65	78
226	174	129	97	76	65	61	62	70	87	113	150	193	229	244	231	195	152	114	87	70	62	61	67	80
217	167	124	94	75	64	60	62	71	87	113	150	191	225	238	224	189	147	111	85	70	62	62	69	83

A-22

Figure A-4 (Sheet 3 of 6)

ECHELLOGRAM SUBSECTION

TAPE 422 - DESTRUCTIVE R/U SIMULATION (COMPLETE SYSTEM), LAMBDA = 2000 ANGST, SEC PSF WIDTH = 50 MICRONS

PTS: 226 TO 250 TOTAL PIXELS = 102400 SUM = 0.1098E 08
 RFCS: 125 TO 275 AVG = 0.1072E 03

66	74	91	122	170	232	291	324	315	270	209	153	110	81	63	53	49	49	55	67	85	107	125	129	116
65	71	87	116	160	216	270	301	293	251	195	143	104	77	61	52	49	50	57	70	90	114	134	138	124
64	69	84	110	150	202	251	279	272	234	182	134	98	74	59	51	49	51	58	73	96	122	143	148	133
62	67	80	104	141	188	234	259	252	217	170	126	92	70	57	50	48	51	60	77	101	130	153	159	143
61	65	77	98	133	176	218	241	235	202	158	118	87	67	55	49	48	52	62	80	107	138	163	169	152
60	63	73	93	125	165	203	225	219	188	148	111	83	65	54	49	48	53	64	84	113	146	173	179	160
58	61	71	89	118	155	190	210	204	176	139	105	79	62	52	48	48	54	66	87	118	154	182	188	168
57	59	68	85	112	146	179	197	191	165	131	99	75	60	51	47	48	54	67	89	122	159	189	195	174
56	58	66	81	106	138	169	186	181	156	124	94	72	58	50	47	48	55	68	91	125	164	194	200	179
54	56	64	78	102	132	161	177	172	149	118	90	70	56	49	46	48	55	69	93	127	166	197	203	181
53	55	62	76	99	127	155	170	166	143	114	87	68	55	48	46	48	55	69	93	128	167	198	205	182
52	53	60	74	96	124	151	166	161	140	111	86	66	54	48	46	48	55	69	93	128	167	198	204	182
50	52	59	73	94	122	148	163	159	138	110	85	66	54	47	46	48	55	69	93	127	166	197	203	181
49	52	59	72	94	121	147	162	158	137	110	84	65	54	47	45	48	55	69	92	126	165	195	201	178
48	51	58	72	94	121	148	163	158	138	110	84	66	54	47	45	48	55	69	92	125	163	192	198	176
48	50	58	72	94	122	149	164	160	139	111	85	66	54	47	45	48	54	69	91	124	161	189	194	173
47	50	58	73	95	124	151	167	163	141	113	86	67	54	48	46	48	54	68	90	122	158	186	191	170
46	50	58	73	97	126	154	170	166	144	115	88	68	55	48	46	48	54	68	90	121	156	183	187	166
46	50	59	75	99	129	158	175	171	148	118	90	69	56	49	46	48	54	68	89	120	154	180	183	162
46	51	60	76	101	133	163	180	176	153	121	92	71	57	49	47	48	55	68	89	119	152	176	179	158
46	51	61	78	104	137	169	187	182	158	125	95	73	58	50	47	49	55	67	88	117	148	171	173	152
47	52	63	81	106	143	176	194	190	164	130	99	75	60	51	48	49	55	67	87	115	145	165	167	147
47	53	65	84	114	150	185	204	199	172	136	103	78	62	53	49	50	55	67	86	113	141	160	160	141
48	55	68	89	120	158	195	216	210	182	144	108	82	64	54	50	50	56	67	85	110	137	154	153	134
49	57	71	94	127	169	208	230	224	193	152	114	86	67	56	51	51	56	67	85	109	133	149	147	128
51	59	75	99	136	181	223	246	239	207	163	122	91	70	58	53	52	57	67	85	107	130	144	141	123
52	62	79	106	146	194	240	265	258	222	174	130	96	74	61	54	53	58	68	85	106	127	139	136	118
54	65	84	113	157	210	259	287	279	240	187	139	102	78	64	56	55	59	69	85	106	125	136	132	114
57	68	89	122	169	227	281	311	302	259	202	149	109	82	67	58	56	60	70	86	106	124	133	128	110
59	72	94	130	182	246	305	338	328	281	219	160	116	87	70	61	58	62	71	87	107	124	132	125	107
61	76	100	140	197	267	332	367	356	305	236	172	124	92	73	63	60	64	73	89	108	125	131	124	105
64	80	107	150	212	288	360	398	386	330	255	185	132	97	77	66	63	66	76	92	111	127	132	123	103
67	84	113	160	228	311	388	430	417	355	273	197	140	103	80	69	65	69	79	96	115	130	134	124	103
69	88	119	170	243	333	416	462	447	380	292	210	148	108	84	72	68	71	83	100	120	135	138	126	104
72	92	126	180	258	354	444	492	476	404	309	222	156	113	88	74	70	75	87	106	127	142	144	130	107
74	96	131	189	272	375	470	521	503	427	326	233	163	118	91	77	73	78	91	112	134	150	150	135	110
77	99	137	197	285	393	493	547	528	447	340	243	170	122	94	80	76	82	96	119	143	159	158	141	113
79	102	142	205	297	409	514	569	549	465	353	251	175	126	97	83	79	86	102	126	152	169	167	147	118
81	105	146	211	307	423	531	588	567	479	363	258	180	129	100	85	82	90	108	134	162	179	177	155	123
83	107	149	217	314	433	544	602	579	489	370	263	183	131	102	87	85	93	114	143	172	191	187	163	128
84	109	152	220	319	440	552	610	587	494	374	265	185	133	103	89	87	97	119	151	183	202	197	170	133
85	110	153	222	322	443	555	612	588	495	374	265	185	134	104	90	90	101	125	159	194	214	208	178	138
86	111	154	223	322	442	553	609	584	491	371	263	184	133	104	92	92	105	131	167	204	225	218	186	143
86	111	153	222	320	438	546	600	575	483	365	259	182	132	104	92	93	108	136	175	214	235	227	193	148
86	111	152	219	315	430	535	587	561	471	356	253	178	130	104	93	95	111	141	182	223	245	236	200	152
86	110	151	216	309	420	520	569	543	455	345	246	173	128	102	92	96	113	145	189	232	255	245	206	156
86	109	149	212	301	407	502	548	522	437	331	236	168	124	101	92	96	115	149	195	240	263	252	212	160
86	108	146	207	293	393	482	524	498	417	316	226	162	121	99	91	97	116	152	200	246	270	259	216	162
85	106	143	202	283	378	461	498	472	395	300	216	155	117	96	90	96	117	154	203	250	275	263	219	164
84	105	140	196	274	363	439	472	446	373	283	204	148	112	94	88	95	117	155	204	252	277	264	219	164
83	103	138	191	264	347	417	446	420	351	267	193	141	110	91	86	94	116	154	203	251	275	262	217	162
82	102	135	186	255	332	396	421	394	329	250	182	133	103	88	84	92	114	151	200	247	270	257	213	158

A-23

ER-267

Figure A-4 (Sheet 4 of 6)

60	81	111	147	182	201	195	169	134	101	78	63	56	56	61	73	95	126	163	197	218	215	189	150	110
62	84	115	154	190	210	205	177	139	105	81	65	58	57	62	75	97	128	165	198	215	210	183	145	107
64	87	120	161	199	221	215	185	146	110	83	67	59	58	64	77	99	131	167	199	215	207	179	141	104
66	91	126	169	209	232	225	194	152	114	86	69	61	60	65	79	102	134	171	202	215	206	176	138	101
69	94	131	177	220	243	236	203	159	119	89	71	63	61	67	81	105	139	176	206	218	206	175	136	100
71	98	137	185	230	254	247	212	165	123	92	73	64	63	69	84	109	144	182	212	222	207	175	135	99
74	102	143	193	239	264	256	220	171	127	95	75	66	65	71	87	114	150	190	220	228	211	176	135	98
76	105	147	199	248	274	265	226	176	130	97	77	67	66	74	91	119	158	199	229	236	216	178	136	95
78	108	151	205	254	281	271	232	180	133	99	79	69	68	76	94	125	166	209	240	245	223	182	138	100
79	110	154	208	259	286	276	235	183	135	101	80	70	70	79	99	131	175	221	252	256	231	187	140	101
80	111	156	211	261	288	278	237	184	136	101	81	71	72	81	103	138	185	233	265	268	239	193	143	103
81	112	156	211	262	288	278	237	183	136	102	81	72	73	84	107	145	194	245	278	280	249	199	147	105
81	112	156	210	260	286	275	234	182	135	101	82	73	75	86	111	151	204	257	292	292	258	205	150	106
81	112	155	208	257	282	271	230	179	133	101	82	74	76	89	115	157	213	269	305	303	267	210	154	108
82	111	154	206	252	276	265	225	175	131	99	81	74	77	91	119	163	222	280	317	315	275	216	157	110
82	111	152	202	247	269	258	220	171	128	98	81	74	78	93	122	169	230	291	328	324	282	220	159	112
82	110	150	198	241	262	251	213	166	125	96	80	74	79	94	125	174	237	300	337	333	289	224	161	113
82	109	149	195	236	255	243	207	162	122	95	79	74	79	96	127	178	243	307	345	340	294	227	163	113
82	109	148	192	231	248	236	201	157	119	93	78	74	79	96	129	181	247	313	351	345	297	229	164	114
82	109	147	189	226	241	229	194	152	115	90	77	73	79	97	130	182	250	316	355	348	299	230	164	114
83	110	146	187	221	235	221	187	147	112	88	75	72	79	97	130	183	251	318	356	349	299	229	163	113
84	110	146	185	216	228	214	180	141	108	86	74	71	78	96	130	183	251	317	355	347	297	227	162	112
84	111	145	183	212	221	206	174	136	105	84	72	70	77	95	129	181	248	313	351	343	293	224	159	110
85	111	145	181	208	215	199	167	131	101	81	71	69	76	94	127	178	244	308	344	336	287	219	156	108
86	113	145	180	204	210	193	161	127	98	79	69	67	74	92	124	174	238	300	335	326	279	213	152	105
88	114	147	180	202	205	187	156	122	95	77	67	66	73	89	120	168	230	290	324	315	269	206	147	102
89	116	149	180	200	201	182	151	118	92	74	66	64	71	87	116	162	221	278	310	302	258	197	141	99
91	118	151	181	199	197	177	146	115	89	73	64	63	69	84	112	155	211	265	296	288	246	188	135	95
93	121	153	183	198	195	174	143	111	87	71	62	61	67	81	107	148	201	251	280	272	232	178	128	90
96	124	157	186	200	194	172	140	109	85	69	61	59	64	78	102	140	189	237	263	256	218	168	121	85
99	129	162	190	203	195	171	138	107	83	68	60	58	62	74	97	133	178	222	246	239	204	157	114	81
103	134	169	197	208	198	171	138	106	82	67	59	56	60	71	92	125	167	207	229	222	190	147	106	76
108	141	178	206	216	203	174	138	106	82	66	58	55	58	68	87	117	155	192	212	206	176	136	99	71

A-25

Figure A-4 (Sheet 6 of 6)

ER-267

ECHELLOGRAM SUBSECTION

TAPE 275 - DESTRUCTIVE R/O SIMULATION (COMPLETE SYSTEM), LAMBDA = 2000 ANGST, SEC PSF WIDTH = 100 MICRONS

PTS: 201 TO 225 TOTAL PIXELS = 102400 SUM = 0.1092E 08
 RECS: 125 TO 275 AVG = 0.1066E 03

313	301	272	232	191	154	125	106	97	98	110	133	165	202	237	263	272	262	238	205	170	138	113	96	88
312	300	270	231	189	153	124	105	97	99	112	136	170	208	244	270	279	269	243	209	173	140	114	96	87
377	295	265	226	186	150	122	104	97	100	113	138	173	212	249	275	284	273	246	211	174	140	113	95	85
299	286	257	220	180	146	119	102	95	99	114	139	174	213	250	277	285	274	246	210	173	139	112	93	83
288	276	248	211	174	141	116	100	94	98	113	138	173	212	249	275	283	271	244	208	170	137	110	91	81
274	263	236	201	166	135	111	97	91	96	111	136	170	209	245	270	277	265	238	203	166	133	107	89	79
260	248	223	190	157	128	106	93	88	93	108	133	166	203	238	262	268	257	230	196	160	129	104	86	76
244	233	209	179	148	121	101	89	85	90	104	128	160	196	229	251	257	246	220	187	154	124	100	83	74
227	217	195	167	138	114	96	84	81	86	100	123	153	187	218	239	244	233	209	178	146	118	96	80	71
210	200	180	154	129	106	90	80	77	82	95	117	145	176	205	225	230	219	196	167	138	112	91	77	69
193	184	166	142	119	99	84	75	73	78	90	110	136	166	192	210	214	204	183	157	129	105	86	73	66
176	168	151	130	109	92	78	71	69	74	85	104	128	154	179	195	199	190	170	146	121	99	82	70	64
160	153	138	119	101	85	73	66	65	70	80	97	119	143	166	180	184	176	158	136	113	93	78	67	62
145	139	125	109	92	78	68	62	61	65	75	91	111	133	153	167	170	162	146	126	106	88	74	65	60
132	126	114	99	85	72	63	58	58	62	71	85	103	124	142	155	158	151	136	118	99	83	70	62	59
120	115	104	91	78	67	59	55	54	58	67	80	97	116	133	144	147	141	127	110	93	79	67	60	56
110	105	95	84	72	62	55	52	52	55	63	75	91	108	124	135	137	132	119	104	88	75	65	59	57
101	97	88	78	67	59	53	49	49	53	60	71	86	102	117	127	129	124	112	98	84	72	63	58	57
95	91	83	73	64	56	50	47	47	50	57	68	82	97	110	119	122	117	106	93	80	69	61	57	56
89	86	78	69	61	53	48	45	45	48	55	65	78	92	105	113	116	111	102	89	77	67	60	56	57
85	82	75	67	58	51	46	44	44	47	53	62	75	88	100	108	111	107	97	86	75	65	59	56	57
82	79	73	65	57	50	45	43	43	45	51	60	72	85	96	104	107	103	94	84	73	64	59	56	58
80	77	71	63	55	49	44	42	42	44	50	59	70	82	93	101	103	100	92	81	72	64	58	57	60
79	76	70	62	55	48	44	41	41	43	49	57	68	80	91	98	100	97	89	80	70	63	59	58	61
78	75	69	62	54	48	43	41	40	43	48	56	66	78	88	96	98	95	87	78	70	63	59	59	63
78	75	69	62	54	48	43	40	40	42	47	55	65	76	86	93	96	93	86	77	69	63	60	60	66
78	75	69	62	54	48	43	40	40	42	47	54	64	75	85	92	94	91	85	77	69	63	60	62	68
79	76	70	62	54	48	43	40	40	42	47	54	63	74	84	91	93	90	84	76	69	64	61	64	71
80	77	71	63	55	48	44	41	40	42	46	54	63	73	83	90	92	90	84	77	69	65	63	66	74
82	78	72	64	56	49	44	41	40	42	47	54	63	73	83	90	93	90	85	77	70	66	65	68	78
84	81	74	66	58	50	45	42	41	43	47	54	63	74	84	91	94	91	86	78	72	67	66	70	81
87	83	77	68	60	52	46	43	42	43	48	55	64	75	85	92	95	93	87	80	73	69	68	73	84
91	87	80	71	62	54	48	44	43	44	49	56	66	77	87	94	97	95	89	82	75	71	70	75	88
96	92	85	75	65	57	50	46	44	46	50	57	67	79	89	97	100	98	92	84	77	73	73	78	91
102	99	91	80	69	60	52	48	46	47	51	59	69	81	92	100	103	101	95	87	80	75	75	81	94
117	106	97	86	74	63	55	50	48	49	53	61	72	84	95	104	107	105	98	90	82	77	77	83	97
119	115	105	93	80	68	58	52	50	51	55	63	75	87	99	108	112	109	102	94	85	80	79	85	100
130	125	115	101	86	73	62	55	52	53	58	66	78	91	104	113	117	114	107	98	89	83	82	88	102
142	137	125	109	93	78	66	58	55	55	60	69	82	96	110	119	123	120	113	102	92	86	84	90	104
155	149	136	118	100	83	70	62	58	58	63	73	86	101	116	126	130	127	119	107	97	89	87	91	106
169	163	148	128	108	89	75	65	61	61	67	77	91	108	123	134	138	135	125	113	101	92	89	93	107
184	176	160	138	115	95	80	69	64	64	70	81	97	114	131	143	147	143	132	119	105	96	91	95	107
198	190	172	148	123	101	84	73	67	67	74	86	102	121	139	152	156	152	140	125	110	99	94	96	108
213	204	184	158	131	107	89	76	70	70	77	90	108	128	147	161	165	160	147	131	115	102	96	97	108
227	217	195	167	138	113	93	79	73	73	81	95	114	135	156	170	175	169	155	137	119	105	98	98	108
240	229	206	176	145	118	97	82	76	76	84	99	119	142	164	179	183	177	162	143	123	108	99	98	107
251	239	215	183	151	122	100	85	78	79	87	103	124	148	171	187	191	184	168	148	127	111	101	99	107
260	248	222	189	155	126	102	87	80	81	90	106	129	154	178	194	199	191	174	152	130	113	102	99	106
267	255	228	193	159	128	104	89	82	83	92	109	133	159	184	200	205	197	179	156	133	114	103	99	105
272	259	231	196	160	129	106	90	83	84	94	112	136	163	189	206	210	201	182	158	135	116	103	99	104
274	260	232	197	161	130	106	91	84	85	96	114	139	167	192	209	213	204	185	160	136	116	103	98	103
274	259	231	196	160	129	106	91	84	86	97	115	140	168	194	211	215	206	186	161	136	116	103	97	101

A-26

ER-267

Figure A-5. Echellogram Subsection - Tape No. 275

99	86	73	61	51	45	40	39	40	43	48	54	59	63	65	63	59	54	49	45	44	45	49	58	72
102	89	75	63	53	46	41	40	41	44	49	55	61	65	67	65	61	55	50	47	45	46	51	60	74
106	92	78	65	54	47	42	41	42	45	50	57	63	67	69	67	63	57	52	48	46	48	53	62	77
110	96	81	67	56	48	44	42	43	47	52	59	65	70	72	70	65	59	54	50	48	49	54	64	80
115	100	84	70	58	50	45	43	44	48	54	61	68	73	75	73	68	62	56	52	49	51	56	66	82
121	105	88	73	61	52	47	45	46	50	57	64	72	77	79	77	72	65	59	54	51	52	57	68	85
127	110	92	76	63	54	49	47	48	53	60	68	76	82	84	82	76	69	62	56	53	54	59	70	87
135	116	97	80	67	57	51	49	51	55	63	72	81	87	89	87	81	73	65	59	55	56	60	71	88
143	123	103	85	70	60	53	51	53	59	67	77	87	93	96	93	86	78	69	62	57	57	62	72	89
152	131	109	90	74	63	56	54	56	62	71	82	93	100	103	100	93	83	73	65	60	59	63	73	90
163	140	116	95	78	66	59	57	59	66	76	88	100	108	111	108	99	88	77	68	62	61	64	74	91
174	149	124	101	82	69	62	60	63	70	81	95	107	116	119	116	106	94	82	72	65	63	66	75	91
186	159	132	107	87	73	65	63	66	75	87	102	116	125	128	124	114	101	87	75	68	65	67	75	91
198	169	139	113	92	77	68	66	70	79	93	109	124	135	138	133	122	107	92	79	70	66	68	76	91
209	179	147	118	96	80	71	69	74	84	99	117	133	145	148	143	130	114	97	83	73	68	69	77	91
220	187	154	124	100	83	74	73	78	89	106	125	143	155	159	152	139	121	103	87	76	70	71	77	91
229	195	159	129	103	86	77	76	81	94	112	133	152	165	169	162	147	128	108	91	79	72	72	78	91
237	201	164	131	106	89	80	78	85	99	118	141	161	176	179	172	156	135	114	95	82	74	73	79	91
242	204	167	134	108	91	82	81	88	103	124	148	170	185	189	181	164	141	118	99	84	76	74	80	92
244	206	168	135	109	92	83	83	92	108	130	155	179	194	198	189	171	147	123	102	86	77	75	80	92
244	206	168	135	109	92	84	85	94	111	135	161	185	201	205	196	176	151	126	104	88	79	76	81	92
241	203	166	134	109	92	85	86	96	114	138	166	190	207	210	200	179	154	128	106	89	80	77	82	93
237	200	163	131	107	92	85	87	97	116	141	169	194	210	213	202	181	155	129	106	90	80	78	82	94
230	195	159	129	106	91	85	87	98	117	142	170	195	211	214	203	181	155	129	106	90	81	78	83	94
223	189	155	125	104	90	84	87	98	117	143	170	195	210	213	201	180	154	128	106	90	81	79	84	96
216	182	150	122	101	88	84	87	98	117	142	169	193	208	210	199	177	151	126	105	89	81	79	85	97
208	176	145	118	99	87	83	86	98	117	141	167	191	205	206	195	174	149	124	103	89	81	80	86	99
200	170	140	115	96	85	82	86	97	116	140	165	188	201	202	190	170	145	122	102	88	81	81	88	101
193	164	135	111	94	84	81	85	97	115	138	163	184	197	197	186	166	142	119	100	87	81	82	90	103
187	158	131	108	92	82	80	85	96	114	137	161	182	193	193	182	162	139	117	99	87	81	83	92	107
180	153	127	105	90	81	79	84	96	114	136	160	179	190	189	177	158	136	114	97	86	82	85	95	111
175	148	123	103	88	80	79	84	96	114	136	158	177	186	185	173	154	133	112	96	86	83	87	98	116
170	144	120	100	87	79	78	84	96	114	135	157	175	183	182	170	151	130	110	95	86	84	89	102	121

A-28

Figure A-5 (Sheet 3 of 6)

ER-267

ECHELLOGRAM SUBSECTION

TAPE 275 - DESTRUCTIVE R/D SIMULATION (COMPLETE SYSTEM), LAMBDA = 2000 ANGST, SEC PSF WIDTH = 100 MICRONS

PTS: 226 TO 250
 RECS: 125 TO 275

TOTAL PIXELS = 102400 SUM = 0.1092E 08
 AVG = 0.1066E 03

88	98	115	139	167	192	209	213	203	181	155	128	104	85	72	66	65	70	81	95	111	124	129	124	109
86	94	109	131	157	180	195	198	189	169	145	120	98	81	70	65	65	72	84	100	118	132	137	132	116
83	90	104	124	147	168	182	185	176	159	136	113	93	78	68	64	66	74	87	105	124	139	145	139	122
81	86	99	117	138	158	171	174	165	149	128	107	89	75	67	64	67	76	90	110	130	146	153	146	128
78	83	94	111	131	149	161	163	155	140	121	102	85	72	65	63	67	77	93	114	135	152	159	152	133
76	80	90	106	124	141	152	154	147	133	115	97	81	70	64	63	67	78	95	117	139	157	163	156	136
73	77	87	101	118	134	144	147	140	127	110	93	79	68	63	62	68	79	97	119	142	160	167	159	139
71	74	84	97	114	129	139	141	135	122	106	90	77	67	62	62	68	80	98	120	143	161	168	161	140
69	72	81	95	110	125	134	137	131	119	103	88	75	66	61	62	68	80	98	120	144	162	169	161	140
67	70	79	92	108	122	132	134	128	117	102	87	74	65	61	61	67	80	98	120	143	161	168	160	140
65	69	78	91	106	121	130	133	127	116	101	86	74	65	61	61	67	79	97	119	142	160	167	159	139
63	68	77	90	106	120	130	132	127	116	101	87	74	65	61	61	67	79	97	118	141	158	165	157	137
62	67	77	90	106	121	131	133	128	117	102	87	75	65	61	61	67	78	96	117	139	156	163	155	135
61	66	77	91	107	122	132	135	130	118	103	88	75	66	61	61	67	78	95	116	137	154	160	152	133
60	66	77	92	108	124	135	138	132	121	105	90	77	67	62	61	67	78	94	115	136	152	157	150	131
60	67	78	93	111	127	138	141	136	123	108	92	78	68	62	62	67	77	93	113	134	149	154	147	128
60	67	79	95	113	130	142	145	139	127	111	94	80	69	63	62	67	77	93	112	131	146	151	143	125
60	68	81	98	117	134	146	150	144	131	114	97	82	71	64	63	67	77	92	110	129	143	147	139	121
61	69	83	101	121	139	152	156	150	136	119	100	85	73	66	64	67	77	91	108	126	139	143	135	118
62	71	86	105	126	145	159	163	157	142	124	105	88	75	67	65	68	76	90	106	123	135	138	130	113
63	74	90	110	132	153	167	171	165	150	130	110	92	78	69	66	68	76	89	104	120	131	133	125	109
65	77	94	116	140	162	177	182	175	159	138	116	96	81	71	67	69	76	88	102	117	127	129	121	105
67	80	99	123	149	173	189	194	187	169	146	123	101	85	74	69	70	76	87	101	114	123	124	116	101
70	85	105	131	159	185	203	208	200	181	157	131	108	89	77	71	71	77	87	99	112	120	120	112	98
73	89	112	140	171	199	218	224	216	195	168	140	114	94	81	73	73	77	87	98	110	117	117	109	94
77	95	120	151	184	215	236	242	233	210	181	150	122	100	85	76	74	78	87	98	109	115	114	106	92
81	101	128	162	199	232	255	262	252	227	195	161	131	106	89	79	77	80	88	98	108	114	112	104	90
85	107	137	174	215	251	277	284	273	246	210	173	139	113	94	83	79	82	89	99	108	113	111	102	88
90	114	147	187	232	272	299	307	295	265	226	186	149	120	99	87	82	84	91	101	109	114	111	102	87
95	121	157	201	249	293	322	331	317	285	242	198	158	127	104	91	86	87	94	103	112	115	112	102	87
100	128	167	215	267	314	346	355	339	304	259	211	168	134	109	95	89	91	98	107	115	118	114	104	88
105	135	177	228	284	334	369	378	361	323	274	223	177	140	115	99	93	95	102	111	119	122	118	106	90
109	142	187	241	301	354	390	400	382	341	289	234	186	147	120	104	97	99	107	117	125	127	122	110	93
114	148	196	253	316	372	410	420	401	358	302	245	194	153	125	108	102	104	112	123	131	133	127	114	96
118	154	204	264	330	389	428	438	417	372	314	254	201	158	129	112	106	109	118	129	138	140	133	119	99
122	159	211	274	342	403	443	453	431	384	323	261	206	163	133	116	111	114	124	136	146	148	140	124	103
125	164	217	281	351	413	455	465	441	392	330	267	210	167	136	120	115	120	131	144	154	156	147	130	107
128	167	221	287	358	421	463	472	448	398	334	270	213	169	139	123	119	125	138	152	162	164	155	136	112
130	170	224	290	362	425	466	475	451	400	336	271	214	170	141	125	123	130	144	159	170	172	162	142	116
131	171	225	291	362	425	466	474	449	398	334	270	214	170	142	128	126	135	150	167	179	180	169	147	120
132	171	225	290	360	422	462	469	444	393	330	266	211	169	142	129	129	140	156	174	186	188	176	153	124
132	170	223	287	356	416	454	461	435	385	323	261	208	167	141	130	132	144	162	181	194	195	182	158	128
132	169	220	282	348	406	443	448	423	374	313	254	203	164	140	130	133	147	167	187	201	202	188	163	131
131	166	216	276	339	395	429	433	408	360	302	245	197	160	138	130	135	150	171	193	207	208	193	167	134
129	163	211	268	329	381	413	416	391	345	290	236	190	156	136	129	136	152	175	197	212	212	198	170	137
127	160	205	260	317	366	395	398	373	329	277	225	182	151	133	128	136	154	177	200	215	216	200	172	138
176	156	199	251	304	350	377	379	355	313	263	215	174	145	129	126	135	154	178	202	217	217	202	173	138
123	153	193	242	292	334	359	359	336	296	249	204	166	140	125	123	133	153	178	201	216	217	201	172	137
121	149	187	233	280	319	341	340	317	279	235	193	158	134	121	120	131	151	175	199	213	214	197	169	135
119	145	181	224	268	303	323	321	299	263	222	182	150	128	116	116	127	147	171	194	208	208	192	164	131
117	142	176	216	257	289	306	304	282	248	209	172	142	121	111	112	123	142	166	187	201	201	185	158	126
115	139	171	209	246	276	291	288	267	234	197	162	135	116	106	108	118	136	159	179	192	191	176	151	120

A-29

Figure A-5 (Sheet 4 of 6)

ER-267

90	113	139	162	177	182	175	159	138	117	99	86	80	81	89	104	123	144	163	175	176	165	146	121	95
94	118	145	169	186	191	183	166	144	122	103	89	83	83	91	106	126	147	165	176	176	165	145	120	94
98	123	151	177	194	199	191	173	150	126	106	92	85	86	94	109	130	151	169	179	179	167	145	120	94
101	128	157	184	202	207	199	179	155	130	109	95	88	89	97	113	134	156	174	184	182	169	147	121	95
105	133	163	190	209	214	205	185	160	134	112	97	90	91	101	118	139	162	180	190	187	173	150	122	96
108	137	168	196	215	220	210	190	163	137	115	100	93	94	105	122	145	169	188	197	193	178	153	125	97
110	140	171	200	219	224	214	193	166	139	117	102	95	97	109	128	152	177	196	205	200	183	157	128	99
112	142	174	203	222	227	216	195	168	141	118	103	97	100	113	133	159	185	205	214	208	190	162	131	101
113	143	175	204	223	227	217	195	168	141	119	105	99	103	117	139	166	194	214	223	217	197	168	135	104
114	143	175	204	222	227	216	194	167	141	119	105	101	106	121	145	174	202	224	232	225	204	173	139	106
114	143	174	202	220	224	213	192	165	139	119	106	102	108	125	150	181	211	233	242	234	211	178	142	109
114	142	173	200	217	221	210	188	163	138	118	106	103	111	129	156	188	219	242	250	241	217	183	146	111
113	141	170	196	213	216	205	185	159	135	116	105	104	113	132	160	194	227	250	258	249	223	188	149	113
112	139	167	193	208	211	200	180	156	133	115	105	104	114	135	165	200	233	258	266	255	228	191	151	115
111	137	165	189	204	206	195	176	152	130	113	104	104	115	137	168	204	239	264	271	260	232	194	153	116
111	136	162	185	199	201	190	171	148	127	111	103	104	116	139	171	208	243	268	276	264	235	196	155	117
110	134	160	181	195	196	185	166	144	124	109	102	104	117	140	173	211	246	271	279	266	237	197	155	117
110	133	157	178	190	191	180	162	140	121	107	100	103	116	140	174	212	248	273	280	267	237	197	155	117
110	132	155	175	186	186	175	157	136	118	104	98	102	116	140	173	212	248	272	279	266	236	196	154	116
110	131	154	172	182	181	170	152	132	114	102	97	100	114	139	172	210	246	270	276	263	233	193	152	115
110	131	152	169	178	176	165	147	128	111	99	94	99	113	137	170	207	242	266	272	258	229	190	149	112
110	130	151	167	174	172	161	143	124	108	96	92	96	110	134	166	203	237	260	265	252	223	185	145	110
110	130	150	165	171	168	157	139	121	105	94	90	94	108	131	162	197	230	252	257	244	216	179	141	106
111	131	149	163	169	165	153	136	118	102	91	87	91	104	127	156	190	222	243	247	235	207	172	135	103
112	131	150	163	167	163	150	133	115	99	89	85	89	101	122	150	183	212	232	237	224	198	164	129	98
114	133	150	163	167	161	148	130	113	97	87	83	86	97	117	144	174	202	221	225	213	188	156	123	94
116	135	152	164	167	160	147	129	111	95	85	80	83	94	112	137	165	191	209	212	201	178	148	117	89
118	138	155	166	168	161	146	128	110	94	83	78	80	90	107	130	156	180	196	199	189	167	139	110	84
122	142	159	170	171	163	147	128	109	93	82	77	78	86	102	123	147	169	184	186	176	156	130	103	79
126	147	165	175	176	166	150	130	110	93	81	75	75	83	96	116	138	158	171	173	164	145	121	96	75
132	154	172	182	182	171	153	132	111	93	81	74	73	79	91	109	129	147	159	161	152	134	112	90	70
138	161	180	190	189	177	158	135	113	94	80	73	71	76	86	102	120	136	147	148	140	124	104	83	65
145	170	189	199	197	184	163	138	115	95	80	72	69	73	82	96	112	126	136	137	129	114	96	77	61

A-31

Figure A-5 (Sheet 6 of 6)

ER-267

ECHELLOGRAM SUBSECTION

TAPE 813 - NON-DESTRUCTIVE R/O SIMULATION (COMPLETE SYSTEM), LAMBDA = 2000 ANGST, SEC PSF WIDTH = 50 MICRONS

PTS: 201 TO 225 TOTAL PIXELS = 102400 SUM = 0.1115E 08
 RECS: 125 TO 275 AVG = 0.1089E 03

357	406	376	291	202	137	96	74	62	57	57	62	74	97	141	207	279	316	294	231	164	114	85	68	61
378	430	397	305	210	141	99	76	64	59	59	64	77	103	149	221	299	338	313	243	171	118	87	69	61
397	451	414	316	216	144	101	77	65	60	60	66	80	107	158	235	318	360	331	255	178	122	88	70	61
411	467	428	325	220	146	102	78	66	61	61	68	83	112	166	248	337	381	349	267	184	125	90	71	62
420	477	435	330	222	147	103	78	66	61	62	69	85	116	173	260	354	400	366	279	191	128	92	72	62
422	479	437	330	222	147	102	78	66	62	63	70	87	119	179	270	368	416	380	288	196	131	93	72	61
419	475	433	326	219	145	101	78	66	62	63	71	88	121	183	277	379	428	390	295	200	133	94	72	61
410	464	423	319	214	142	100	77	66	61	63	71	88	122	185	281	384	434	395	298	201	133	94	72	61
396	448	408	308	207	138	97	75	65	61	63	71	88	122	185	281	384	434	395	297	200	132	93	71	60
379	429	390	294	199	132	94	73	63	60	62	70	87	121	183	277	379	428	388	292	197	130	91	70	59
359	406	369	279	189	127	90	71	62	58	61	68	85	118	178	271	369	416	378	284	191	127	89	69	58
338	381	347	262	178	120	87	69	60	57	59	67	83	115	173	261	355	400	364	274	184	123	87	67	56
315	355	323	245	167	113	82	66	58	55	57	65	80	111	165	249	339	381	346	261	177	118	84	65	55
292	328	299	227	155	106	78	63	56	53	55	63	77	106	157	235	319	359	326	247	167	113	81	63	54
268	301	274	208	143	99	73	60	53	51	53	60	74	100	148	220	297	334	304	230	157	107	77	61	52
244	273	249	190	132	92	69	57	51	49	51	58	70	94	138	204	274	308	280	213	147	100	73	58	50
221	247	225	173	121	85	65	54	49	47	49	55	67	89	129	189	252	282	257	197	136	94	70	56	49
199	222	203	157	111	79	61	51	46	45	47	52	63	83	120	174	232	259	236	181	126	88	66	54	48
179	199	182	141	101	73	57	48	44	43	45	50	60	79	111	161	213	238	218	167	118	83	63	52	46
161	179	163	127	91	67	53	46	42	41	43	48	57	74	104	150	198	220	201	156	110	79	60	50	45
146	161	147	115	83	62	50	43	40	40	41	46	54	70	98	140	184	205	187	145	103	74	58	49	44
134	147	134	105	77	58	47	41	39	38	40	44	52	66	92	131	172	191	175	135	96	70	55	47	44
124	136	124	97	71	54	44	39	37	37	38	42	50	63	87	124	162	179	163	126	91	67	53	46	43
116	127	116	91	67	51	42	38	36	36	37	41	48	61	83	117	153	169	154	119	86	64	51	45	43
110	120	109	86	64	49	41	37	35	35	36	40	46	58	80	112	146	161	147	114	82	61	50	45	43
105	114	105	82	61	47	40	36	34	34	35	39	45	56	77	108	140	154	141	109	79	60	49	44	43
102	111	101	80	60	46	39	35	33	33	34	38	44	55	74	104	135	149	136	106	77	58	49	44	43
100	109	99	78	58	45	38	34	33	33	34	37	43	53	72	101	131	144	132	103	75	57	48	44	43
99	107	98	77	58	45	37	34	32	32	33	36	42	52	70	98	127	140	128	100	74	57	48	44	44
98	107	97	77	57	44	37	34	32	32	33	36	41	51	69	95	123	136	124	98	72	56	48	45	45
98	107	97	77	57	44	37	33	32	32	33	36	41	50	68	93	120	133	121	96	71	56	48	45	45
96	107	98	77	57	44	37	34	32	32	33	35	40	50	67	92	118	130	119	94	71	56	48	46	46
99	108	98	77	58	45	37	34	32	32	33	35	40	50	66	90	116	128	117	93	70	56	49	46	48
100	109	99	78	58	45	38	34	32	32	33	35	40	50	66	90	116	127	117	93	70	56	49	47	49
103	111	101	80	60	46	38	34	33	32	33	36	41	50	66	91	116	128	118	94	71	57	50	48	50
106	115	105	82	61	47	39	35	33	33	34	36	41	50	67	92	118	130	119	95	72	58	51	49	51
110	119	109	86	63	49	40	36	34	33	34	37	42	51	68	93	120	132	122	97	73	59	52	50	53
116	126	114	90	66	51	42	37	35	34	35	37	43	52	70	96	123	136	124	99	75	60	53	52	54
123	134	122	95	70	53	43	38	36	35	36	38	44	54	71	98	126	139	128	102	77	61	54	53	55
132	144	131	102	74	56	45	39	37	36	37	39	45	55	74	102	131	145	133	105	79	63	56	54	57
144	157	142	110	80	59	47	41	38	37	38	40	46	57	76	106	137	151	138	109	82	65	57	55	58
158	173	156	120	86	63	50	43	39	38	39	42	48	59	80	111	143	158	145	114	85	67	59	57	59
174	191	172	131	93	67	53	45	41	39	40	43	50	62	84	116	151	166	152	119	89	69	60	58	60
192	210	189	144	100	72	56	47	43	41	42	45	52	65	88	123	160	176	161	126	93	72	62	59	61
212	232	208	157	109	77	59	49	44	42	43	46	54	68	94	132	171	188	171	133	97	75	64	60	62
232	255	228	171	117	82	62	52	46	44	45	48	57	72	100	141	183	201	183	141	102	77	65	61	63
253	278	248	186	126	87	66	54	48	46	46	50	59	77	107	151	196	216	195	150	107	81	67	62	63
275	302	269	200	135	93	69	56	50	47	48	52	62	81	113	161	210	230	208	159	113	84	69	63	64
296	325	290	215	144	98	72	58	51	49	49	54	65	85	120	171	223	245	221	168	118	87	71	64	64
316	348	309	229	153	103	75	61	53	50	51	56	67	88	126	180	236	260	234	177	124	90	72	65	65
335	368	327	241	160	107	78	62	55	51	52	58	69	92	131	190	249	274	246	185	129	93	74	66	65
350	386	342	252	167	111	80	64	56	53	54	59	71	95	137	198	260	287	257	193	134	95	75	67	65

A-32

Figure A-6. Echellogram Subsection - Tape No. 813

137	105	75	54	43	36	32	30	30	30	32	37	46	59	73	80	73	59	46	37	33	31	32	33	37
137	105	75	54	43	36	32	30	30	30	32	37	46	59	74	80	74	60	46	38	33	32	32	34	38
137	106	75	55	43	36	33	30	30	30	32	37	46	60	75	82	75	61	47	38	34	32	33	35	38
140	107	76	55	43	37	33	31	30	31	33	38	47	61	77	84	77	62	48	39	34	33	33	35	39
143	110	78	56	44	37	33	31	30	31	33	38	48	63	79	86	79	63	49	40	35	33	34	36	40
147	113	80	58	45	38	34	32	31	31	34	39	49	65	81	88	81	65	50	40	36	34	34	37	41
152	116	82	59	46	39	34	32	31	32	35	40	51	66	83	91	84	67	51	41	36	35	35	38	42
159	121	85	61	47	40	35	33	32	33	35	41	52	69	86	94	87	69	53	43	37	36	36	39	44
166	126	88	63	49	41	36	34	33	34	37	43	54	72	90	99	90	72	55	44	38	36	37	39	45
174	132	92	66	50	42	37	35	34	35	38	44	57	75	95	104	95	76	57	46	40	37	38	40	46
183	139	96	68	52	43	38	36	35	36	39	46	59	79	101	110	101	80	60	47	41	38	39	41	46
193	146	101	71	54	45	40	37	36	37	41	48	63	85	107	118	108	85	63	49	42	39	39	42	47
204	154	107	75	57	47	41	38	37	39	43	51	67	91	116	127	116	91	67	52	44	41	40	43	48
218	164	113	79	59	49	43	40	39	40	45	54	71	98	125	138	125	98	71	54	46	42	41	43	49
234	176	120	83	62	51	44	41	40	42	47	57	76	105	136	149	136	105	76	57	47	43	42	44	49
252	188	128	88	65	53	46	43	42	44	49	61	82	114	147	162	147	113	81	60	49	44	43	45	50
272	202	137	93	69	55	48	44	44	46	52	65	88	123	159	175	158	121	86	64	51	46	44	46	50
292	217	146	98	72	58	50	46	45	48	55	69	95	133	173	189	171	130	92	67	54	47	45	46	51
313	231	154	104	75	60	51	48	47	50	58	74	102	144	187	204	184	139	98	71	56	49	46	47	51
333	245	163	109	78	62	53	49	49	52	61	78	110	155	201	220	198	149	104	74	58	50	47	48	52
351	258	171	113	81	64	55	51	50	54	64	83	117	166	216	237	212	160	110	78	60	52	48	48	52
367	269	177	117	84	66	56	52	52	56	67	87	124	178	232	255	227	170	117	82	63	53	49	49	53
379	278	182	120	86	67	58	53	53	58	70	92	131	189	248	272	242	181	123	85	65	54	50	50	53
386	283	186	122	87	68	59	54	55	60	72	96	139	200	262	287	256	190	129	88	67	56	51	50	54
388	284	187	123	88	69	59	55	56	61	75	100	145	210	275	301	267	198	133	91	68	57	52	51	54
385	282	186	123	88	69	60	56	57	63	77	103	150	217	284	311	276	204	137	93	70	58	52	52	55
379	277	183	122	87	69	60	56	57	64	78	106	154	222	290	317	281	208	139	95	71	58	53	52	56
368	270	179	120	86	69	60	57	58	65	79	108	156	225	293	319	282	209	140	95	71	59	53	53	56
356	261	174	117	85	68	60	57	58	65	80	109	157	225	292	317	281	208	140	95	71	59	54	53	57
341	251	168	114	84	68	59	57	58	65	81	109	157	224	289	313	277	205	138	95	71	59	54	54	58
326	240	162	110	82	67	59	56	58	66	81	110	157	222	284	306	270	200	136	94	71	59	54	54	59
311	230	156	107	80	66	58	56	58	66	81	110	156	219	277	298	262	195	133	92	70	59	55	55	60
297	219	149	104	78	64	58	56	58	66	82	110	156	216	271	289	254	189	129	91	70	59	55	56	61

Figure A-6. (Sheet 3 of 6)

ECHLLOGRAM SUBSECTION

TAPE 813 - NON-DESTRUCTIVE R/D SIMULATION(COMPLETE SYSTEM), LAMBDA = 2000 ANGST, SEC PSF WIDTH = 50 MICRONS

PTS: 226 TO 250
RECS: 125 TO 275

TOTAL PIXELS = 102400 SUM = 0.1115E 08
AVG = 0.1089E 03

59	63	72	91	126	190	288	391	440	399	300	201	133	93	70	57	50	47	47	52	63	83	114	144	155
59	62	70	88	121	180	270	366	411	373	281	190	126	89	68	56	49	47	48	53	66	89	122	155	166
59	61	68	84	115	169	252	340	382	347	262	178	119	85	65	55	49	47	49	55	69	95	131	166	178
58	60	66	81	109	159	235	316	354	321	243	166	112	81	63	53	48	47	50	57	73	101	141	179	191
58	59	64	78	103	149	219	293	328	298	226	155	106	77	61	52	48	47	51	59	76	107	151	193	206
57	57	62	74	98	140	204	272	304	276	210	145	100	73	59	51	47	48	52	61	80	113	161	207	222
56	56	61	71	93	131	191	253	282	256	196	136	94	70	57	50	47	48	52	63	84	120	172	221	237
55	55	59	68	88	124	178	236	262	239	182	127	89	67	55	49	47	48	53	65	88	127	182	235	252
55	54	57	66	84	117	167	220	245	222	170	119	84	64	53	48	46	48	54	67	91	132	191	247	264
53	52	55	64	80	111	158	207	229	208	160	112	80	62	52	47	46	48	55	68	93	137	198	250	275
52	51	54	61	77	106	150	195	216	196	150	106	76	59	51	46	46	48	55	69	95	140	203	263	281
51	50	53	60	74	102	143	187	206	187	143	101	73	58	49	46	45	48	55	70	96	142	206	266	285
50	49	51	58	72	98	138	180	198	180	138	98	71	56	49	45	45	48	56	70	97	143	207	267	286
49	48	50	57	71	96	135	175	193	175	134	95	70	55	48	45	45	48	56	70	97	143	206	267	286
48	47	49	56	70	95	133	173	191	173	132	94	69	55	48	45	45	48	56	70	97	142	205	264	283
47	46	49	56	69	94	132	172	190	172	132	94	68	54	47	44	45	48	55	70	96	141	203	261	279
46	46	48	55	69	94	133	173	191	173	132	94	68	54	47	44	45	48	55	69	95	139	200	257	275
45	45	48	55	69	95	134	175	193	175	134	95	69	55	47	44	45	48	55	69	95	138	197	253	270
44	45	48	55	70	96	136	178	196	178	136	96	70	55	48	45	45	48	55	69	94	136	194	248	264
43	44	48	56	71	98	139	182	201	182	139	98	71	56	48	45	45	48	55	69	94	135	192	244	259
43	44	48	56	72	100	142	187	207	187	142	100	72	57	49	45	45	48	55	69	94	135	189	239	252
43	44	49	57	74	103	147	193	213	192	147	103	74	58	50	46	45	48	55	69	93	133	186	232	244
43	45	49	59	76	106	152	199	220	199	151	106	76	59	50	46	46	48	55	68	93	131	181	225	235
43	45	50	60	78	110	158	207	229	207	157	110	78	61	52	47	46	49	55	68	92	129	176	217	225
43	46	52	63	82	116	166	218	241	217	165	115	81	63	53	48	47	49	55	68	91	126	171	208	214
43	47	53	65	86	123	176	231	254	229	173	120	85	65	55	49	48	49	55	68	90	124	165	199	204
44	48	55	68	91	131	188	246	271	243	184	127	89	68	56	51	48	50	56	68	90	122	161	190	193
45	49	58	72	97	140	202	264	291	261	196	135	94	71	58	52	50	51	56	68	90	121	157	183	183
46	51	60	76	104	150	218	285	313	281	210	144	100	75	61	54	51	52	57	69	90	120	154	176	175
47	53	63	81	111	162	235	309	340	303	227	154	106	78	64	56	52	53	58	70	91	120	151	171	167
49	55	66	85	119	175	256	336	369	329	245	166	113	83	66	58	54	54	59	71	92	120	149	166	161
50	57	70	91	128	189	278	366	402	358	266	178	120	88	70	60	55	55	60	72	93	122	149	163	155
52	60	73	96	137	205	301	398	438	390	288	192	129	93	73	62	57	57	62	74	96	124	149	160	150
53	62	77	102	146	220	326	433	476	423	312	207	137	98	76	65	59	59	64	77	99	128	152	160	147
55	65	81	108	156	237	352	468	515	457	336	221	146	103	80	67	61	61	66	80	103	133	156	161	146
57	67	84	114	166	253	377	502	553	491	360	236	154	109	84	70	64	63	69	83	109	140	163	165	147
59	70	88	119	175	268	402	535	590	523	382	250	163	114	87	73	66	65	71	88	115	148	171	171	149
60	72	91	125	183	283	424	567	625	553	404	263	170	118	90	75	68	68	75	92	122	157	181	178	153
62	74	94	130	191	296	445	595	656	580	423	275	177	123	93	78	70	70	78	97	130	168	192	187	158
64	76	97	134	198	307	463	620	683	604	440	285	183	127	96	80	72	73	81	103	139	179	204	197	164
65	78	100	137	204	317	478	640	705	623	453	293	188	130	98	82	75	75	85	109	148	192	218	208	170
66	79	102	140	209	325	490	655	721	637	463	299	192	132	100	84	76	78	89	115	158	206	232	219	177
67	80	103	143	212	329	497	663	730	645	468	303	194	134	102	85	78	80	92	121	168	219	246	231	185
68	81	104	144	214	332	499	665	732	646	469	303	195	134	102	86	79	82	96	127	177	232	261	242	192
69	82	104	144	214	331	497	661	726	641	465	301	194	134	103	86	80	84	99	133	186	245	274	254	198
69	82	104	144	213	329	491	651	714	630	458	297	191	133	102	87	81	85	102	138	195	257	288	264	205
70	82	104	143	211	324	482	636	696	613	446	290	188	131	101	86	82	87	105	143	204	269	300	274	211
70	82	103	142	209	318	470	617	672	591	430	281	183	128	100	86	82	88	107	148	212	280	312	284	217
70	81	102	140	205	311	455	593	644	566	412	270	177	125	98	85	82	88	109	151	219	290	323	293	222
70	81	101	138	201	302	439	568	613	538	392	258	170	121	96	84	81	89	110	154	224	298	332	300	226
69	80	100	135	197	293	422	541	580	508	371	245	163	117	93	82	80	88	111	156	228	304	338	305	229
69	79	98	133	192	285	405	514	548	478	350	232	155	112	90	80	79	88	111	157	229	306	340	306	229

A-35

Figure A-6. (Sheet 4 of 6)

43	54	73	105	151	198	217	195	148	103	74	58	51	49	50	56	68	90	127	178	229	262	258	215	156
44	56	76	109	158	206	227	203	154	107	76	60	52	49	51	57	69	92	129	179	227	255	247	204	148
45	57	78	114	164	215	237	213	160	111	79	62	53	50	52	57	70	93	131	181	227	250	238	195	141
47	59	81	118	172	226	249	223	168	116	82	63	55	51	53	58	71	95	134	184	227	246	231	187	135
48	61	84	123	180	237	261	234	176	121	85	65	56	52	54	60	73	98	138	188	230	244	225	180	130
49	63	88	129	189	249	275	246	184	126	88	67	57	54	55	61	75	101	142	193	233	244	221	175	126
51	66	91	135	198	262	289	258	193	131	91	69	59	55	56	63	77	105	148	200	239	246	218	171	122
52	68	95	141	208	274	302	270	201	136	94	71	60	56	57	64	80	109	155	208	247	250	218	168	120
54	70	99	147	216	286	315	280	208	141	97	73	62	58	59	66	83	114	162	218	257	256	219	167	118
55	72	102	152	224	296	326	290	215	145	99	75	63	59	60	68	86	119	171	230	269	264	223	167	117
56	73	104	156	230	304	334	297	220	148	101	76	64	60	62	71	90	125	181	244	283	275	228	168	117
57	75	106	158	234	309	340	302	224	150	103	77	65	61	64	73	94	132	192	259	298	286	234	171	118
58	75	107	160	235	311	342	304	225	151	104	78	66	63	65	75	97	139	203	274	315	299	241	174	119
58	76	107	160	236	311	341	304	225	151	104	79	67	63	67	78	101	146	214	289	331	313	249	177	121
59	77	108	160	234	308	338	300	223	150	104	79	67	64	68	80	105	152	225	305	348	326	257	181	122
59	77	108	159	232	303	331	294	219	148	103	79	68	65	69	82	109	159	236	320	364	339	265	185	124
60	77	108	158	228	297	323	287	214	145	101	78	68	66	70	84	112	165	246	334	379	351	272	188	125
60	77	107	156	224	290	314	279	208	142	100	77	68	66	71	86	115	170	255	346	393	362	278	191	127
60	77	107	155	220	282	305	270	202	138	98	77	67	66	72	87	118	175	263	357	405	371	284	193	127
61	77	107	153	216	275	295	261	195	135	96	75	67	66	72	88	120	179	269	366	414	379	288	195	128
61	78	107	153	213	268	286	252	189	131	93	74	66	66	73	89	122	182	274	373	422	384	291	196	128
62	78	108	153	211	262	277	243	182	124	91	73	66	66	73	89	122	184	277	378	426	388	292	196	128
62	79	109	153	209	256	268	234	175	122	89	71	65	65	72	89	123	184	279	379	428	388	292	195	127
63	80	110	154	206	249	258	224	168	118	86	70	64	64	72	89	122	183	278	378	426	386	290	193	126
63	81	111	154	204	243	249	215	161	114	84	68	63	63	71	88	121	181	275	374	421	381	285	190	124
64	82	113	155	203	238	240	206	154	109	81	67	61	62	70	86	119	178	269	366	412	373	279	186	121
65	84	114	157	202	233	232	198	148	105	79	65	60	61	68	84	116	174	262	356	400	362	271	181	118
66	85	117	160	203	229	225	190	142	102	76	64	59	60	67	82	113	168	253	343	386	350	262	175	115
67	87	120	162	203	226	218	183	136	98	74	62	58	59	65	80	109	162	243	329	370	335	251	168	111
68	89	123	166	205	224	213	176	131	95	72	61	56	57	63	77	105	155	231	313	351	319	240	161	106
70	91	126	170	208	223	208	171	127	92	70	59	55	56	61	74	100	147	219	296	332	301	227	153	101
72	94	131	175	212	223	205	166	123	89	69	58	54	54	59	72	96	139	207	278	311	282	213	144	96
74	98	136	182	213	226	204	163	120	88	67	57	53	53	58	69	91	131	194	260	290	263	199	135	90

Figure A-6. (Sheet 6 of 6)

ECHHELLOGRAM SUBSECTION

TAPE 1107 - DESTRUCTIVE R/O SIMULATION (COMPLETE SYSTEM), LAMBDA = 1216 ANGST, SEC PSF WIDTH = 41 MICRONS

PYS: 201 TO 225
 RECS: 125 TO 275

TOTAL PIXELS = 100864 SUM = 0.1093E 08
 AVG = 0.1084E 03

498	519	435	306	194	121	81	61	52	49	53	63	87	136	221	333	428	445	375	265	170	108	73	56	48
496	515	431	302	191	120	80	60	51	49	53	64	89	140	227	344	442	460	386	272	173	109	74	56	47
486	505	422	295	187	117	79	60	51	49	53	65	90	142	231	351	450	468	392	275	174	110	74	55	47
470	488	407	285	180	114	77	59	50	49	53	65	90	142	232	352	452	469	392	274	173	109	73	55	46
450	466	389	272	173	109	74	57	49	48	52	64	89	141	230	348	446	462	386	270	170	107	72	54	45
426	441	368	258	164	104	71	55	48	47	51	63	88	138	225	340	435	450	375	262	166	104	70	53	44
400	414	346	242	154	99	68	53	47	46	50	61	85	134	217	328	420	434	361	252	160	101	68	51	43
373	386	322	226	144	93	65	51	45	44	49	59	82	128	208	313	400	413	344	241	153	97	66	50	42
345	356	297	209	134	87	61	49	43	43	47	57	79	122	196	295	376	389	324	227	145	92	63	48	41
316	325	271	191	123	81	58	46	42	41	45	55	75	115	184	275	350	361	302	212	136	87	60	47	40
286	295	246	174	113	75	54	44	40	40	43	52	71	107	170	254	322	333	278	196	126	82	57	45	39
258	266	222	158	103	69	51	42	38	38	41	49	66	100	157	233	295	304	254	180	117	76	54	43	38
231	238	200	142	94	64	47	39	36	36	39	47	62	93	145	213	270	278	233	165	108	72	52	41	36
207	212	178	128	85	59	44	37	34	34	37	44	59	86	134	196	247	254	213	152	100	67	49	40	36
184	189	159	114	77	54	41	35	33	33	36	42	55	81	124	181	227	234	197	141	93	63	47	38	35
165	169	142	103	70	49	38	33	31	31	34	40	52	76	115	168	211	217	182	131	87	60	45	37	34
150	153	129	93	64	46	36	32	30	30	33	38	49	71	108	157	196	202	169	121	81	56	43	36	34
138	140	118	86	59	43	34	30	29	29	31	37	47	67	102	147	184	188	158	113	76	53	41	35	33
128	130	110	80	55	40	33	29	28	28	30	35	45	64	96	138	173	177	148	106	72	51	40	35	33
120	122	103	75	52	38	31	28	27	27	29	34	43	61	91	131	164	167	140	101	68	49	39	34	33
114	116	98	72	50	37	30	27	26	26	28	33	41	59	88	126	156	160	134	96	66	47	38	34	33
110	112	94	69	48	36	29	26	25	26	28	32	40	57	84	121	150	154	129	93	64	46	37	34	33
107	109	92	67	47	35	29	26	25	25	27	31	39	55	82	117	145	149	125	90	62	45	37	34	34
106	108	91	67	47	35	28	26	25	25	27	30	38	53	79	113	141	144	121	88	61	45	37	34	34
105	107	90	66	46	34	28	25	24	25	26	30	37	52	77	110	137	140	117	85	59	44	37	35	36
105	107	90	66	46	34	28	25	24	24	26	30	37	51	75	107	133	136	114	83	59	44	37	35	36
105	107	90	66	46	34	28	25	24	24	26	29	36	50	74	104	129	132	112	82	58	44	37	36	37
106	108	91	66	47	34	28	25	24	24	26	29	36	50	73	103	127	130	110	81	58	44	38	36	38
107	109	92	67	47	35	29	26	24	24	26	29	36	49	72	102	126	129	109	81	58	44	38	37	39
109	111	94	69	48	36	29	26	25	25	26	29	36	50	72	102	126	130	110	81	58	45	39	38	40
112	114	96	71	49	36	30	26	25	25	26	30	37	50	73	103	128	131	111	82	59	46	40	39	42
117	119	100	73	51	38	30	27	25	25	27	30	37	51	75	105	131	134	114	84	60	47	41	40	43
123	125	105	77	54	39	31	28	26	26	27	31	38	52	76	108	134	137	116	86	62	48	42	41	44
131	133	112	82	57	41	33	29	27	27	28	32	39	53	78	111	137	141	120	88	63	49	43	42	45
141	144	121	88	60	43	34	30	28	27	29	32	40	55	81	115	142	146	124	92	65	50	44	43	46
155	158	132	96	65	46	36	31	29	28	30	33	41	57	84	120	149	153	129	95	67	52	45	44	48
171	174	146	104	70	49	38	32	30	29	31	35	43	60	88	126	156	160	135	99	70	53	46	45	49
189	193	161	115	76	53	40	34	31	30	32	36	45	63	93	132	165	169	143	104	73	55	47	46	49
210	214	178	126	83	56	42	35	32	32	33	38	47	66	98	141	175	179	151	110	77	57	49	47	50
233	237	196	138	90	61	45	37	34	33	34	39	50	70	105	151	187	192	161	117	81	60	50	48	51
254	262	216	151	98	65	48	39	35	34	36	41	53	75	113	162	201	206	172	124	85	62	52	49	51
293	287	237	165	106	69	50	41	36	35	37	43	56	81	122	175	217	221	184	132	89	65	53	50	52
308	313	257	178	114	74	53	43	38	37	39	45	59	86	131	188	233	237	197	140	94	67	54	50	52
334	339	278	192	121	78	56	44	39	38	40	47	62	91	139	201	249	253	210	149	99	70	56	51	53
358	363	298	205	129	82	58	46	41	39	42	49	65	96	148	213	265	270	223	157	104	72	57	52	53
381	386	316	216	135	86	60	48	42	40	43	51	68	101	155	225	280	285	235	165	108	74	58	52	53
401	406	331	226	141	89	62	49	43	41	44	52	70	105	163	236	294	299	247	172	112	77	59	53	53
417	422	344	235	146	92	64	50	44	42	45	54	73	109	170	247	307	312	257	179	116	78	60	53	53
428	433	353	240	149	94	65	51	44	43	46	55	75	113	176	256	318	323	265	184	119	80	61	53	52
435	440	358	243	151	95	66	51	45	44	47	56	77	116	181	263	327	331	271	188	121	81	61	53	52
438	442	359	244	151	95	66	52	45	44	47	57	78	119	185	269	333	336	275	190	122	81	61	53	52
435	438	356	242	150	95	66	52	45	44	48	58	79	120	187	271	335	339	277	191	122	82	61	53	52

A-38

ER-267

Figure A-7. Eschellogram Subsection - Tape No. 1107

135	96	64	44	33	28	25	23	23	25	28	36	50	68	83	85	72	54	39	31	27	26	26	29	34
139	99	65	45	34	28	25	24	24	25	29	37	51	70	85	87	74	55	40	31	27	26	27	30	35
144	102	68	46	35	29	26	24	24	26	29	38	53	72	88	90	77	57	41	32	28	27	28	31	36
150	106	70	48	36	30	26	25	25	26	30	39	54	75	91	93	79	59	43	33	29	27	28	31	37
157	111	73	50	37	30	27	25	25	27	31	41	57	78	96	98	83	62	44	34	29	28	29	32	38
165	116	76	52	38	31	28	26	26	28	32	42	59	82	101	103	87	65	46	36	30	29	30	33	39
173	122	80	54	40	32	29	27	27	29	34	44	63	87	107	109	93	69	49	37	31	30	30	34	40
183	128	84	56	41	34	30	28	28	30	35	47	67	93	115	117	99	73	52	39	33	31	31	34	41
194	136	88	59	43	35	31	29	29	31	37	50	72	101	124	127	107	79	55	41	34	31	32	35	42
207	145	94	62	45	36	32	30	30	33	39	53	77	109	135	138	117	85	59	43	35	32	33	36	42
223	155	100	66	48	38	33	31	32	34	42	57	84	119	147	151	127	91	63	45	37	33	33	36	43
240	167	107	70	50	40	35	33	33	36	45	62	91	129	161	164	137	99	67	48	38	34	34	37	43
260	180	115	74	53	42	36	34	34	38	48	66	99	141	175	178	149	106	71	50	40	35	35	37	43
280	194	122	79	55	43	38	35	36	40	51	72	107	153	190	194	161	114	76	53	41	36	35	38	44
301	207	130	83	58	45	39	37	38	43	54	78	117	167	206	210	174	123	81	56	43	37	36	38	44
321	220	138	87	60	47	40	38	39	45	58	83	126	181	223	227	188	132	86	59	45	39	37	39	44
340	232	144	91	63	48	42	39	41	47	61	89	136	195	241	245	202	142	92	62	47	40	38	39	45
356	243	150	94	65	50	43	41	42	49	65	95	146	210	260	264	217	151	98	65	48	41	38	40	45
369	251	155	97	66	51	44	42	44	51	68	101	155	225	279	283	232	161	103	68	50	42	39	40	46
377	255	158	98	67	52	45	43	45	53	71	107	165	239	297	300	246	170	108	71	52	43	40	41	46
379	257	159	99	68	53	45	44	46	55	74	112	174	252	312	315	258	177	112	73	53	44	40	41	47
377	255	158	99	68	53	46	44	47	56	77	116	181	262	324	327	266	183	115	75	54	44	41	42	48
370	251	155	98	68	53	46	45	48	58	79	120	186	269	332	334	272	186	117	76	55	45	41	42	48
360	244	152	96	67	53	46	45	48	59	81	122	189	272	335	337	274	188	118	77	55	45	42	43	49
347	236	147	94	66	52	46	45	49	59	82	124	191	273	335	335	272	187	118	77	55	46	42	43	50
332	227	142	91	65	52	46	45	49	60	82	124	190	271	331	330	268	184	116	76	55	46	42	44	51
317	216	137	89	63	51	46	45	49	60	83	124	189	267	324	323	262	180	114	75	55	46	43	44	52
301	206	131	86	62	50	45	45	49	60	83	124	187	262	316	313	254	175	112	74	55	46	43	45	53
287	196	125	83	60	49	45	45	49	61	84	124	186	257	307	303	245	169	108	72	54	46	43	46	55
273	187	120	80	59	49	45	45	49	61	84	125	185	253	298	292	236	163	105	71	54	46	44	47	56
259	178	115	77	58	48	44	45	50	62	86	127	185	249	291	282	227	157	102	69	53	46	44	48	58
247	169	110	75	56	47	44	44	50	62	87	128	185	246	283	273	219	151	99	68	52	46	45	49	61
235	161	106	72	55	47	44	45	50	63	88	130	186	243	276	263	210	146	96	67	52	46	46	51	63

Figure A-7 (Sheet 3 of 6)

ECHELLOGRAM SUBSECTION

TAPE 1107 - DESTRUCTIVE R/O SIMULATION (COMPLETE SYSTEM), LAMBDA = 1216 ANGST, SEC PSF WIDTH = 41 MICRONS

PTS: 226 TO 250 TOTAL PIXELS = 100864 SUM = 0.1093E 08
 RECS: 125 TO 275 AVG = 0.1084E 03

45	47	55	73	109	170	251	317	326	272	191	124	81	57	45	40	38	40	47	63	95	146	207	245	230
44	46	53	70	102	159	233	294	302	252	178	116	76	55	44	39	38	40	49	66	101	156	222	263	248
44	45	51	66	96	148	216	272	280	234	166	108	72	52	43	38	38	41	50	69	106	166	237	281	264
43	44	49	63	91	139	202	253	260	217	154	101	68	50	41	38	38	42	51	72	112	176	251	297	279
42	42	48	60	86	130	189	236	242	202	144	95	65	48	40	37	38	42	53	75	116	183	261	310	290
41	41	46	58	82	123	178	222	227	190	135	89	61	46	39	37	38	42	53	76	119	188	269	319	298
40	40	45	56	78	118	169	211	216	180	128	85	59	45	38	36	37	42	54	77	121	192	274	324	303
39	39	44	54	76	113	163	202	207	172	123	82	57	44	38	36	37	43	54	78	122	193	275	326	305
38	38	43	53	74	110	158	196	201	167	119	80	56	43	37	36	37	42	54	78	122	192	274	325	304
37	38	42	52	73	108	155	193	197	165	117	78	55	43	37	35	37	42	54	78	121	191	272	322	301
36	37	41	52	72	108	154	192	197	164	117	78	54	42	37	35	37	42	54	77	120	189	269	317	297
36	37	41	51	72	108	155	193	197	165	117	78	54	42	37	35	37	42	54	76	119	186	265	312	292
35	36	41	51	72	109	156	195	200	166	118	79	55	42	37	35	37	42	53	76	118	184	260	306	286
34	36	41	52	73	110	159	198	203	169	120	80	55	43	37	35	37	42	53	75	117	181	256	300	280
34	36	41	52	74	112	162	203	208	173	123	81	56	43	37	36	37	42	53	75	116	179	251	294	274
34	36	41	53	76	115	167	209	214	178	126	83	57	44	38	36	37	42	53	75	115	177	247	287	266
33	36	42	54	78	119	172	215	220	183	130	86	59	45	38	36	37	42	53	75	115	175	241	278	258
33	36	43	55	80	123	178	223	228	190	134	88	60	46	39	37	37	42	53	75	113	171	234	268	247
34	37	44	57	83	128	185	232	237	197	139	92	62	47	40	37	38	42	53	74	111	167	226	257	236
34	38	45	60	88	134	195	243	249	207	146	95	65	49	41	38	38	42	52	73	109	162	217	245	224
35	39	47	63	93	143	207	258	263	218	153	100	68	50	42	38	38	42	52	72	107	157	207	232	211
35	40	49	66	99	153	221	275	280	232	163	106	71	52	43	39	39	43	52	72	106	152	199	220	199
36	41	51	71	106	164	238	295	301	248	174	113	75	55	45	40	40	43	53	72	105	149	191	209	188
37	43	54	75	114	177	257	319	324	268	187	120	79	58	47	41	41	44	53	73	104	146	185	199	177
38	45	57	81	123	192	279	347	352	290	202	129	85	61	48	43	42	45	54	73	104	144	179	191	168
40	47	61	87	133	209	304	378	383	315	219	139	90	64	51	44	43	45	55	74	105	143	175	183	160
41	49	65	93	144	227	331	412	418	344	238	150	97	68	53	46	44	47	56	75	106	143	172	177	153
43	52	68	100	156	247	362	451	457	375	258	162	103	72	56	48	45	48	58	77	108	144	170	172	147
44	54	73	107	169	269	394	491	498	408	280	175	110	76	58	50	47	49	59	80	111	146	170	169	142
46	57	77	114	181	290	427	533	540	442	302	188	117	80	61	52	49	51	62	84	116	151	172	168	139
48	60	81	121	194	312	460	575	583	475	324	200	125	84	64	54	50	53	65	88	123	158	178	170	138
50	62	85	128	206	333	492	615	623	508	346	213	132	88	67	56	52	56	68	93	130	167	185	174	139
51	65	89	134	218	353	522	653	662	538	365	224	138	92	69	58	54	58	72	99	139	178	195	180	142
53	67	92	141	229	371	550	688	696	566	384	235	144	96	72	60	56	61	76	106	149	190	206	187	145
54	69	96	146	238	388	574	719	727	590	399	244	149	99	74	62	58	63	80	113	160	203	218	196	149
56	71	98	151	246	401	595	744	752	610	412	251	153	102	76	64	60	66	85	121	172	218	232	205	155
57	72	101	154	253	412	610	763	771	625	421	256	156	104	77	65	62	69	90	129	185	234	247	216	160
58	73	102	157	258	419	620	775	782	633	427	259	158	105	78	66	64	72	94	138	198	250	263	227	166
58	74	103	159	260	423	624	779	785	635	428	260	159	105	79	67	65	74	99	146	211	266	278	237	171
59	75	104	160	261	422	622	775	780	631	425	258	158	105	79	68	67	77	104	154	223	282	292	247	177
59	75	104	159	259	419	615	763	767	620	417	254	156	105	79	69	68	79	108	162	235	296	306	257	182
60	75	104	158	257	412	603	745	748	604	407	248	153	103	79	69	69	81	112	169	246	311	320	266	187
60	74	103	157	253	404	586	722	722	582	393	240	149	101	78	68	69	83	115	176	257	324	333	275	191
59	74	102	155	248	393	566	693	691	557	376	231	144	99	77	68	70	84	119	182	267	337	345	284	196
59	73	101	152	242	380	544	661	657	529	357	221	138	96	75	67	70	85	121	187	276	348	355	291	199
59	73	99	149	236	367	520	628	621	499	338	209	132	92	73	66	69	85	123	191	282	355	362	295	201
58	72	98	146	230	354	496	594	584	469	318	198	126	89	71	65	68	85	123	192	285	359	365	297	202
58	71	96	144	224	342	472	560	547	438	297	186	119	85	69	63	67	84	122	192	284	358	363	295	199
57	70	95	141	219	329	449	526	511	408	277	174	113	81	66	62	66	82	120	188	279	352	356	288	195
57	69	94	139	214	317	426	494	475	378	257	163	106	77	64	60	64	80	117	183	271	341	345	279	188
56	68	93	137	209	307	406	463	442	350	239	152	100	74	61	58	62	78	113	176	259	326	329	266	180
56	68	92	136	206	298	388	437	412	325	222	142	95	70	59	55	60	75	108	167	246	308	311	251	170

A-41

Figure A-7 (Sheet 4 of 6)

ER-267

44	61	94	147	215	268	272	224	157	101	68	51	43	42	45	54	73	109	161	218	257	259	223	165	109
45	64	99	155	226	282	287	236	164	106	70	53	45	43	46	55	76	113	166	223	259	257	217	159	105
47	67	103	163	238	297	302	248	172	110	73	54	46	44	47	57	79	118	173	230	263	256	213	154	101
48	69	108	171	251	312	317	260	180	115	76	56	47	45	48	59	82	123	181	239	270	258	210	150	99
50	72	113	179	262	326	331	271	187	119	78	57	48	46	50	61	86	129	190	250	279	262	210	148	97
52	75	117	186	272	339	343	281	193	122	80	59	49	47	51	64	90	137	202	263	290	268	212	148	96
53	77	121	192	280	349	353	288	198	125	82	60	50	48	53	66	95	145	215	279	304	277	215	148	96
54	78	123	195	286	356	360	294	202	127	83	61	51	50	55	69	100	154	228	296	320	287	220	149	96
54	79	124	197	289	359	363	296	203	128	84	62	52	51	56	72	105	163	243	314	337	299	225	151	97
55	80	125	198	289	359	362	296	203	128	84	62	53	52	58	75	110	173	257	333	355	312	232	154	98
55	80	125	197	287	356	358	292	201	127	84	62	54	54	61	80	121	191	286	369	390	337	245	160	100
56	80	125	196	283	350	352	287	197	125	83	62	54	54	62	83	125	200	300	386	406	348	251	162	101
56	80	124	194	278	342	343	279	192	123	82	62	54	54	62	83	125	200	300	386	406	348	251	162	101
56	80	123	191	272	332	332	271	187	120	81	61	54	55	64	85	130	208	312	402	421	359	256	164	102
56	80	122	188	265	323	322	262	181	117	79	61	54	55	64	87	134	215	323	415	434	367	261	166	103
57	80	122	185	259	313	311	253	175	113	77	60	54	55	65	89	137	221	332	427	445	375	264	167	103
57	81	122	183	254	304	300	244	169	110	75	59	53	55	66	90	139	225	339	435	453	380	266	167	103
58	82	123	183	250	296	290	234	163	106	73	58	53	55	66	90	141	228	344	441	458	383	268	167	103
58	83	124	182	246	287	279	225	156	103	71	57	52	55	66	91	141	229	346	444	460	384	267	167	102
59	84	125	182	241	278	268	215	149	99	69	55	51	54	65	90	141	229	346	443	459	382	265	165	101
60	85	126	181	237	269	257	205	143	95	67	54	50	54	65	89	140	227	343	439	454	377	261	162	99
61	87	128	181	233	261	246	196	136	91	65	53	50	53	64	88	137	223	337	431	445	369	255	158	97
62	89	130	183	231	254	237	187	130	87	63	52	48	52	62	86	134	217	328	419	432	359	248	154	95
64	91	133	184	229	248	228	179	124	84	61	50	47	50	61	84	130	210	317	404	417	346	239	149	92
65	93	136	187	228	242	220	171	119	81	59	49	46	49	59	81	125	202	303	387	399	331	230	143	89
67	96	140	190	228	238	212	164	114	78	57	48	45	48	57	78	120	193	289	368	380	315	219	137	85
69	99	144	194	229	234	206	158	110	75	56	46	44	47	55	75	114	183	273	347	358	298	207	130	81
71	103	149	199	232	233	201	153	106	73	54	45	43	45	53	72	108	172	257	326	336	279	194	122	76
73	107	156	206	237	234	199	149	103	71	53	44	42	44	51	68	102	161	240	304	313	260	181	114	72
77	113	165	217	245	237	198	147	101	70	52	44	41	42	49	65	96	151	223	282	290	241	168	106	67
81	120	175	229	257	244	200	146	100	69	51	43	40	41	47	61	90	140	206	260	267	222	155	99	63
85	128	188	245	271	253	203	146	99	68	51	42	39	40	45	58	84	130	190	239	246	204	143	91	59
90	137	202	262	247	264	209	148	100	68	51	42	38	39	43	55	78	120	174	219	224	186	131	84	55

A-43

Figure A-7 (Sheet 6 of 6)

APPENDIX B

EXPANSION FORMULAE FOR HANKEL TRANSFORM OF TRUNCATED GAUSSIAN POINT SPREAD FUNCTION

B.1 INTRODUCTION

The calculation of the two-dimensional Fourier transform of an axially symmetric point spread function (PSF) may be reduced to the Hankel transform of the radial PSF. In this Appendix we derive an infinite series by partial integration for the case of a circular Gaussian profile truncated by a clear circular aperture. An alternative formula, which is obtained by interchanging the u and dv variables in the partial integration, is quoted from the literature (Reference 5). These formulae yield the well known results of the diffraction pattern of a clear circular aperture and the Gaussian MTF in the limiting cases of $r_0/\sigma \ll 1$ and $r_0/\sigma \gg 1$, respectively, where r_0 is the radius of the truncating aperture, and σ is the standard deviation of the Gaussian profile.

B.2 EVALUATION OF HANKEL TRANSFORM

We start with the Hankel transform expression,

$$M(s) = (1/\sigma^2) \int_0^{r_0} J_0(2\pi rs) \exp(-r^2/2\sigma^2) r dr, \quad (\text{B-1})$$

where J_0 is the Bessel function of order zero, and s is spatial frequency. Letting $z = 2\pi rs$ and $\delta = 2\pi\sigma s$ the integral (B-1) becomes

$$M = (1/\delta^2) \int_0^{z_0} J_0(z) \exp(-z^2/2\delta^2) z dz, \quad (\text{B-2})$$

where

$$z_0 = 2\pi r_0 s.$$

We now integrate by parts, letting $u=J_0(z)$ and $dv = \exp(-z^2/2\delta^2) dz$, and using the relation $(1/z)(d/dz) (J_n(z)/z^n) = -J_{n+1}(z)/z^{n+1}$.

Thus

$$M = -J_0(z)\exp(-z^2/2\delta^2) \Big|_0^{z_0} - \int_0^{z_0} (J_1(z)/z)\exp(-z^2/2\delta^2) dz.$$

Integrating by parts again gives

$$M = -J_0(z)\exp(-z^2/2\delta^2) \Big|_0^{z_0} + \delta^2 (J_1(z)/z)\exp(-z^2/2\delta^2) \Big|_0^{z_0} \\ + \delta^2 \int_0^{z_0} (J_2(z)/z^2)\exp(-z^2/2\delta^2) dz.$$

Continuing this process and evaluating the upper and lower limits of integration with the help of the limit: $\lim_{z \rightarrow 0} (J_n(z)/z^n) = (1/2^n n!)$ we get the infinite series

$$M = 1 - J_0(z_0)\exp(-z_0^2/2\sigma^2) - \delta^2 [1/2 - (J_1(z_0)/z_0)\exp(-z_0^2/2\sigma^2)] \\ + \delta^4 [1/2^2 2! - (J_2(z_0)/z_0^2)\exp(-z_0^2/2\sigma^2)] \\ - \delta^6 [1/2^3 3! - (J_3(z_0)/z_0^3)\exp(-z_0^2/2\sigma^2)] \\ + \dots$$

which can be separated into the sum of two infinite series:

$$M = 1 - \delta^2/2 + (1/2!) (\delta^2/2)^2 - (1/3!) (\delta^2/2)^3 + \dots \\ - \exp(-z_0^2/2\sigma^2) [J_0(z_0) - \delta^2 J_1(z_0)/z_0 + \delta^4 J_2(z_0)/z_0^2 \\ + \delta^6 J_3(z_0)/z_0^3 - \dots].$$

The first series is recognizable as the expansion of $\exp(-\delta^2/2)$; hence the expansion formula of the Hankel transform is written, finally, as

$$M(s) = \exp(-2\pi^2 \sigma^2 s^2) - \exp(-r_o^2/2\sigma^2) \sum_{n=0}^{\infty} (-4\pi^2 \sigma^2 s^2)^n J_n(2\pi r_o s)/(2\pi r_o s)^n, \quad (B-3)$$

where z_o and δ have been replaced by their corresponding parameters.

In the limit $r_o/\sigma \gg 1$, (B-3) clearly reduces to the MTF of a Gaussian PSF. It is evident that the series diverges for any fixed r_o/σ for s large enough. Hence, the usefulness of the formula is limited to the region $2\pi\sigma s/(r_o/\sigma) < 1$.

B.3 ALTERNATIVE FORMULA FOR THE REGION $2\pi\sigma s/(r_o/\sigma) > 1$

In Reference 5 a similar calculation is performed with the u and dv interchanged in the partial integration. The result in our notation is

$$M(s) = \frac{(r_o/\sigma)^2}{\exp(r_o^2/2\sigma^2)-1} \sum_{n=0}^{\infty} (r_o/\sigma)^{2n} J_{n+1}(2\pi r_o s)/(2\pi r_o s)^{n+1}, \quad (B-4)$$

which reduces in the limit $r_o/\sigma \ll 1$ to

$M(s) \cong 2 J_1(2\pi r_o s)/(2\pi r_o s)$, which is the well-known Fraunhofer diffraction pattern for a clear circular aperture illuminated by an incoherent plane wave. It is evident that this series converges only in the region $2\pi\sigma s/(r_o/\sigma) > 1$, so that the two formulae (B-3) and (B-4) are complementary.

B.4 COMMENT

In practice, the two expansion formulae may provide an aid in analysis, but in numerical computations involving the use of a computer it is probably faster and more accurate to perform a direct numerical integration of (B-1) using the polynomial approximation to the Bessel function J_o and Simpson's rule, which was ultimately done in this study. An attempt to numerically evaluate (B-3) on the computer using an IBM Scientific Software Package

subroutine for the J_n ran into difficulty since the subroutine apparently is not accurate for the small argument region of the J_n , i.e., in the region $2\pi r_0 s \ll 1$.